Steelmaking Operation and Refining Process of Electric Arc Furnace (EAF) in Melting Plant

This thesis is submitted to the Department of Mechanical Engineering of Chittagong University of Engineering & Technology as a partial fulfillment of requirement for the degree of

Master of Engineering

IN MECHANICAL ENGINEERING

Submitted by

Atikuzzaman Billah

Student ID: 16MME028P

Supervised By

Dr. Md. Abu Mowazzem Hossain

Associate Professor, Department of Mechanical Engineering

Department of Mechanical Engineering

Chittagong University of Engineering & Technology

Approval

The thesis titled **"Steel Making Operation and Refining Process of Electric Arc Furnace (EAF) in Melting Plant**" submitted by Atikuzzaman Billah, ID-16MME028P , Session: 2016-2017 has been accepted as satisfactory in partial fulfillment of the requirement for the degree of Master of Engineering (M.Eng.) in Mechanical Engineering dated on ……...

Board of Examiners

1.	**Dr. Md. Abu Mowazzem Hossain** Associate Professor, Department of Mechanical Engineering, CUET	**Chairman** **(Supervisor)**
2.	**Head** Department of Mechanical Engineering, CUET	**Member** **(Ex-Officio)**
3.	**Dr. Md. Arafat Rahman** Professor, Department of Mechanical Engineering, CUET	**Member**
4.	**Dr. Md Rabiul Islam Sarker** Professor, Department of Mechanical Engineering, RUET	**Member** **(External)**

Declaration

I hereby declare that this thesis represents my own work which has been done after registration for the degree of M.Eng. in Mechanical Engineering at CUET, has not been previously included in a thesis or dissertation submitted to this or any other institution for a degree, diploma or other qualification.

Name: Atikuzzaman Billah

Student ID:16MME028P

Acknowledgement

First, I would like to express my gratitude to Almighty Allah for the opportunity to pursue my Master's in Engineering at this university and for the patience and strength to complete my project.

I wish to extend my deepest appreciation to my project supervisor, Dr. Md. Abu Mowazzem Hossain, for his unwavering support and guidance throughout my research. His encouragement and enthusiasm were a constant source of motivation for me. I am truly grateful for his excellent advice, insightful comments, and suggestions throughout this research journey. Whenever I faced challenges, his proper guidance proved invaluable.

I would also like to express my sincere thanks to Prof. Dr. Mohammad Mizanur Rahman, Head of the Department of Mechanical Engineering at CUET, for his support during my research. I am profoundly grateful to my committee members, Prof. Dr. Md. Arafat Rahman from the Department of Mechanical Engineering at CUET and Prof. Dr. Md. Rabiul Islam Sarker from the Department of Mechanical Engineering at RUET, for their time, expertise, and critical evaluation of my work. Their thoughtful comments, suggestions, and academic rigor have greatly contributed to the refinement of this thesis.

I wish to acknowledge the support of Mr. Saful Islam, Manager of the Abul Khair Steel (AKS) Melting Unit, and the EAF operation team. Their wholehearted support and commitment to my research were evident through discussions on the operational process and meetings to analyze the project results.

Additionally, I extend my sincere appreciation to the faculty and staff of CUET for providing a stimulating academic environment and access to valuable resources that facilitated my research endeavors.

Last but certainly not least, I owe an immeasurable debt of gratitude to my family. Their unwavering love, encouragement, belief in my abilities, and sacrifices made to ensure my success have been invaluable.

Dedication

This dissertation is dedicated to my father late Mohasin Billah and my family.

Abstract

Steel production through electric arc furnace (EAF) technology has emerged as an essential process in contemporary metallurgy, particularly in terms of its adaptability and resource flexibility. The EAF represents one of the most prevalent methods for steel manufacturing, primarily utilized in the casting and rolling phases within steel plants. The inception of the first EAF dates back to the early 20th century. The inherent versatility of the electric arc furnace allows it to cater to the dynamic demands for steel materials, which has facilitated the development of mini steel plants focused on producing various grades of steel products from steel scrap and alternative charge materials.

In EAF operations, steel scrap serves as the principal raw material; however, challenges such as limited scrap availability and the need for low-residual or high-purity iron sources have necessitated the incorporation of direct reduced iron (DRI), hot briquetted iron (HBI), pig iron, and hot metal in the steelmaking process. Significant advancements in the operational aspects of EAF steel production have enhanced its contribution to global steel output. According to the World Steel Association, electric arc furnaces account for approximately 30% to 35% of the total steel production worldwide. Over the past three decades, numerous innovations in EAF steelmaking have been implemented to minimize power consumption, optimize tap-to-tap timings, reduce electrode usage, and lessen refractory wear.

This study critically analyzes the steelmaking and refining processes employed at AbulKhair Steel (AKS) melting plant in Bangladesh. An examination of the significance of raw materials in the steelmaking process forms a central component of this research. Various parameters, including specific electrical energy consumption, tap-to-tap timing, lime consumption, carbon consumption, and electrode consumption, were examined across four distinct charging mixture ratios (MR). A comparative analysis of these parameters was conducted graphically, with a focus on determining the most cost-effective and productive mixture ratio for the steelmaking process. Among the evaluated mixtures, the MR-2, consisting of 87.7% scrap (comprising 67.7% shredded scrap and 20% heavy melting scrap) and 12.3% pig iron, demonstrated the most favorable results, establishing its efficiency relative to the other raw material mixtures examined. The findings indicate that the lowest specific power consumption, tap-to-tap (TTT), and electrode consumption were recorded for MR-2, in contrast to the other ratios. In contrast, MR-4 exhibited the highest specific electrical energy consumption, TTT, lime consumption, and electrode consumption. Interestingly, carbon consumption was highest in MR-1, which contained a significant amount of

scrap with 10% hot briquetted iron (HBI) and 5% pig iron. The presence of FeO in HBI necessitates greater carbon consumption to produce carbon monoxide (CO) gas.

সারসংক্ষেপ

ইলেকট্রিক আক ফানেস প্রযুক্তির মাধ্যমে স্টীল উৎপাদন সমসাময়িক মেটালাজিতে একটি অত্যাবশ্যকীয় প্রক্রিয়া হিসেবে আবিভুত হয়েছে, বিশেষ কওে এর অভিযোজন যোগ্যতা এবং কাচামাল ব্যবহাওে সহজলভ্যতার জন্য।স্টীল উৎপাদনে ইএএফ হচ্ছে প্রচলিত পদ্বতিগুলোর মধ্যে অন্যতম, যা প্রাথমিকভাবে স্টীলপস্ন্যান্টের মধ্যে ঢালাই ও রোলিং এ ব্যবহৃতহয়।প্রথম ইএএফ এর সুচনা হয় ২০ শতকের গোড়ার দিকে।ইলেকট্রিক আক ফানেসের অন্তনিহিত বহুমুখিতা এটাকে স্টীল সামগ্রীর বিভিন্ন চাহিদা পুরণ করে, যাহা স্টীল স্ক্র্যাপ ও বিকল্প চাজ ম্যাটেরিয়াল হতে বিভিন্ন গ্রেডের স্টীল প্রোডাক্ট তৈরী কওে মিনি স্টীলপস্ন্যান্টের বিকাশকে সহজতর করেছে।

ইএএফ অপারেশনে স্টীল স্ক্র্যাপ প্রধান কাচামাল হিসেবে ব্যবহৃত হয়,যাই হোক সিমীত স্ক্র্যাপের প্রাপ্যতা এবং লো রেসিডিউয়াল বা উচ্চ আয়রন উৎসের চ্যালেঞ্জগুলো মোকাবেলা করতে ডিআরআই, এইচবিআই,পিগআয়রন ও হট মেটাল স্টীল উৎপাদনের প্রক্রিয়ায় অন্তভুক্ত করার প্রয়োজনীয়তা তেরী করেছে।ইএএফ অপারেশনে গুরন্নত্বপূণ অগ্রগতির জন্য বিশ্বব্যপী স্টীল উৎপাদনে এর অবদান বাড়িয়েছে।বিশ্ব স্টীল সংসত্মার তথ্য মতে, মোট স্টীল উৎপাদনের ৩০-৩৫% স্টীল আক ফানেস এর মাধ্যমে হয়।গত তিন দশকে ইএএফ এর মাধ্যমে স্টীল তৈরির প্রক্রিয়ায় বিদ্যুত খরচ কমাতে, ট্যাপ টু ট্যাপ টাইমিং অপটিমাইজ করতে ,ইলেকট্রোডের ব্যবহার কমাতে এবং রিফ্র্যাকটরির ড়ায় রোধ করার জন্য অনেক উদ্বাবনী প্রয়োগ করা হয়েছে।

এই গবেষনাটি বাংলাদেশের আবুল খায়ের স্টীল মেল্টিং পস্ন্যান্টের স্টীল উৎপাদন ও রিফাইনিং প্রক্রিয়াটির উপর সুড়াভাবে বিশেস্নষন করা হয়েছে। এই গবেষনার প্রধান উপকরন হলো স্টীল উৎপাদনে কাচামালের প্রভাব পরীড়্গা করা।স্পেসিফিক ইলেকট্রিক্যাল পাওয়ার কনজাম্পশন,ট্যাপ টু ট্যাপ টাইমিং, লাইম কনজাম্পশন, কাবন কনজাম্পশন এবং ইলেকট্রোড কনজাম্পশন সহ বিভিন্ন প্যারামিটার চারটি স্বতন্ত্র কাচামাল /চাজিং মিকশ্চার রেশিও দিয়ে পরীড়্গা করা হয়।চারটি স্বতন্ত্র চাজিং মিক্সার রেশিও দিয়ে এই প্যারামিটার গুলোর তুলনামূলক বিশেস্নষন গ্রাফিক্যালি দেখানো হয়েছে এবং স্টীল উৎপাদনে সবচেয়ে কস্টইফেক্টিভ ও প্রোডাক্টিভ মিক্সার রেশিও নিণয়ে ফোকাস করা হয়েছে ।মূল্যায়নকৃত মিক্সারগুলোরমধ্যে মিক্সার রেশিও -২ যার মধ্যে ৮৭.৭ % স্ক্র্যাপ (৬৭.৭% স্রেডেড স্ক্র্যাপ ও ২০% হেভি মেল্টিং স্ক্র্যাপ) এবং ১২.৩ % পিগ আয়রন বিদ্যমান , যাহা অন্যান্য মিক্সার রেশিও গুলোর মধ্যে পরীড়্গায় সবচেয়ে অনুকূলীয় ফলাফল ও ভালো পারফরম্যান্স দেখিয়েছে।ফলাফল হলো মিক্সার রেশিও -২ এ স্পেসিফিক ইলেকট্রিক্যাল পাওয়ার কনজাম্পশন,ট্যাপ টু ট্যাপ টাইমিং এবং ইলেকট্রোড কনজাম্পশন অন্যান্য মিক্সার রেশিওর চেয়ে তুলনামূলকভাবে অনেক কম।অন্যদিকে মিক্সার রেশিও -৪ এ স্পেসিফিক ইলেকট্রিক্যাল পাওয়ার কনজাম্পশন,ট্যাপ টু ট্যাপ টাইমিং, লাইম কনসাম্পশন এবং ইলেকট্রোড কনজাম্পশন তুলনামূলকভাবে বেশী প্রদশন করে।মজার বিষয়হলো, মিক্সার রেশিও -১ এ কাবন কনজাম্পশন সবচেয়ে বেশী ছিল, যেটিতে ১০% এইচবিআই এবং ৫% পিগ আয়রন সহ উলেস্নখযোগ্য পরিমান স্ক্র্যাপ রয়েছে।এইচবিআই (HBI) তে আয়রন অক্সাইড (FeO) এর উপস্থিতির জন্য কাবনমনোঅক্সাইড(CO)গ্যাস তেরী করতে বেশী পরিমান কাবন কনজাম্পশন হয়।

Table of Contents

Approval ..... **i**
Board of Examiners ..... **i**
Declaration ..... **ii**
Acknowledgement ..... **iii**
Dedication ..... **iv**
Abstract ..... **v**
সারসংক্ষেপ ..... **vii**
List of Figures ..... **x**
List of Tables ..... **xv**
Chapter 01 Introduction **1**
1.1 BACKGROUND 1
1.2 SHORT HISTORY OF EAF STEEL MAKING 1
1.3 STEEL PRODUCTION PERSPECTIVE IN BANGLADESH 4
1.4 MOTIVATION AND OBJECTIVES 5
1.5 PROJECT OUTLINE 6
Chapter -02 Introduction to Electric Arc Furnace **7**
2.1 BACKGROUND 7
2.2 TYPES OF ELECTRIC ARC FURNACE 8
2.2.1 AC Electric Arc Furnace 8
2.2.2 DC Electric Arc Furnace 9
2.2.3 Advantages of DC Electric arc Furnace over AC furnace 9
2.2.4 Design of DC Electric Arc Furnace 10
2.3 COMPONENTS AND STRUCTURE OF DC ELECTRIC ARC FURNACE 13
2.3.1 Furnace Platform and Tilting System 13
2.3.1.1 Furnace Platform 13
2.3.1.2 Furnace Tilting System 15
2.3.1.3 Platform Locking System 15
2.3.2 Shell and Cooled Panels 15
2.3.2.1 Slagging Door 17
2.3.3 Cooled Roof 17
2.3.4 Eccentric Bottom tapping (EBT) 18
2.3.5 Roof Lifting and Rotating Unit 19

2.3.6 Electrode Lifting Unit....20
2.3.7 Conductive Electrode-Holder Arms....21
2.3.8 EAF Electrical System....21
2.3.8.1 Step down Transformer....21
2.3.8.2 EAF Transformer....22
2.3.8.3 DC Power....22
2.3.8.4 Cathode Secondary Circuit....22
2.3.8.5 Anode Secondary Circuit....22
2.3.8.6 Anode Electrical Connection....22
2.3.9 Electrode Spray Cooling....23
2.3.10 Water-Cooled Bottom Anodes....23
2.3.10.1 Anode cooling water system....23
2.3.11 Cooled Flexible Cables....24
2.3.12 Supply of Alternative Energy....24
2.3.12.1 Carbon pipe....25
2.3.12.2 Water Cooled Supersonic Oxy-Carbon Lance....26
2.3.13 Bottom Stirring....27
2.3.14 Refractories for Electric Furnace Steelmaking....28
2.3.14.1 Refractory Lining of EAF Roof....29
2.3.14.2 Side Wall....29
2.3.14.3 Bottom of Hearth....30
2.3.14.4 Bottom Anode Design....31
2.3.14.5 Refractory Wear Mechanism....31
2.3.15 Graphite Electrode....32
2.3.15.1 Electrode Wear mechanism....32
2.3.15.3 Development of Special DC Electrode Grades....33
2.3.16 Electric Arc Furnace Fume suction Plant....33
2.3.17 Grease Lubrication System....34
2.3.18 Cooling System....35
2.3.19 Hydraulic System....35
2.3.20 Electrodes Conditioning Centre....36
2.4 RAW MATERIALS IN EAF....36
2.4.1 Scrap....36
2.4.2 Direct Reduced Iron (DRI)....38

2.4.3 Hot Briquetted Iron (HBI) 38
2.4.4 Pig Iron (PI) 39
2.4.5 Hot Metal (Molten Pig Iron) 39
2.4.6 Other Charge Materials 39
2.4.6.1 Carbon 40
2.4.6.2 Lime and Dolomite Lime 41
2.5 OXYGEN LANCING IN EAF 41
2.6 POST COMBUSTION IN EAF 42
2.7 SCRAP PREHEATING SYSTEM IN EAF 43
2.7.1 Bucket Preheating System 44
2.7.2 Continuous Preheating System or Consteel Process 44
2.8 SHAFT FURNACE 45
2.9 CHEMICAL REACTIONS IN THE FURNACE 46
Chapter -03 Steelmaking Operation and Refining Process 48
3.1 INTRODUCTION 48
3.2 STEEL PRODUCTION 49
3.3 ELECTRIC ARC FURNACE SPECIFICATION 50
3.4 EAF OPERATION 51
3.4.1 Charging 52
3.3.2 Melting 56
3.3.2.1 HBI/DRI Continuous Feeding and Melting 57
3.3.3 Refining 58
3.3.4 Deslagging 64
3.3.5 Tapping 65
3.3.6 Furnace Turnaround 65
3.3.7 Furnace Heat Balance 66
3.5 IMPACT OF RAW MATERIALS ON STEEL MAKING OPERATION 66
Chapter-04 Data collection and Methodology 76
4.1 DATA CAPTURING 76
4.2 METHODOLOGY 76
4.2.1 Process Sequence of 85% Scrap, 5% Pi and 10% HBI Mixture 78
Chapter -05 Data Analysis and Discussion 82
5.1 INTRODUCTION 82
5.2 DATA ANALYSIS 82

5.2.1 Graphical Representation of four mixture ratios 82
5.2.2 Comparative Analysis.....85
5.3 DISCUSSION 91
Chapter –06 Conclusion and Recommendations 93
6.1 CONCLUSION 93
6.2 RECOMMENDATIONS 94
References 95
Appendices 100

List of Figures

Figure 1. 1 World steel crude production [adopted from 5]. 2
Figure 1. 3 Electric Arc Furnace development criteria [adopted from 7].....3
Figure 1. 4 Current demand and forecast of rebar [adopted from 8]. 5
Figure 2. 1 Technology development in steel arc furnace by time (year) [adopted from 20]. 8
Figure 2. 2 AC and DC electric arc furnace layout [adopted from 21]. 9
Figure 2. 3 Configuration of a DC EAF with single graphite electrode and bottom anode [2]....10
Figure 2. 4 Configuration of a DC EAF with two graphite electrode and four bottom anodes [2]. 11
Figure 2. 5 Configuration of a DC EAF with single electrode and four bottom anodes [2].....11
Figure 2. 6 Different design bottom anode connections [adopted from 24]. 12
Figure 2. 7 Typical arrangement of billet anode at EAF bottom area [24].....13
Figure 2. 8 EAF structure [adopted from 2]. 13
Figure 2. 9 Schematics of furnace Platform unit (where, 1. Pins for shell centering, 2. Platform, 3. Rolling guides, 4. Foundation columns, 5.Link for rotational cylinder, 6.Level for tilting locking, 7.Cylinder for tilting locking, 8. Tilting cylinder) [26]. 14
Figure 2. 10 A typical of shell structure schematic (1. Bottom shell, 2.Top shell, 3. Slagging door) [adopted from 26].....16
Figure 2. 11 Upper shell and water cooled panel [adopted from 2]. 17
Figure 2. 12 Schematics of slagging door (1.cylinder protection, 2.chain, 3. Cylinder, 4.door panel) [adopted 26]. 17
Figure 2. 13 A typical EAF roof (AKS, a well-known steel melting plant in Chittagong) [27]. .18
Figure 2. 14 Eccentric bottom tapping configuration [adopted from 25]. 19
Figure 2. 15 Cylindrical position: (101) electrode regulation cylinder, (102) Roof lifting cylinder (103) Roof rotation cylinder, (104) Tilting cylinder,(105)Platform locking cylinder, (106) locking cylinder (107)Slagging door cylinder (108) EBT opening cylinder (109) EBT locking cylinder [adopted from 26]. 20
Figure 2. 16 Electrode lifting column (at AKS Melting Ltd, Chittagong) [27].....20
Figure 2. 17 Current Conducting arms [adopted from 25]. 21
Figure 2. 18 A typical EAF injection system [adopted from 25].....25
Figure 2. 19 A typical model of oxygen-jet and carbon pipe installation [adopted from 31]. 26
Figure 2. 20 A typical PARPI slag door supersonic lance [Adopted from 31]. 27
Figure 2. 21 Bottom stirring system (A) Direct contact & (B) Indirect contact at EAF [Adopted from 32]. 28

Figure 2. 22 A schematics of different zone of refractories of bottom tapping EAF [Adopted from 33]. 28
Figure 2. 23 Bottom assembly of EAF [Adopted from 34]. 30
Figure 2. 24 Typical off gas system flow sheets [Adopted from 24]. 34
Figure 2. 25 EAF Hydraulic system [setup at AKS melting plant in Chittagong, ref. 27]. 35
Figure 2. 26 Schematic diagram of bucket preheating system [Adopted from 25]. 44
Figure 2. 27 Schematic diagram of consteel process [adopted from 43]. 45
Figure 2. 28 A schematic diagram of finger shaft furnace [adopted from 42]. 46
Figure 2. 29 Fundamental mechanism and chemical reaction [adopted from 31]. 47
Figure 3. 1 EAF operation process flow diagram [AKSML, Chittagong]....52
Figure 3. 2 Scrap bucket loading pattern [adopted from 31]. 54
Figure 3. 3 Placing of the Bucket above the Furnace [31]....55
Figure 3. 4 Emptying of the Bucket into the Furnace [31]. 55
Figure 3. 5 Scrap charged into the furnace [31]....55
Figure 3. 6 Melting process [AKS melting plant in Chittagong]. 57
Figure 3. 7 Refining process flowchart [52]. 59
Figure 3. 8 The solubility of MgO for slags that are dual saturated with respect to CaO and MgO at 1600^0C [57]. 63
Figure 3. 9 EBT Furnace Tapping [AKS melting plant in Chittagong]....65
Figure 3. 10 Specific electrical energy consumption versus DRI charging ratio [47]. 68
Figure 3. 11 The specific energy consumption versus metallization degree (%) with respect to different percentage addition of DRI to the scrap [47]. 69
Figure 3. 12 Specific energy consumption versus DRI temperature with carbon % [47]. 70
Figure 3. 13 Specific energy consumption versus DRI metallization % with carbon content % [47]. 70
Figure 3. 14 Specific energy consumption versus gangue % (DRI) with efficiency [47]. 70
Figure 3. 15 Electrical energy consumption versus percentage of hot metal charged [62]. 73
Figure 3. 16 Furnace productivity versus hot metal charged percentage [62]. 74
Figure 3. 17 Specific energy consumption versus raw materials ratio with input power [66]. 75
Figure 4. 1 Flowchart of EAF operation and steel making process. 78
Figure 5. 1 MR -1 [Scrap -85 % (Shredded – 55% + HMS – 30%), Pig Iron – 5%, HBI – 10%] 84
Figure 5. 2 MR-2 [Scrap -87.7 % (Shredded – 67.7% + HMS – 20%), Pig Iron – 12.30%]. 84
Figure 5. 3 MR– 3 [Scrap -72 % (Shredded – 50% + HMS – 22%), Pig Iron – 15%, HBI – 13%]. 85

Figure 5. 4 MR– 4[Scrap -60 % (Shredded – 40% + HMS – 20%), Pig Iron – 12%, HBI – 28%]. 85
Figure 5. 5 Comparison of specific power consumption for the four mixture ratios.....87
Figure 5. 6 Comparison of tap-to-tap timing (TTT) for the four mixture ratios.....88
Figure 5. 7 Comparison of lime consumption for the four mixture ratios. 89
Figure 5. 8 Comparison of carbon consumption for the four mixture ratios. 90
Figure 5. 9 Comparison of electrode consumption for the four mixture ratios. 91

List of the Tables

Table 2. 1 Properties of different refractories used in EAF roof [34].....29
Table 2. 2 Properties of sidewall refractory in EAF [34] 29
Table 2. 3 The properties of gunning & patching refractories [34]. 30
Table 2. 4 Electrode properties [25,26] 32
Table 2. 5 Different categories scrap and other ferrous raw materials chemical properties [2] ...37
Table 2. 6 Typical characteristics of pig iron [31]. 39
Table 2. 7 Charged carbon characteristics [31]. 40
Table 2. 8 Injected carbon characteristics [31] 40
Table 2. 9 Lime and dolomite lime chemical properties [31].....41
Table 2. 10 Benefits and concern for post combustion [25] 42
Table 3. 1 EAF technical specification of AKS melting plant at Chittagong.....50
Table 3. 2 Chemical energy packages (Flow rates) [31] 51
Table 3. 3 Slag composition of EAF [50] 64
Table 3. 4 Heat balance of old and new modern EAF [50] 66
Table 3. 5 Typical properties of DRI [62]. 72
Table 3. 6 Comparative analysis of DRI & average scarp at AM Mexico [63] 73
Table 4. 1 Technical parameters of specific raw materials tapped Steel [AKS melting plant in Chittagong] 81

Chapter 01
Introduction

1.1 BACKGROUND

An electric arc furnace (EAF) is an enclosed facility designed for the melting of steel scrap and iron materials through the intense heat generated by an electric arc. This innovative melting technology allows for the production of molten steel by initiating a chemical reaction that carefully controls carbon composition and temperature. After the liquid steel is produced, it undergoes a ladle treatment before being transferred to a continuous caster, where it is formed into semi-finished products such as billets and slabs. EAFs serve a dual purpose: they can be utilized not only for producing steel but also for creating cast iron in workshops and secondary steel in industrial settings. The operational capacity of these furnaces can range significantly, accommodating loads from as little as 1 ton up to an impressive 400 tons. During industrial operations, the temperatures within an EAF can soar to around 1800°C to achieve the desired molten steel state [1]. The process within an electric arc furnace involves melting ferrous materials using a powerful electric current, with both alternating current (AC) and direct current (DC) options available. In order to refine the steel and eliminate undesirable metallic impurities, oxygen is injected into the furnace during the refining process. Additionally, fuels may be introduced to minimize electricity consumption, enhancing efficiency. One notable distinction between an electric arc furnace and an induction furnace is the flexibility in the charge material. In an EAF, the charge materials are directly exposed to the electric arc, which is generated by the current passing through the electrodes. This unique aspect allows for a more varied range of scrap materials to be used, making the electric arc furnace a versatile choice in steelmaking [1].

1.2 SHORT HISTORY OF EAF STEEL MAKING

In 1890, Paul He'roult invented the first AC electric arc furnace in France, marking a significant advancement in metallurgical technology. The technology has been its first commercial implementation in the United States in 1906. At the dawn of the twentieth century, the electric arc furnace (EAF) began to emerge as an innovative solution for steel production, characterized by its relatively low electrical energy consumption during initial operations. Early models of the furnace had capacities ranging from 1 ton to 15 tons and played a crucial role in the production of specialized grades of steel at elevated temperatures, necessitating extended refining processes [2]. The application of EAF technology gained traction with the advent of billet casting in 1960,

wherein EAFs were utilized to supply billet casters for the production of rebar and wire rod. It is noted that in 1963, the first ultra-high power furnace was installed in the USA, revolutionizing the capabilities of steel manufacturing [3]. By 1985, the introduction of thin slab casting and rolling led to the production of flat products, signaling a new era in electric steelmaking and establishing a significant niche in global steel production [4].

The 1990s witnessed a significant increase in the use of direct current (DC) furnace technology, facilitated by advancements in high-power solid-state rectifiers, which led to a growing demand for steel production through scrap melting. In 1990, Tokyo Steel installed a 130-ton DC arc furnace at its Kyushu plant [5]. Over the next two decades, advancements in electric arc furnace technology have concentrated on several key areas: reducing tap-to-tap time, increasing transformer power, utilizing ultra-high power furnaces, and minimizing the consumption of electrodes and refractory materials. The introduction of foamy slag in the steel melting process has significantly improved productivity in electric arc furnace (EAF) operations. According to the World Steel Association, approximately 25% of global steel production is achieved using electric arc furnaces, while the remaining 75% is produced through blast furnace and basic oxygen furnace methods. Open hearth furnaces account for only 0.4% of global steel production [5]. In 2018, total global crude steel production reached 1,840 million metric tons, reflecting a growth rate of 15% compared to 2016 and 2017. Trends in steel production and the evolution of electric arc furnace technology are illustrated in Figure 1.1.

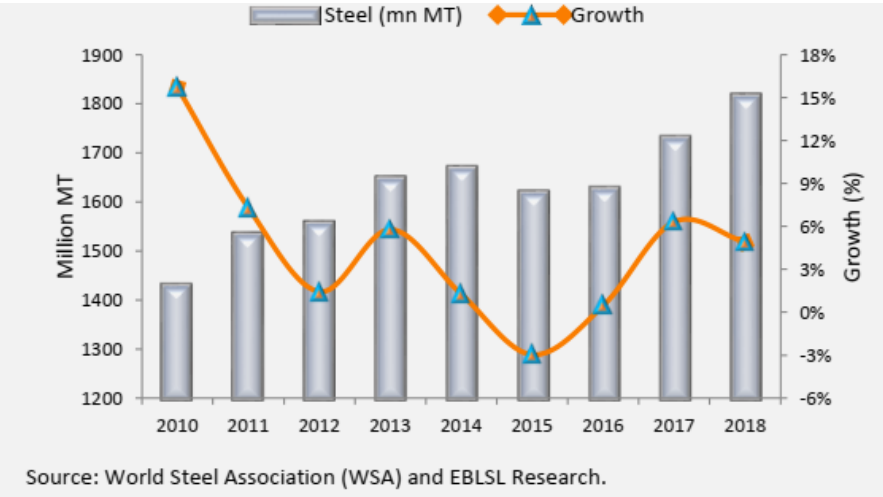


Figure 1. 1 World steel crude production [adopted from 5].

As the capacity of EAF increased over the years, the production of various grades of steel became highly competitive. By 2006, EAFs accounted for 55% of total steel production in the U.S., according to the US Geological Survey (USGS) [6].The advancement of Electric Arc Furnace (EAF) technology began in 1965, leading to a significant reduction in electric energy

consumption, decreasing from 630 kWh per ton to 345 kWh per ton. Additionally, the tap-to-tap timing improved from 180 minutes to just 40 minutes, and electrode consumption was reduced from 6.5 kg per ton to 1.1 kg per ton. The capacity of ultra-high power furnaces expanded from 50 tons to 300 tons, with power levels increasing from 250 KVA to 1000 KVA per ton [7].

Moreover, various furnace transformers have been developed to accommodate different furnace capacities, including a 300-ton EAF that is currently installed in Turkey with 300 MVA [3]. Recent developments in EAF technology feature the implementation of ultra-high power supply systems, the use of oxy-fuel burners, eccentric bottom tapping (EBT), bath stirring for improved homogeneity, electrode cooling, cooled water panels, and the production of foamy slag [8]. The criteria for the development of Electric Arc Furnaces are illustrated in Figure 1.2.

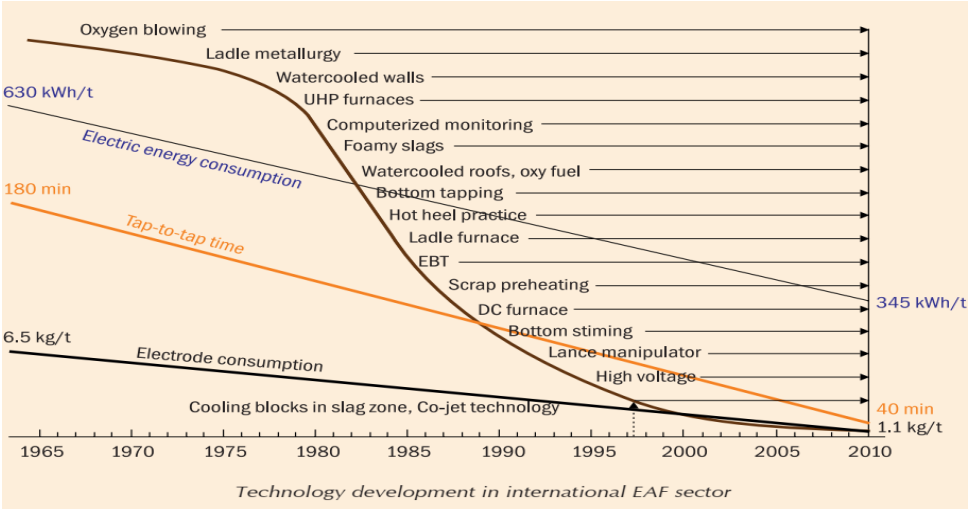


Figure 1. 2 Electric Arc Furnace development criteria [adopted from 7].

A study referenced in [7] indicates that greenhouse gas (GHG) emissions from electric arc furnaces are significantly lower than those from integrated steel plants, such as blast furnaces and basic oxygen furnaces. According to a 2013 survey by the World Steel Association, which analyzed data from 72 blast furnaces and electric arc furnaces, the CO_2 intensity was 2.26 tons of CO_2 per ton of crude steel for blast furnaces and basic oxygen furnaces, while it was only 0.62 tons of CO_2 per ton of crude steel for electric arc furnaces. This reduced greenhouse gas emission is attributed to several techniques implemented in electric arc furnaces, including scrap preheating, oxy-fuel burners, post-combustion, and other energy-efficient methods that lower electrical energy consumption. It is worth noting that electricity accounts for approximately 60% of EAF steelmaking costs. As a result, various methods have been developed over the past 20 years to reduce electricity and production costs [8-10]. Industries have sought to decrease power consumption by utilizing both chemical and electrical energy, which has led to reduced tap-to-tap timing and enhanced continuous casting production [10].

1.3 STEEL PRODUCTION PERSPECTIVE IN BANGLADESH

Bangladesh has experienced a remarkable increase in its demand for raw materials essential for steel production, alongside significant advancements in steel technology as we have developed and expand our steel market. The thriving economy hinges on the vibrant evolution of the steel sector, which has fostered an increased utilization of steel in various industries. As one of the fundamental raw materials for infrastructural development, steel plays a crucial role in projects ranging from bridges and buildings to roads and railways. Fortunately, Bangladesh boasts a long and rich heritage of skill in steel manufacturing and the production of diverse steel products that has persisted for many years [5]. Currently, the country produces long steel products such as rebar, angles, beams, and channels to support the development of its infrastructure. In recent years, the demand for long steel products has increased significantly. The steel industry today is thriving, largely due to investments from major corporations, which have led to product diversification and transformation in production processes [11]. Presently, the total steel demand in the country is 7.5 million metric tons, with local production at 7.0 million metric tons and an additional 0.5 million metric tons of billets imported from abroad. Iron scrap is a key raw material for billet production in our steel-making plants. A total of 5.5 million metric tons of scrap is imported, along with 0.8 million metric tons sourced from the shipbreaking industry, while the remaining 0.7 million metric tons is collected from domestic sources [11,12].The current demand and forecast for rebar are presented in Figure 1.3, illustrating the trends and projections in the market.

In Bangladesh, the steel manufacturing sector is primarily led by several key companies, including BSRM, AKS, GPH, KSRM, Golden Isphat, Anwar Isphat, and Bayezid Steel. Together, these mills have a significant combined production capacity of around 9 million metric tonnes of steel each year [12]. It is important to note that Bangladesh does not have integrated steel mills that utilize advanced blast furnace and basic oxygen furnace technologies for steel production. Instead, the country's steel industry mainly depends on innovative processes involving electric arc and induction furnaces. These methods allow steel manufacturers to recycle and process scrap metal, which they convert into high-quality finished steel products, thereby adding considerable value to the material [5].

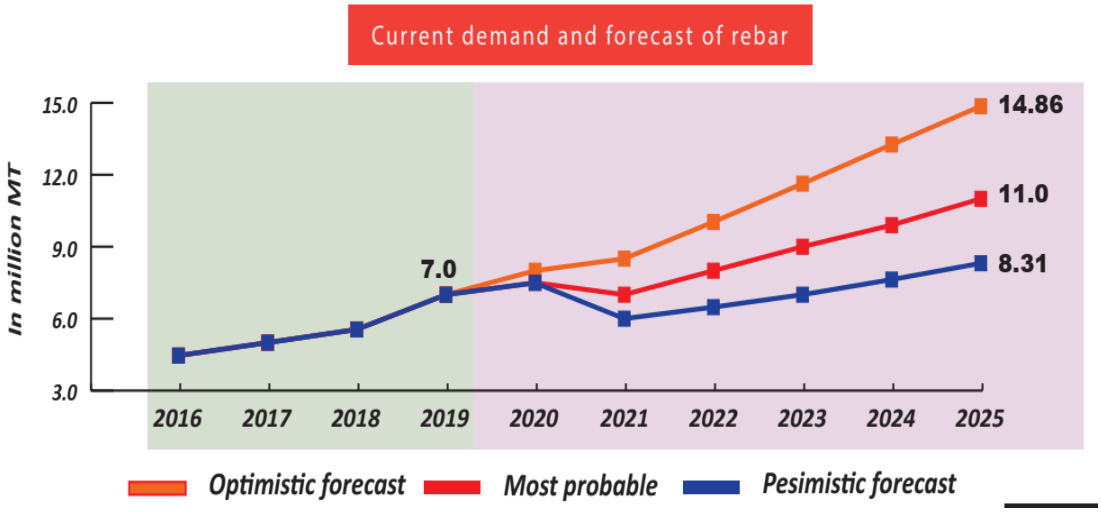


Figure 1.3 Current demand and forecast of rebar [adopted from 8].

1.4 MOTIVATION AND OBJECTIVES

i. To study and observe the methods of steelmaking and refining in Electric Arc Furnaces (EAF)
ii. To compare specific power/energy consumption, tap-to-tap timing (TTT), lime consumption, carbon consumption, and electrode consumption in relation to different raw materials and mixtures during the melting process.
iii. To analyze the impact of direct reduced iron (DRI), hot briquetted iron (HBI), pig iron (PI), and hot metal (molten pig iron) used proportionally with steel scrap in the steel manufacturing process.

As a rapidly developing nation, Bangladesh's growth heavily hinges on its infrastructure, which is significantly built using steel. Since the steel industry, particularly electric arc steel production, requires significant energy consumption. It is crucial to study energy use and explore reduction methods to compete effectively in the global market. In this context, the energy consumption associated with electric arc furnaces (EAF) plays a vital role in enhancing cost-effectiveness, reducing environmental footprint, and optimizing overall operational performance. By conducting a thorough analysis of specific power usage, tap-to-tap timing, and material utilization during the melting processes, manufacturers can achieve greater cost efficiency, deliver higher quality products, and promote sustainability within the steel production sector.

Moreover, a close examination of the ratios of Direct Reduced Iron (DRI), Hot Briquetted Iron (HBI), pig iron, and scrap metal can empower manufacturers to make more informed decisions. Such insights are essential for refining production practices, ultimately leading to improved operational outcomes and contributing to the nation's economic advancement.

1.5 PROJECT OUTLINE

This project report, titled “Steel Making Operations and Refining Processes of the Electric Arc Furnace (EAF) in Melting Plants,” includes background studies, a review of the literature on steelmaking processes, an overview of steelmaking operations and refining processes, and performance analyses based on various charging mixtures. The entire report is organized as follows:

Chapter 1: Introduction

In this chapter, the history of steelmaking using Electric Arc Furnace (EAF) technology and the perspective of steel production in Bangladesh are explained. The chapter also outlines the motivation and objectives.

Chapter 2: Literature Review

This chapter provides a comprehensive overview of Electric Arc Furnaces (EAFs), examining the various types of EAFs and their constituent components. Additionally, the performance analysis of these furnaces is presented, along with an exploration of their inherent limitations.

Chapter 3: Steelmaking operation and refining process

The chapter detailed the intricate operation process of an electric arc furnace, outlining each critical step: charging, melting, refining, de-slagging, tapping, and finally, the furnace turnaround. It also explored how the quality and type of raw materials used significantly influence the efficiency and effectiveness of the steelmaking process.

Chapter 4: Data collection and methodology

This chapter explores the data collection methods used in the steelmaking and refining processes, along with the project methodology that supports these operations.

Chapter 5: Results and Discussion

All related data is represented graphically to analyze the work results and project outcomes, as explained in the discussion.

Chapter 6: Conclusion and Recommendation

This chapter provides an overview of the project's findings, discusses the limitations of the work, and offers recommendations for further study.

Chapter -02
Introduction to Electric Arc Furnace

2.1 BACKGROUND

The steelmaking process includes three main types of facilities: electric arc furnaces (EAF), induction furnaces, and integrated steel mills. There is a fundamental difference among these manufacturing plants. Induction furnaces and EAF plants, often referred to as minimills, produce steel primarily through the melting of scrap metal. In contrast, integrated steel plants manufacture steel from iron ore utilizing blast furnaces (BF) and basic oxygen furnaces (BOF). In the integrated steelmaking process, iron ore in the form of sinter or pellets is processed in a blast furnace along with limestone and coke to produce molten pig iron, also known as hot metal. This liquid pig iron, which contains approximately 4% dissolved carbon, is then tapped from the blast furnace and transferred to the basic oxygen furnace (BOF). The metallic charge of the BOF typically consists of 60% to 70% molten pig iron from the blast furnace and 30% to 40% steel scrap [13].

In an electric arc furnace, an electric arc is transferred from the electrodes to the metal, generating heat through the metal's electrical resistance. This heat facilitates the melting of the metal charge. The electric arc effectively converts electrical energy into heat, which is then transferred to the molten metal through radiation and heat resistance [14]. In the steel-making process within an electric arc furnace, direct reduced iron (DRI), hot briquetted iron (HBI), pig iron, and fluxes are charged along with additional scrap. To refine the steel and control the carbon content during the EAF process, oxygen is injected, and fluxes are added. In addition to the electric arc, other heating sources utilized in the steelmaking process include chemical reactions, oxy-fuel burners, carbon lancing, and the post-combustion of carbon monoxide (CO) [15].

The development of single-phase and two-phase arc furnaces has evolved into three-phase electric arc furnaces. Initially used only for ordinary steel, these furnaces now also produce alloy steels. Their popularity in steel production stems from efficient conversion of electrical energy into heat, allowing for high melting capacity in smaller furnaces [16]. Advances in electrical energy production, installation of water-cooled units, continuous feeding, and automated control have enabled large-scale use of electric arc furnaces in the past decade [17].

It has produced various grades of carbon steel, alloy steel, and stainless steel, available in both long and flat product forms. In this process, sponge iron and iron carbide are commonly utilized alongside scrap metal, particularly when steel scrap is in short supply and to reduce the presence of undesirable tramp elements [18]. It worth noting that the EAF exhibits a substantial electricity

consumption that can potentially match the energy requirements of an entire city [19]. This significant energy utilization, particularly concerning electricity and water, represents a critical challenge within the steel industry that necessitates prompt and focused intervention. The urgent need to address these issues is essential for promoting sustainability and efficiency in steel production processes. Improvements in the EAF operation process and design have significantly contributed to energy efficiency. As reported in reference [20], electricity consumption in the arc furnace decreased from 630 kWh per ton in 1965 to 280 kWh per ton in 2015 as shown in Figure 2.1. Additionally, the total tap-to-tap (TTT) time has been reduced from 180 minutes to just 40 minutes.

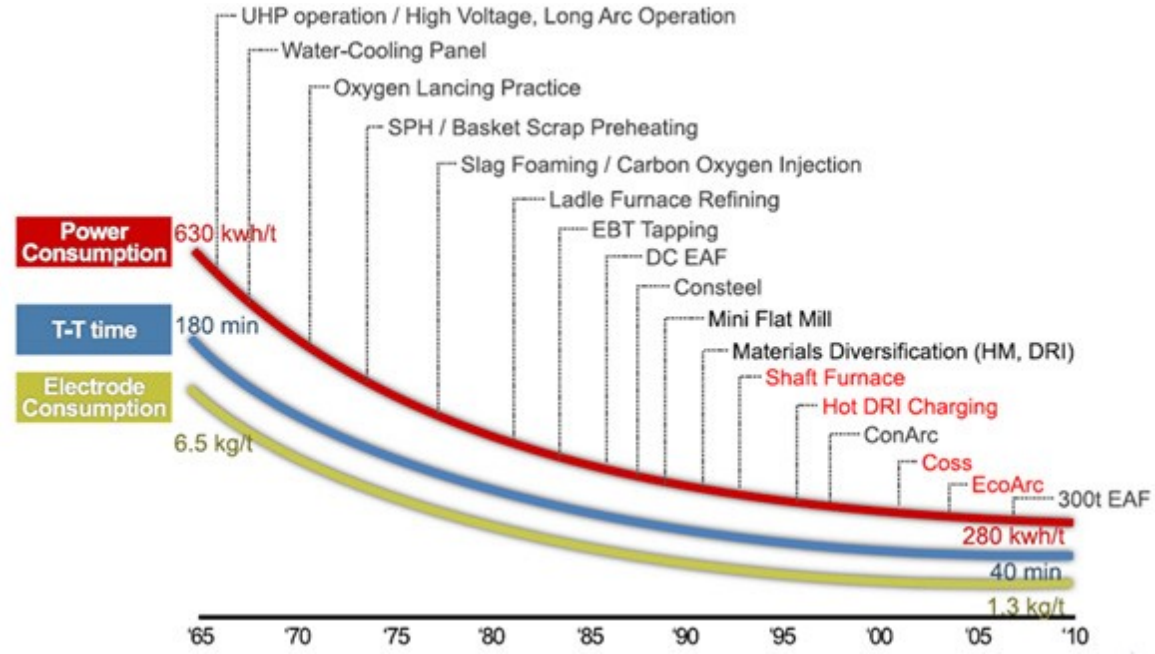


Figure 2. 1 Technology development in steel arc furnace by time (year) [adopted from 20].

2.2 TYPES OF ELECTRIC ARC FURNACE

Electric Arc Furnaces (EAF) are essential to the steelmaking industry and various metallurgical processes. These advanced furnaces utilize electrical energy to produce intense heat, enabling the efficient melting of scrap steel and other raw materials. While there are several types of EAF, the two most commonly used today are alternating current (AC) and direct current (DC) EAF [18].

2.2.1 AC Electric Arc Furnace

In an AC electric arc furnace, alternating current flows between a primary electrode and three additional electrodes through a metallic charge composed primarily of steel scrap. In this setup, the steel scrap functions as the anode, while the graphite electrodes serve as the cathodes. As the current arcs across the electrodes, intense heat is generated through arc radiation, effectively raising the temperature of the charge material to facilitate the smelting and refining process. This

method harnesses the power of electricity to transform metallic scrap into molten steel, ready for further processing [15,18].

2.2.2 DC Electric Arc Furnace

In a direct current (DC) electric arc furnace, the process begins with the flow of direct current through a graphite electrode, which serves as the cathode. This electrode directs electricity to the anode, a component that is integrated into the lower section of the furnace. As electricity travels between the cathode and the anode, it generates an electric arc, which produces intense heat through arc radiation. This heating mechanism effectively raises the temperature within the furnace, allowing for the melting and processing of materials [15,18]. The arrangement of both AC and DC electric arc furnaces is illustrated in Figure 2.2.

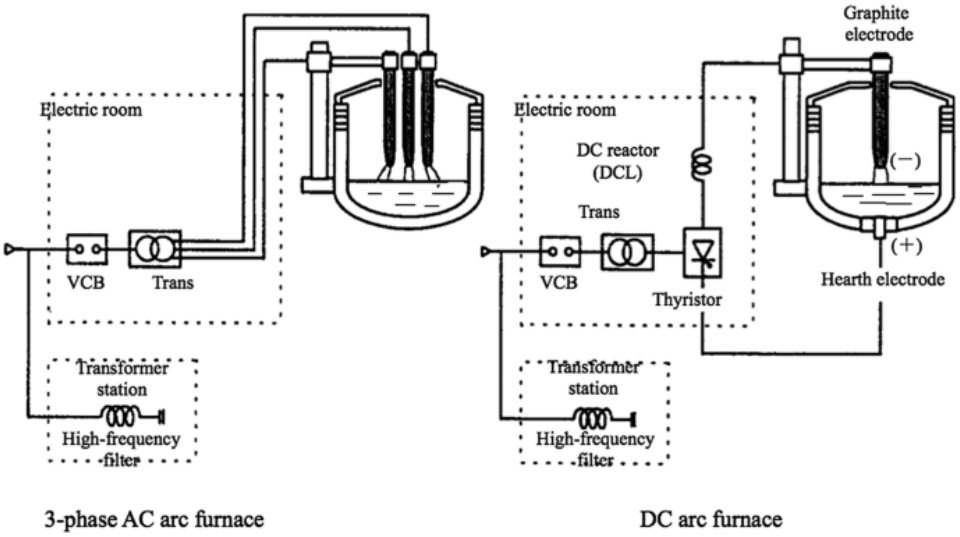


Figure 2. 2 AC and DC electric arc furnace layout [adopted from 21].

2.2.3 Advantages of DC Electric arc Furnace over AC furnace

The DC electric arc furnace is recognized for its superior efficiency compared to the traditional AC arc furnace. This distinction is highlighted by several key advantages that the DC arc furnace offers, making it a preferred choice in many applications. The advantages of DC EAF in comparison to AC furnaces are delineated below [22].

- One of the most notable benefits is the reduced electrode consumption in DC furnaces. In comparison to AC furnaces, which experience higher tip consumption and substantial side consumption of electrodes, DC furnaces boast a remarkable 40% to 50% reduction in total electrode usage. This efficiency not only translates to cost savings but also to a more sustainable operation.
- DC furnaces demonstrate lower power consumption, which further enhances their operational efficiency

- DC furnace allows for reduced refractory consumption in the sidewalls, leading to longer-lasting components and reduced maintenance requirements
- Melting process in a DC furnace is characterized by a more uniform temperature distribution, ensuring a consistent and efficient melting of materials.
- In DC furnace significant reduction in flicker, achieved through the application of a reactor that minimizes resonance, ultimately leading to a smoother operation and enhanced control over the melting process.
- Another advantage of the DC electric arc furnace is its lower noise levels.

The architecture of the DC furnace is such that graphite electrodes serve as the cathode, while the bottom electrode acts as the anode, located at the furnace's base. To establish a stable electrical path between these electrodes, a practice known as hot healing is implemented. When starting up a DC furnace from a cold state, an initial mixture of scrap metal and slag is utilized to create this electrical pathway. Furthermore, the DC arc furnace benefits from a more stable arc due to the presence of foamy slag, which enhances the efficiency of the melting process when compared to AC furnaces. Though DC furnaces typically incur higher installation and capital costs, their maintenance expenses tend to be lower, making them a wise investment over time [9,23].

2.2.4 Design of DC Electric Arc Furnace

DC electric arc furnaces come in various designs, each tailored for specific operational needs [2]. Below are three distinct configurations:

(a) Single Graphite Electrode with a Bottom Anode

In this design, the furnace utilizes one graphite electrode, serving as the cathode, positioned above the charge material and an anode, located at the bottom of the furnace. The electric arc is generated between these two electrodes, facilitating the intense heat required for melting and processing metal, as illustrated in Figure 2.3.

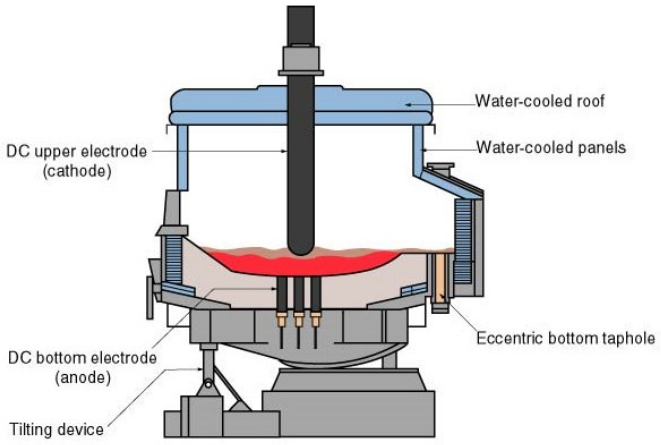


Figure 2. 3 Configuration of a DC EAF with single graphite electrode and bottom anode [2].

(b) Two graphite electrodes with four anodes

In this setup, the furnace incorporates two graphite electrodes functioning as cathodes in conjunction with four anodes situated at the bottom. This arrangement allows for enhanced arc stability and energy efficiency, as depicted in Figure 2.4.

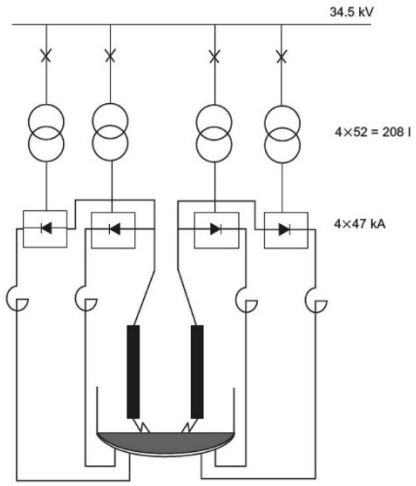


Figure 2. 4 Configuration of a DC EAF with two graphite electrode and four bottom anodes [2].

(c) Single Electrode with Four Bottom Anodes

This design features one graphite electrode acting as the cathode, paired with four anodes positioned at the furnace bottom. This configuration provides a robust arc formation, ensuring efficient energy transfer for melting operations. The electrical schematic for this setup is displayed in Figure 2.5.

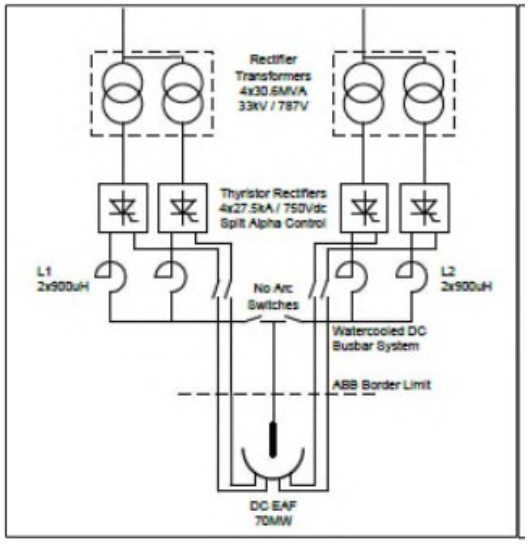


Figure 2. 5 Configuration of a DC EAF with single electrode and four bottom anodes [2].

Each of these designs presents unique advantages that cater to specific operational requirements in the smelting process. In a DC electric arc furnace, a return electrode (anode) is essential for completing the electrical circuit necessary for arc generation. This anode is situated at the base of the furnace shell. A hot heel is employed to bridge the electrical connection between the graphite electrode and the bottom anode.

Various types of bottom anodes are utilized in DC arc furnaces, including: (i) metal pin return electrodes with non-conductive refractories, (ii) billet electrodes, (iii) metal fin electrodes, and (iv) conductive bottom refractories. These configurations are illustrated in Figure 2.6[24].

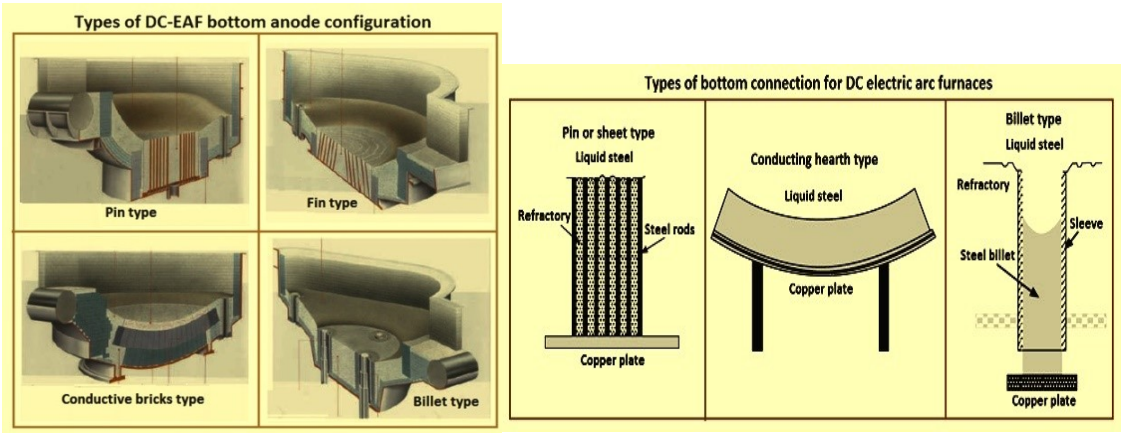


Figure 2. 6 Different design bottom anode connections [adopted from 24].

In Bangladesh, a well-known melting plant features a DC electric arc furnace that utilizes one graphite electrode as the cathode and four bottom anodes of the billet type. The billet-type anode DC EAF consists of one to four steel billets, with a diameter ranging from approximately 100 mm to 150 mm, and a maximum possible size of 250 mm, depending on the furnace's specifications as reported in ref. [24]. Each bottom anode is designed to handle a current capacity of 40 KA to 45 KA. The top surface of the billets makes contact with the molten bath, which is regulated through water cooling. A copper housing encases the billet body, allowing for the circulation of cooling water. An insulating casing separates the billet from the copper housing, and the copper base is also connected to the billet, facilitating the connection of the electrical line. Due to the effective cooling provided by the water circulation, the billet anodes do not fully melt. Additionally, a thermocouple monitors the temperatures of both the bottom anodes and the cooling water. A typical arrangement of a billet anode is shown in Figure 2.7.

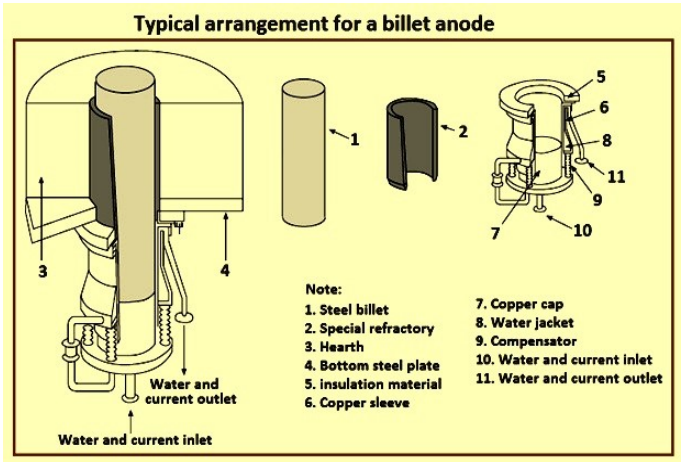


Figure 2. 7 Typical arrangement of billet anode at EAF bottom area [24].

2.3 COMPONENTS AND STRUCTURE OF DC ELECTRIC ARC FURNACE

The EAF typically features a cylindrical design, consisting of two main components: the upper shell and the bottom shell. The upper shell is cylindrical, while the bottom shell has a spherical dish shape. This design allows for the upper shell to be easily separated from the bottom shell, minimizing downtime required for replacements. Once the upper shell is removed, the bottom shell can also be swiftly taken out. The EAF includes various components that support its structure, facilitate movement, provide electrical power, and house auxiliary equipment either on the furnace itself or around its perimeter. The sidewalls and roof of the furnace are constructed from water-cooled panels [25]. A depiction of the furnace structure can be found in Figure 2.8.

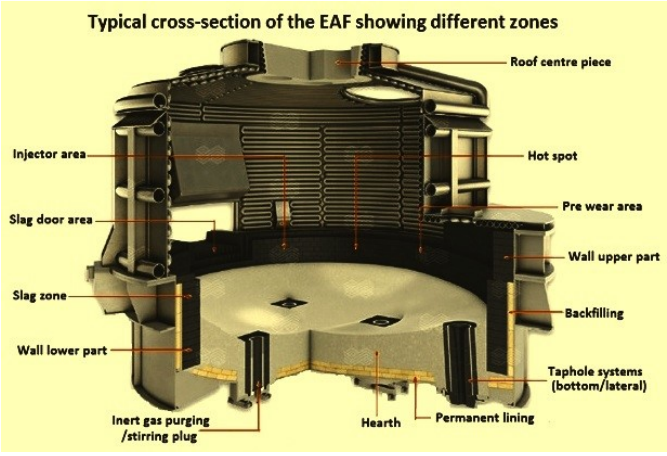


Figure 2. 8 EAF structure [adopted from 2].

2.3.1 Furnace Platform and Tilting System

2.3.1.1 Furnace Platform

The platform is built from a fabricated steel box frame that provides structural support for both the furnace shell and the electrode superstructure. This design allows for the quick and easy

replacement of the shell. Integrated into the platform are steel plate rockers that enable the furnace to tilt between the slagging and tapping positions. The rotation mechanism operates on rocker bases, which are also made from steel plate and feature spaced teeth along their length that interlock with corresponding depth teeth on the rocker beam. These rocker bases are firmly anchored to concrete foundations [26]. The furnace platform system supports several essential components, including the furnace shell, the roof structure, the roof lifting and rotation frame, and the electrode holder column and arm.

To protect the casting system from the heat emitted by molten steel, a refractory wall is installed, supported by specially designed mechanical anchoring devices. During the tapping of molten steel and the removal of slag, all components tilt together with the platform. The design of the tilting platform and rocker placement ensures that, in the event of a hydraulic failure, the furnace automatically tilts back to the slag side. The tilting cradles, secured beneath the platform, slide and rotate on metal bases anchored to the foundations during operation. The spacing of the cradles promotes excellent transversal stability, while their curvature radius ensures movement stability throughout the tilting process [26].

During the charging of the furnace and the melting of scrap, the furnace is maintained in a horizontal position by dual mechanical levers equipped with hydraulic cylinders that have a double-acting drive system. Figure 2.9 illustrates the furnace platform unit, which includes components such as pins for shell centering, the platform itself, rolling guides, foundation columns, a link for the rotational cylinder, a level for tilting locking, a cylinder for tilting locking, and the tilting cylinder.

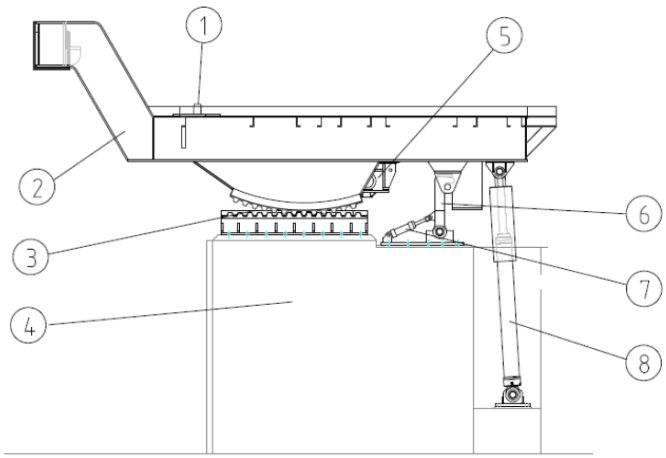


Figure 2. 9 Schematics of furnace Platform unit (where, 1. Pins for shell centering, 2. Platform, 3. Rolling guides, 4. Foundation columns, 5.Link for rotational cylinder, 6.Level for tilting locking, 7.Cylinder for tilting locking, 8. Tilting cylinder) [26].

2.3.1.2 Furnace Tilting System

The EAF is designed to tilt for both de-slagging and tapping operations. During de-slagging, the furnace is tilted backward, while it is tilted forward during tapping. For conventional spout tapping, the tilting angle reaches 45° to ensure complete tapping of the furnace. In the case of bottom tapping furnaces, the maximum tilting angle is between 15 to 20° [25]. The tilting of the furnace is managed by two large hydraulic cylinders, which are operated by a hydraulic central unit. These cylinders are securely anchored to the foundations and connected sideways to the platform leading to the slagging door. Additionally, they are protected from heat and falling debris (such as scrap metal) by a reinforced concrete wall that is lined with refractory bricks [26].

2.3.1.3 Platform Locking System

Two locking devices are implemented on the supporting platform to prevent the furnace from inadvertently tilting toward the slagging position during the scrap charging and melting processes. These devices feature two bush-pin mechanical stops, operated by double-acting hydraulic cylinders. The stop pin effectively absorbs impact stresses during the loading of scrap metal, preventing these stresses from being transferred to the tilting system [26].

2.3.2 Shell and Cooled Panels

The EAF features a cylindrical design, with a spherical bottom plate defining its base. The upper section consists of a cylindrical shell topped by a flat spherical roof. Most contemporary EAFs employ a split-shell configuration, allowing the upper shell to be rapidly detached from the lower section. This design significantly minimizes downtime associated with upper shell replacements. Following the removal of the top cover, the lower furnace can also be efficiently replaced [25]. Typically, the lower shell adopts an oval shape, constructed from robust steel plates that are fully welded and reinforced with bead structures. A refractory lining safeguards the bottom shell, with ramming applied to enhance durability. The thickness of the steel base ranges from 25 mm to 50 mm, while the refractory lining measures between 750 mm and 900 mm referenced in [26].

The upper shell integrates specifically shaped cooling panels that optimize cooling efficiency across all furnace zones. This modular design not only replaces traditional refractory linings but also enhances the shell's capacity. In addition, the cooling panels can be individually closed and removed, with dimensions allowing for installation at strategic distances from the slag, thereby minimizing refractory material requirements [26]. A typical depiction of the shell structure is illustrated in Figure 2.10, which includes the bottom shell, top shell, and slagging door.

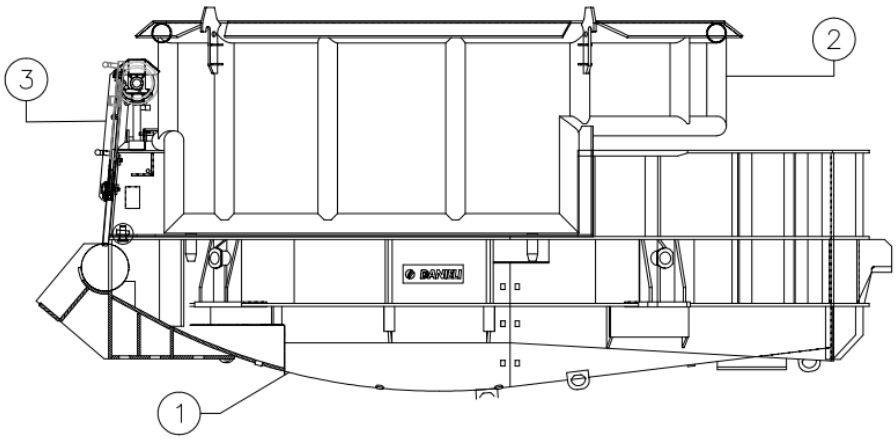


Figure 2. 10 A typical of shell structure schematic (1. Bottom shell, 2.Top shell, 3. Slagging door) [adopted from 26].

Modern electric EAFs feature water-cooled panels mounted on a water-cooled cage, allowing for easy panel replacement with minimal downtime. The lifespan of these panels is influenced by factors such as water quantity and quality, flow speed, input pressure, and the materials used in piping [25]. The panels effectively absorb heat energy while maintaining the integrity of the furnace shell, enduring high thermal and mechanical loads. Therefore, choosing the right piping materials is crucial to balance wall thickness for strength and heat transfer efficiency. Boiler tube grade steel is usually used for the panels, with copper tubing applied in high heat load scenarios [25]. The construction features of the upper shell and water-cooled panel are illustrated in Figure 2.11. The panels are affixed to the shell wall using brackets, forming a cohesive unit with the furnace, yet they can be easily detached from the outer structure.

Each panel is linked to the collector via a network of pipes outfitted with ON/OFF valves. Additionally, each drain section of the circuit is equipped with a measuring diaphragm and a thermistor, which enable precise regulation of the cooling flow rate and continuous temperature monitoring in each circuit. The configuration includes a total of 12 cooled panels located at the top/upper shell and one panel positioned at the slagging door, as seen at the AKS Melting Plant.



Figure 2. 11 Upper shell and water cooled panel [adopted from 2].

2.3.2.1 Slagging Door

The slagging door is made up of a cooled panel designed according to the specifications mentioned earlier. It operates using a hydraulic cylinder that enables the door to open and close (lift and lower) through a chain-and-sheave mechanism. For the safety of personnel, the door can remain closed while scrap is being charged. Figure 2.12 show the schematics of the slagging door.

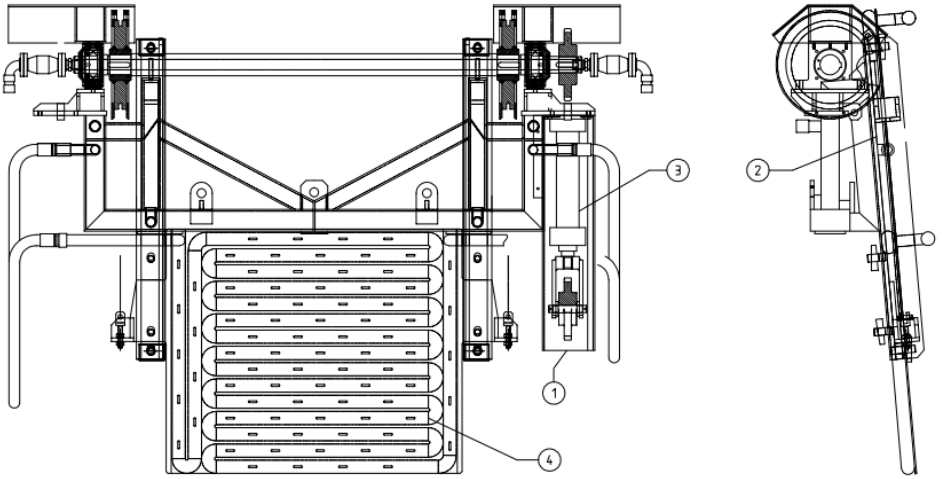


Figure 2. 12 Schematics of slagging door (1.cylinder protection, 2.chain, 3. Cylinder, 4.door panel) [adopted 26].

2.3.3 Cooled Roof

A typical Electric Arc Furnace (EAF) roof consists of a tubular support structure with steel panels suspended beneath it. Its primary purpose is to cover the furnace shell. A central opening is designed to accommodate the refractory roof, which includes a hole for the electrode. Additionally, the delta refractory section has an opening that allows for the movement of the electrode while ensuring a safety clearance between the electrode and the water-cooled panel during arcing.

Furthermore, a small independent roof features a fifth opening for charging alloy and lime, making it easy to remove and replace if necessary. Opposite the roof lifting system, there is an oval opening for connecting the fume suction elbow, which is also referred to as the fourth hole for the fume evacuation system [25,26]. A typical EAF roof is illustrated in Figure 2.13.

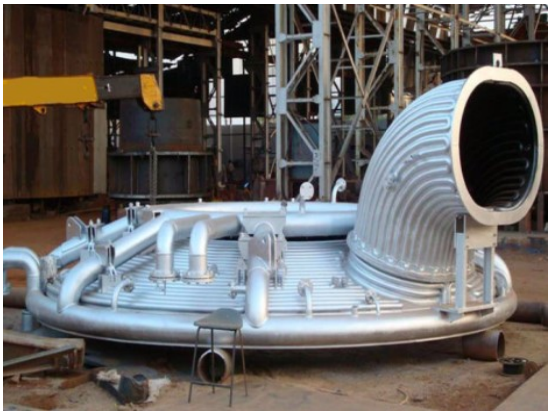


Figure 2. 13 A typical EAF roof (AKS, a well-known steel melting plant in Chittagong) [27].

This system effectively cools the roof without requiring a substantial refractory coating. The entire structure is equipped with appropriate brackets designed to support grouting and subsequently, slag. The panels are secured to the roof using tie rods, irrespective of the furnace's position during the melting process. Each panel is connected to the discharger and discharge collector through pipes fitted with ON/OFF valves. Moreover, thermometers are installed in the discharge circuit to monitor its condition, and measuring membranes are incorporated to ensure proper distribution of the flow rate. The AKS configuration is as follows:

- Total of three cooled panels on the roof
- One cooled panel at the elbow side
- One cooled panel at the fifth hole.

2.3.4 Eccentric Bottom tapping (EBT)

An eccentric bottom tapping (EBT) mechanism is integrated into the bottom section of the furnace. This setup facilitates slag-free tapping, minimizes steel temperature losses during the tapping process, and supports hot heel practices. The EBT design enables a clear and focused casting, which results in a significant reduction in overall tapping time. This efficiency helps maintain low levels of undesirable elements, such as O_2, N_2, and H_2, while also reducing temperature losses [26]. In the bottom tapping system, the ladle is precisely positioned beneath the furnace either via a ladle car or a ladle turret arm [25]. Molten steel is directly collected in the ladle, allowing for subsequent treatments within the reheating furnace without the need for slag removal. This method

streamlines the process and enhances the efficiency of steel handling and processing [26]. The configuration and functionality of the EBT are illustrated in Figure 2.14.

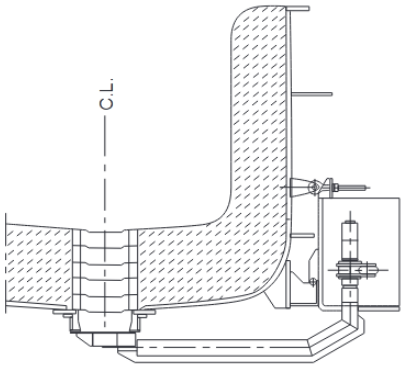


Figure 2. 14 Eccentric bottom tapping configuration [adopted from 25].

The tapping hole is packed with fire sand, and the closing mechanism functions on a "drawer closure" principle, actuated by a hydraulic system. The EBT opening and closing mechanism is pivotally mounted to the outer shell, facilitating precise adjustment of the spacing between the fixed and movable components of the drawer closure system. Furthermore, this design allows for straightforward disassembly, enabling efficient maintenance operations [26].

2.3.5 Roof Lifting and Rotating Unit

The roof lifting and rotating unit is comprised of a base structure fitted with a platform. It operates through a double-acting cylinder and a large thrust bearing device, enabling both lifting and rotation. The roof-supporting column bridge and the electrode-supporting column arms are moved via this device. Typically, the roof and electrode holder can rotate together or independently. The movement of the electrodes allows them to rotate while the roof remains in contact with the furnace shell, facilitating the removal and replacement of the delta section without needing to detach the roof. The swiveling angle is managed by a linear transducer fixed onto the cylinder. The roof is securely attached to the lifting assembly using a water-cooled lifting fork, which is bolted to the roof and constructed from welded steel plates. The lifting device comprises a lifting piston guided by two anti-friction bushings and powered by a double-acting hydraulic cylinder [25,26]. The schematics of cylindrical position is presented in Figure 2.15.

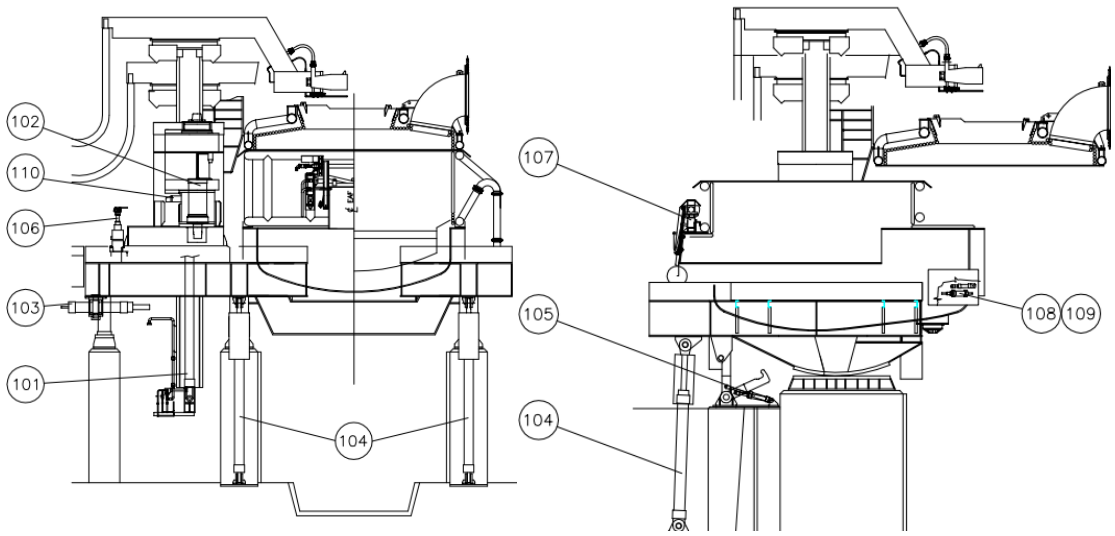


Figure 2. 15 Cylindrical position: (101) electrode regulation cylinder, (102) Roof lifting cylinder (103) Roof rotation cylinder, (104) Tilting cylinder, (105) Platform locking cylinder, (106) locking cylinder (107) Slagging door cylinder (108) EBT opening cylinder (109) EBT locking cylinder [adopted from 26].

2.3.6 Electrode Lifting Unit

The electrode lifting column features a robust steel structure with triangular guide bars welded to it. These guide bars move on four pairs of guide wheels mounted on housing brackets, allowing for accurate vertical positioning of the electrode. Each column is powered by a hydraulic cylinder, anchored at the base and connected to the column. Mechanical stops enable secure locking during manual operation. For automatic regulation during arcing, movement speeds range from 30 to 35 cm per second, while manual adjustments are at 15 to 20 cm per second. As illustrated in Figure 2.16, the support column includes a hole for clearance from the tie rod, facilitating precise electrode positioning over the roof's refractory lining [26].

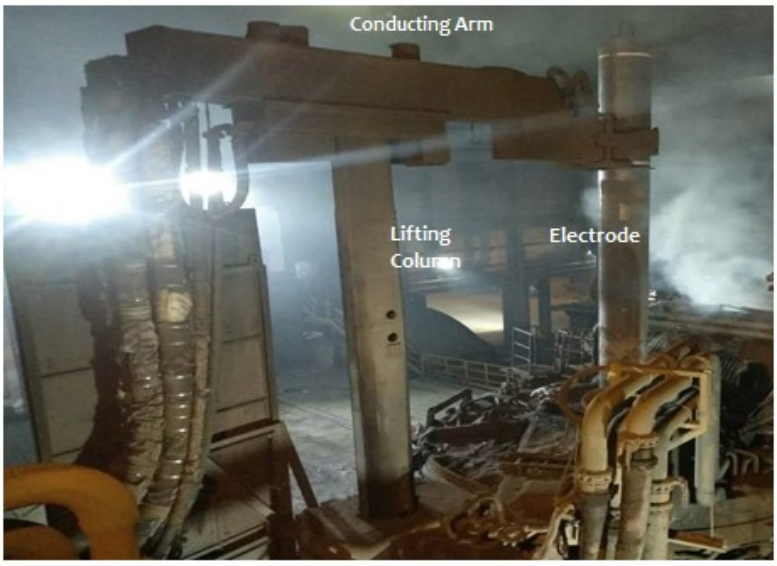


Figure 2. 16 Electrode lifting column (at AKS Melting Ltd, Chittagong) [27].

2.3.7 Conductive Electrode-Holder Arms

In conventional Electric Arc Furnace (EAF) designs, electrical current is delivered to the electrodes via bus tubes, but new installations often use current-conducting arms made from copper-plated steel or aluminum [25]. These arms channel secondary current directly. Electrode holders and contact pads connect the bus tubes or conducting arms to the graphite electrodes. Forged copper and non-magnetic steel clamps at the furnace front secure the electrodes with a pusher/tensioner assembly that maintains electrode stability, even during pressure drops in the hydraulic circuit [28]. A hydraulic cylinder facilitates electrode release by overcoming the disc spring's resistance. The electrode holder allows positional adjustments, essential for regulating the electrode circle diameter and placement within the roof housing. The clamping mechanism ensures a secure connection, and with current-carrying arms, insulation is unnecessary as the arm is part of the electrical circuit [26]. The schematic of current conducting arms at AKS is shown in Figure 2.17.

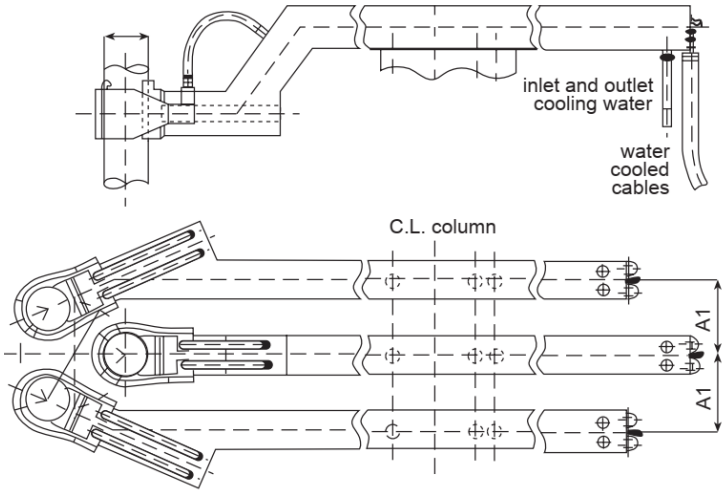


Figure 2. 17 Current Conducting arms [adopted from 25].

2.3.8 EAF Electrical System

2.3.8.1 Step down Transformer

A step-down transformer is utilized in the EAF electrical system to supply power from the high-voltage line of the national grid to the EAF transformer. This transformer reduces the voltage from 233 kV (high voltage) to 33 kV (medium voltage). It serves as the primary source transformer. The main circuit breaker is employed to disconnect the grid current from the step-down transformer, while a vacuum circuit breaker (VCB) is used to isolate the power supplied to the EAF transformer from the step-down transformer [28].

2.3.8.2 EAF Transformer

The EAF transformer is essential for supplying electrical power to the furnace. It receives high voltage and low current from a step-down transformer and converts this input into high current and low voltage power suitable for the EAF. The transformer is located in close proximity to the EAF. Additionally, it is equipped with a tap changer that allows for adjustments across different stages of current and voltage. Over the past 50 years, the input power for EAFs has significantly increased alongside advancements in EAF technology. In the 1960s, the typical power rating for EAFs ranged from 250 to 300 KVA per ton. Today, with the latest technological developments, this rating has risen to between 900 and 1000 KVA per ton for ultra-high power EAFs [28]

2.3.8.3 DC Power

The Thyristor Rectifier and DC reactor work in conjunction with the EAF transformer in a DC electric arc furnace. The secondary AC power generated by the EAF transformer is converted into DC power through the thyristor rectifier. This DC power is then supplied to the graphite electrode, which serves as the cathode, while each anode is managed by the rectifier. This electrical power supply enables operation at an optimal secondary voltage and allows for appropriate control of the firing angle in the rectifier units. This setup reduces harmonics generation and ensures stable arcing conditions [26].

2.3.8.4 Cathode Secondary Circuit

In the EAF, the cathode secondary circuit connects the transformer to flexible current cables for the electrode holder arms. It primarily consists of cooled copper pipes supported by a welded structure with lead supports. This circuit has two sections: one connects the rectifier output to the smoothing reactor, and the other links the reactor to the water-cooled cables. The facility also has a closure for the furnace-side opening near the transformer [26].

2.3.8.5 Anode Secondary Circuit

In an EAF, there is an anode secondary circuit positioned beneath the furnace. This circuit establishes the electrical connection between the converters and the water-cooled cables. It links the rectifier to the water-cooled cables for the bottom anodes and is constructed from a water-cooled pipe. The connections to the rectifier utilize flexible copper components to accommodate the vibrations generated by electromechanical forces [26].

2.3.8.6 Anode Electrical Connection

A water-cooled copper pipe connects the water-cooled cables to the bottom anodes through flexible copper connections and clamping devices that operate using springs. One end of the water-cooled cables is securely bolted to a machined copper surface on the copper pipes, while the other

end connects to the electrode clamps. The clamping devices consist of a copper pad for efficient current conduction and a stainless steel band [26].

2.3.9 Electrode Spray Cooling

To enhance the efficiency of electrode cooling and reduce consumption in modern furnaces, a spray ring is strategically placed at the base of the electrode holder to facilitate effective spray cooling. As water is atomized and sprayed, it evaporates along the electrode's surface before it can reach the furnace roof, thus providing optimal thermal management. In contrast, traditional furnaces often incorporate additional strategies to mitigate electrode heating, such as utilizing water-cooled graphite segments adjacent to the electrode holder and applying specialized thermal coatings to further improve their resistance to high temperatures [25].

2.3.10 Water-Cooled Bottom Anodes

Water-cooled anodes are situated at the bottom of the furnace and are responsible for conducting the electrical current from this location. There are four anodes embedded in the furnace's lower section. The metallic anode consists of several components [26]:

- An upper section made of low-carbon steel, which is wire-welded to an underlying intermediate section
- The intermediate section is also made from low-carbon steel and is welded to a lower section made of copper that is internally water-cooled
- The lower copper section is welded to a water-cooled copper tube, which is connected to the clamping device
- An inner component, the stainless steel conveyor, ensures the supply of cooling demineralized water.

2.3.10.1 Anode cooling water system

The anode cooling system operates as an independent circuit, distinct from the other cooling water circuits associated with the furnace. This specialized cooling circuit utilizes demineralized water, ensuring optimal performance. The properties of the water, including conductivity and pH levels, along with critical operational parameters such as temperature, pressure, and flow rate, are subjected to continuous monitoring by the furnace control system. This vigilant oversight is essential for maintaining the integrity and efficiency of the cooling process [26].

2.3.11 Cooled Flexible Cables

The cooled current cable is electrically connected to the secondary circuit, which consists of a cooled copper tube, via an electrode holder that requires four cables for each phase. Typically, this cable has a dual-hose design—one internal and one external—around copper conductors that are positioned between them. These conductors are insulated with a rubber sleeve, which is further protected by a screen covering the other conductors, ensuring optimal current distribution. The ribbed rubber sleeve enhances cooling efficiency [26].

Each conductor is made of highly conductive copper strands, chosen for their diameter, which allows for maximum elasticity and flexibility. At the cable's end on the electrode arm, a specialized swivel is included to minimize cable twisting, ultimately extending the cable's lifespan. Cooling occurs through water circulating within the inner rubber tube, which is safeguarded by an insulating sheath that protects against heat and abrasion. Additionally, the triangular arrangement of the cables ensures satisfactory reactance symmetry throughout the entire secondary system. The connection point is located on the wall of the transformer room [26].

2.3.12 Supply of Alternative Energy

Alternative energy is employed in Electric Arc Furnaces (EAF) to enhance the melting process by injecting solids and gases via oxy-fuel burners and an oxygen-carbon lancing system. This approach facilitates additional heat generation through chemical reactions involving the products inside the furnace, effectively reducing overall electrical energy consumption. The efficiency of the burners peaks when the scrap is at a lower temperature. Constructed from high alloy or stainless steel, these burners are equipped with water cooling to maintain optimal operating conditions. Typically, three or four burners are strategically positioned along the sidewall, optimizing their effectiveness in penetrating cold spots within the charge [25,29,30]. The EAF injection system is illustrated in the accompanying Figure 2.18.

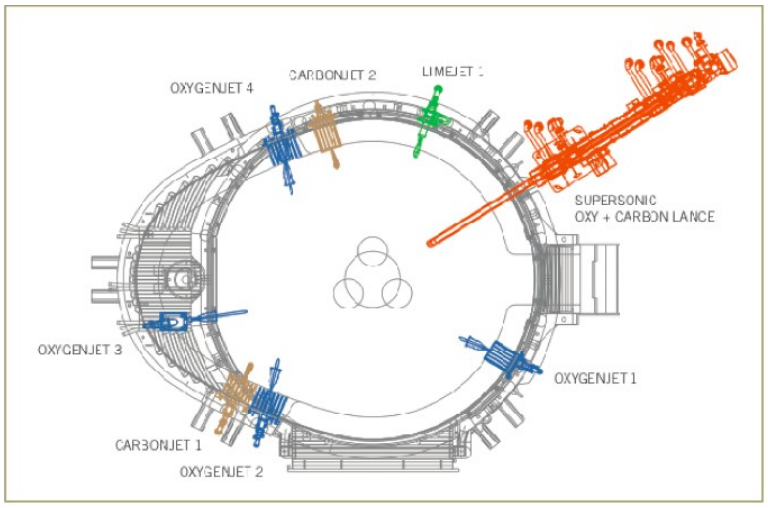


Figure 2. 18 A typical EAF injection system [adopted from 25].

In an injection system, multiple modules are integrated to supply alternative energy in the Electric Arc Furnace (EAF). These modules can function both as burners and as injectors for oxygen and carbon, depending on the various phases of EAF operation. To facilitate this, two tools have been developed: the oxygen-jet and the carbon-jet [31].

- **Oxygen-Jet**

The injectors feature a specialized head, comprising a central nozzle for supersonic oxygen flow and annular nozzles for both oxygen and fuel flows. This configuration initially acts as a burner and subsequently as a supersonic injector. During power-off stages, such as tapping, charging, and turnaround, air is routed through the nozzle to prevent clogging. It is important to note that during the lancing phase, the air needed to clean the pipeline is supplied through dedicated air nozzles [31].

- **Carbon-Jet**

The carbon-jet system is employed to regulate the carbon content in molten steel, which is crucial for achieving the desired material properties. This system is especially significant in the production of specific steel grades that require precise control of carbon levels, such as high-carbon steels and alloys [31].

2.3.12.1 Carbon pipe

A pipe situated next to the oxygen jet and positioned within the same copper plate serves as the nozzle for coal flow. Air circulates through this pipe to prevent clogging. All stages of injection are controlled automatically. To succinctly describe melting operations utilizing these modules, it is essential to recognize that the transitions between work stages are managed by furnace automation. Thus far, the modules can be essentially characterized as oxygen and carbon injectors. The primary function of the oxygen jet is to supply oxygen and carbon to the process, thereby

enhancing the overall energy supply, while also significantly improving the performance of the foam slag.

This objective is critically important due to its impact on arc efficiency and stability, consumption of electrodes and refractories, heat dissipation in water-cooled panels, and noise reduction. By precisely adjusting the carbon and oxygen flow ratios of the modular injector, one can alter the physical and chemical conditions within the slag, shifting the overall environment from balanced to either oxidizing or reducing.

The advantages of installing modules on a furnace should be evaluated from a broader perspective, considering their influence on overall production management. The module supplies the majority of the oxygen required for the decarburization of the charge and for the combustion of elements in the scrap, providing necessary energy throughout the melting and superheating phases. The use of oxygen is crucial for enhancing the decarburization rate and facilitating efficient post-combustion of CO. A typical installation of the oxygen jet and carbon pipe is illustrated in Figure 2.19.

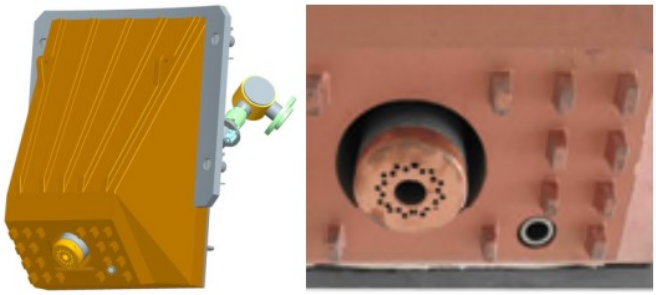


Figure 2. 19 A typical model of oxygen-jet and carbon pipe installation [adopted from 31].

2.3.12.2 Water Cooled Supersonic Oxy-Carbon Lance

The lance is positioned at a specific angle in front of the slag door to facilitate effective oxygen penetration into the bath and carbon incorporation into the slag. The lances can be adjusted to approach the bath as needed. Figure 2.20 illustrates the PARPI slag door supersonic lance (Lance). The primary function of the supersonic oxygen lance is to inject oxygen into the liquid steel bath while also introducing carbon, achieving several key outcomes [31]:

- Decarburization of the steel bath;
- Rapid formation of foamy slag (by minimizing the distance between the nozzle and the bath level);
- Post-combustion of carbon monoxide, which generates thermal energy beneficial for the melting process;
- Enhanced stirring of the liquid steel bath due to a high oxygen injection rate.



Figure 2. 20 A typical PARPI slag door supersonic lance [Adopted from 31].

2.3.13 Bottom Stirring

Inert gas injection is the most widely utilized method in Electric Arc Furnaces (EAF) to promote uniformity within the liquid bath. This bottom stirring technique enhances the management of temperature and chemical composition of the molten steel while reducing the consumption of electrodes and refractories. Argon and nitrogen are introduced through porous plugs situated at the bottom of the ladle to facilitate metal stirring and enhance the mixing of metal and slag, which accelerates thermal and chemical homogenization as well as reactions [32].

Bottom stirring can be performed using either direct or indirect contact plugs. In the case of indirect contact, the plug does not come into direct contact with the molten metal. The gas distribution is more extensive with an indirect contact plug compared to a direct contact plug, as illustrated in Figure 2.21.

When employing two porous plugs, the control of gas flow rates and consumption for the bottom stirring is managed through two independent lines, which can be used simultaneously. Depending on the specific phase of the metallurgical process, either one or both lines can be activated to meet the necessary gas flow rates. Additionally, it is recommended that the cleaning of the porous plates be conducted every two to three castings by injecting inert gas or compressed air.

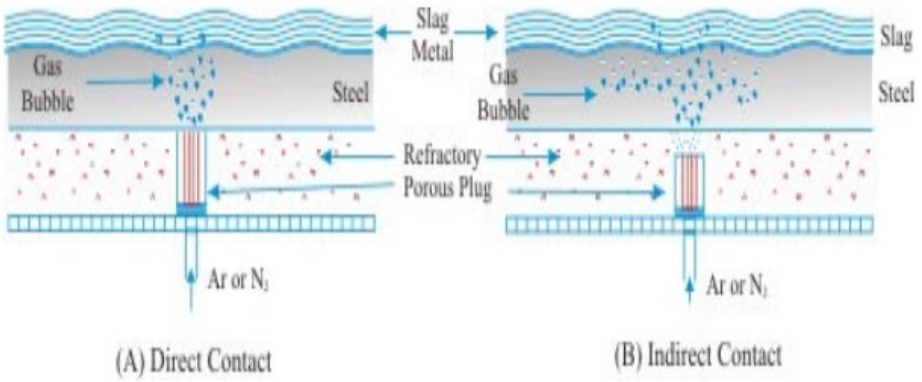


Figure 2. 21 Bottom stirring system (A) Direct contact & (B) Indirect contact at EAF [Adopted from 32].

2.3.14 Refractories for Electric Furnace Steelmaking

Refractories used in electric arc furnaces (EAF) are carefully selected based on furnace design and operational procedures to withstand high temperatures and thermal shock. The wear rate of refractories in EAFs is significantly higher compared to other types of steelmaking equipment. Therefore, it is essential to choose the appropriate refractory lining to achieve better economic benefits. Several key factors should be considered when selecting the right refractory lining for an EAF [33,34]:

- Operation temperatures ranging from 1600°C to 1700°C, which are very high.
- Chemical interactions between slag materials and the refractory lining.
- Irregular charging of scrap, which leads to significant thermal shock.
- The direct impact of the electric arc.
- The use of oxy-fuel burners and oxygen lancing, which affects the design and performance of the refractories and accelerates wear.

In electric arc furnace steelmaking, different zones require specific types of refractories. Figure 2.22 illustrates the various zones within bottom-tapping electric furnaces.

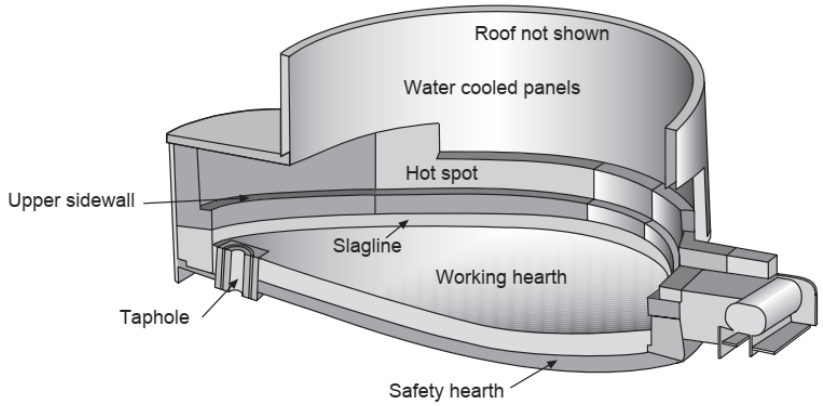


Figure 2. 22 A schematics of different zone of refractories of bottom tapping EAF [Adopted from 33].

2.3.14.1 Refractory Lining of EAF Roof

The furnace roof is subjected to high temperatures, mechanical shocks, and chemical exposure during the charging and melting processes. It is vulnerable to corrosive slag and FeO vapor. Traditionally, high alumina bricks have been used for the refractory lining of the roof. However, with the introduction of Ultra High Power (UHP) furnaces, Magnesite and Magnesia-C (MgO-C) are now being utilized for roof linings. In the delta section, precast pre-fired blocks are currently employed. Modern furnaces feature a roof entirely surrounded by cooling panels, over which a thin refractory lining is applied using gunned castable refractory [34]. The properties of various refractory linings in the roof area are presented in Table 2.1.

Table 2. 1 Properties of different refractories used in EAF roof [34]

Type of refractory	Unit	High alumina bricks		Basic bricks	High alumina precast	
Area of application		Outer ring	Roof top	Entire roof	Delta section	
Chemical properties						
SiO_2	%	10.5 - 15.5	5.5 - 7.5	3.5 - 4.5	6.5 - 9.5	4.5 - 5.5
Al_2O_3	%	76 - 80	85 - 90	Nil	70 - 80	80 - 85
Fe_2O_3	%	1.5 - 2.5	1.2 - 1.5	1.5 - 2.5	1.2 - 1.8	1.2 - 1.8
MgO	%	Nil	Nil	62 - 65	2.5 - 3.5	Nil
Cr_2O_3	%	Nil	8.5 - 10.5	11.5 - 12.5	Nil	10
Physical properties						
App. porosity	%	18 - 19	13 - 16	12.5 - 14.5	4.5 - 6.5	4.5 - 6.4
Bulk density	g/cc	2.75	3.05	3.05	2.65	2.72
Cold crushing strength	Kg/cm^2	440 - 520	700 - 900	850 - 960	> 1200	> 1200
Thermal expansion at 1500^0C	%	1.65	1.27	1.9	1.2	1.2

2.3.14.2 Side Wall

The side wall refers to the cylindrical portion of the zone that extends vertically from the bottom of the metal zone to the top of the slag zone, including the free board. Currently, magnesite, dolomite, magnesia-carbon (MgO-C), and chrome-magnesite are utilized in sidewall refractories. The slag line and hot spot area are critical zones within the electric arc furnace (EAF). At present, MgO-C bricks are employed as refractories in these regions. The properties of various refractories used in the sidewall are presented in Table 2.2.

Table 2. 2 Properties of sidewall refractory in EAF [34]

Properties	Unit	MgO-C unburnt bricks			MgO - Cr2O3 bricks (Direct bonded)	
		Type A	Type B	Type C	Type D	Type E
Application areas		Tapping hole	Hotspot	Slag zone	Slag line	Slag line tap. hole
Chemical properties						
SiO_2	%	0.5 - 1.5	0.5 - 1.6	1.5 - 2.5	1.5	1.5 - 2.5
MgO	%	82 - 84	84 - 86	74 - 78	60 - 65	65 - 70
Cr_2O_3	%	NA	NA	NA	20 - 22	16 - 20
Fixed C	%	14 - 16	10.5 - 12.5	> 20	NA	NA
Physical properties						
App. porosity	%	2.5	3.6	3.9	13 - 16	13 -16
bulk density	g/cc	2.98	3.04	2.83	3.25	3.27
Cold crushing strength	kg/cm^2	450 - 500	550 - 650	400 - 450	860 - 900	940 - 980
Mod. of rupture at 1400^0C	kg/cm^3	80 -100	140 -150	60 -80	110 -120	125 -135

2.3.14.3 Bottom of Hearth

In an EAF, the bottom of the hearth is divided into two sections: the sub-hearth and the working hearth. Magnesite bricks are utilized in the sub-hearth, with high-temperature fired magnesite and high alumina bricks positioned at the base of the sub-hearth nearest the shell to provide protection against overheating.

The working hearth features a monolithic refractory lining made from magnesite-based ramming mass or MgO-C bricks. In this monolithic lining, dry MgO ramming masses are used to enhance strength during the heating process. During the initial construction, large profile carbonaceous bricks are implemented in the hearth, while ramming masses are employed for intermediate repairs [34].

Furthermore, in the EBT electric arc furnace, specific components such as tap hole sleeves and an end block are essential for the design of the tap hole. The tap hole sleeves are crafted from high-purity magnesia, incorporating 10% carbon content. The bottom assembly and tap hole configuration are illustrated in Figure 2.23.

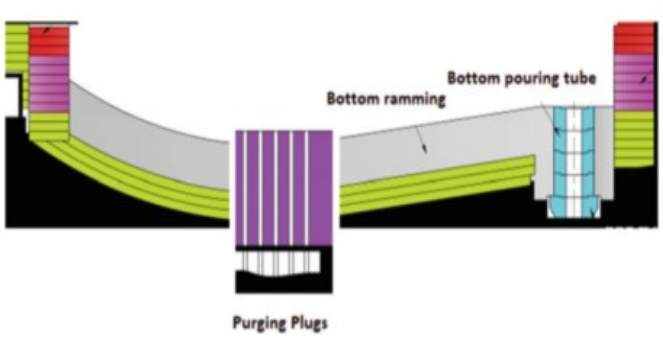


Figure 2. 23 Bottom assembly of EAF [Adopted from 34].

It is noted that the maintenance of the refractory lining is performed using the gunning process. A gunning material with a higher MgO content is employed to repair the hot spot and tap hole areas in high-power and high-capacity furnaces. Currently, the damaged refractory wear profile is analyzed using a laser scanner, and its thickness is restored through gunning. By applying the gunning mix, all voids and cracks in the patched brickwork can be effectively filled [34]. The properties of gunning and patching refractories are detailed in Table 2.3.

Table 2. 3 The properties of gunning & patching refractories [34].

Item		Gunning Material(I)	Gunning Material(II)	Thermal self-flow patching material
MgO min%		85	80	75
CaO max%		6	4	
C min%				10
Bulk density min g/cc	110^0C x24 h	2.3	2.3	2.2
	1500^0C x3 h	2.5	2.5	1000^0C x3 h

Cold crushing strength min MPa	110^{0}C x24 h	8	8	12
	1500^{0}C x3 h	25	25	1000^{0}C x3 h
Modulus of rupture at RT min MPa	110^{0}C x24 h	2.5	2.5	2
	1500^{0}C x3 h	4	4	(1400^{0}C)

2.3.14.4 Bottom Anode Design

In DC electric arc furnaces, various types of anodes are utilized in the bottom area, including:

- Metal pin electrodes combined with non-conductive refractories
- Thick steel billets serving as electrodes
- Metal fins functioning as electrodes
- Conductive bottom refractory materials.

The bottom hearth area is lined with a six-inch thick magnesia-carbon ramming mix that contains a carbon content of 5-10% by weight. Above this layer, three tiers of magnesia-carbon bricks are installed as an intermediate layer, with a carbon content of 10-14% by weight. The remainder of the hearth is lined with magnesia-based ramming masses. Additionally, the billet anode is embedded within the ramming mass refractories [34].

2.3.14.5 Refractory Wear Mechanism

The EAF is subject to various forms of refractory wear during its operation, necessitating careful consideration in the design process to effectively manage these wear mechanisms. The different types of refractory wear identified include [33]:

Corrosion: This form of wear occurs as a result of chemical reactions between metal oxides present in the slag and the materials comprising the refractory lining.

Oxidation: Oxidative wear results from chemical interactions between oxygen or FeO present in the slag and the carbon components within the refractory lining, leading to degradation of the material.

Erosion: The high temperatures of molten steel or slag can physically abrade the surface of the refractory lining, leading to material loss through erosion.

Melting: The unshielded electric arc generates temperatures that exceed the melting points of all commercially available refractories, contributing to material failure.

Hydration: Refractories, particularly those containing MgO and lime, are susceptible to damage from hydration when exposed to water or steam, which may infiltrate from the cooling systems.

Spalling: Rapid temperature fluctuations can induce stresses within the refractory lining material. When these stresses surpass the inherent strength of the refractory, it can result in cracking and subsequent compromise of the refractory integrity.

In light of these wear mechanisms, it is vital to implement design strategies that mitigate their effects in order to enhance the longevity and performance of the refractory lining in electric arc furnace operations.

2.3.15 Graphite Electrode

The graphite electrode plays a vital role in facilitating the transfer of electrical power from the main input source during the melting process. By establishing a conductive pathway with the bottom anode, it generates an electric arc that effectively melts the charge materials inside the furnace. It is essential for this electrode to maintain a consistent electric power supply within the furnace environment, particularly under the extreme temperatures generated during operation. Over the past two decades, advancements in electric arc furnace (EAF) technology have led to significant improvements in the design and functionality of graphite electrodes. These enhancements have resulted in electrodes that are better equipped to deliver high levels of power to the furnace, ultimately boosting operational efficiency and effectiveness in metallurgical processes [25].

Nowadays, ultra-high power (UHP) graphite electrodes are essential components in various industrial applications, particularly in electric arc furnaces. These electrodes should exhibit exceptional electrical conductivity, ensuring efficient energy transfer during operation. Additionally, they must possess high mechanical strength to withstand the intense conditions encountered in their applications. An important characteristic of UHP graphite electrodes is their low ash content, which is crucial for maintaining the purity of the final product. In the following section, Table 2.4 provides a detailed overview of the properties of these electrodes.

Table 2. 4 Electrode properties [25,26]

Properties		Unit	UHP	
			300 – 600mm	650 – 800mm
Electric resistivity	Electrode	μΩm	4.8 - 5.8	4.6 - 5.8
	Nipple		3.8 - 4.5	3.8 - 4.5
Flexural strength	Electrode	Mpa	10.0 - 14.0	10.0 - 14.0
	Nipple		20.0 - 26.0	20.0 - 26.0
Young's modulus	Electrode	Gpa	9.0 - 13.0	10.0 - 14.0
	Nipple		15.0 - 18.0	15.0 - 18.0
Bulk density	Electrode	≥ g/cm^3	1.68 - 1.74	1.70 - 1.74
	Nipple		1.77 - 1.82	1.78 - 1.84
CTE (100 - 600^{0}C)	Electrode	x 10^{-}6/^{0}C	1.1 - 1.4	1.1 - 1.4
	Nipple		0.9 - 1.2	0.9 - 1.2
Ash			0.3	0.3

2.3.15.1 Electrode Wear mechanism

Several factors influence electrode consumption. Essentially, electrode wear occurs through both continuous and discontinuous processes. Approximately 90% of the total consumption is

attributed to continuous wear, which results from tip consumption (sublimation) and sidewall oxidation. In contrast, discontinuous consumption includes processes such as electrode breakage, butt losses, and electrode tip spalling [25].

2.3.15.3 Development of Special DC Electrode Grades

Graphite electrode manufacturers are advancing the properties of direct current (DC) electrodes in response to the evolving requirements of electric arc furnace (EAF) technology. Recent innovations include the introduction of a new electrode nipple system specifically designed for DC operations. Key modifications include:

Enhanced nipple strength: Incorporation of high-strength nipples with a lower thermal expansion coefficient has been implemented to minimize joint resistance, thereby reducing thermal stress and the risk of rupture.

Reduced electrode resistivity: Efforts to decrease specific electrode resistivity are in place to alleviate thermal stresses, particularly those resulting from heating at the electrode center.

Improved thermal conductivity: Enhancements in transverse thermal conductivity facilitate efficient heat transfer from the electrode center to the surface, promoting more uniform temperature distribution.

Lowered thermal expansion coefficient: A reduction in the thermal expansion coefficient of the electrodes is aimed at mitigating thermal stress arising from expansion.

Uniformity and coarseness modifications: The development of uniformity and controlled coarseness in electrode structure is crucial for enhancing resistance to crack initiation and propagation.

These modifications collectively contribute to the performance and longevity of DC electrodes in EAF applications.

2.3.16 Electric Arc Furnace Fume suction Plant

The fume suction and elimination from the electric arc furnace are managed by a dedicated independent system. Fumes are collected via an exhaust elbow made of water-cooled piping, which is appropriately installed on the roof. A slight negative pressure within the furnace facilitates the collection and discharge of the fumes and dust generated during the process. This low pressure is maintained to prevent excessive airflow into the plant, which could disrupt the

metallurgical process. The elbow features a water-cooled flange constructed from steel pipes, serving as the interface with the mobile fume duct [26].

The fume suction system, also known as the off-gas system for electric arc furnaces, consists of containment, cooling, and collection components to ensure effective fume control within the standard regulatory framework. The containment elements comprise fourth-hole ducting, elbows, and fans. Cooling is achieved through water-cooled ducting, dilution air cooling, and natural and forced draft heat exchangers. Particulate collection elements include baghouses, along with scrubbers and electrostatic precipitators [25].

The total fume treatment system typically comprises two primary components: a direct evacuation system, which encompasses containment, cooling, and collection processes, and a secondary quick capture system, which is characterized by a canopy hood integrated into the roof of the melt shop. A representative illustration of a typical off-gas system is provided in Figure 2.24.

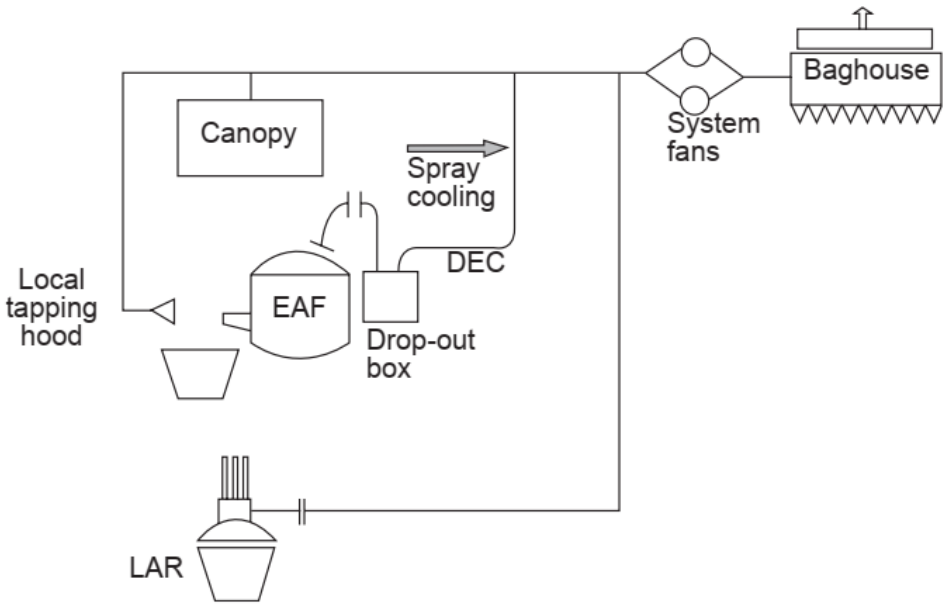


Figure 2. 24 Typical off gas system flow sheets [Adopted from 24].

2.3.17 Grease Lubrication System

In an EAF, the double-line centralized system featuring an automatic inverter comprises several key components. At its core is a motor pump connected to a tank, which plays a crucial role in the system's operation. This setup includes drive electric equipment that ensures efficient performance. Various filters are integrated to maintain the quality of the fluids circulating within the system. To facilitate the connections with users, such as guide wheel columns, a roof lifting column, and a rotation thrust bearing, both rigid and flexible pipes are utilized. These pipes are engineered to handle the system's demands while ensuring reliability. An important safety feature

of this system is a signal that alerts operators when the grease level inside the tank is insufficient, preventing potential issues and ensuring smooth operation [26].

2.3.18 Cooling System

The water cooling system is a critical component of the Electric Arc Furnace (EAF) structure. There are various types of cooling systems, including transformer cooling, delta closure cooling, duct cooling, and electrode holder cooling. These systems typically utilize a closed-loop circuit that circulates water through sensitive equipment. The water in the closed circuit flows through a heat exchanger to dissipate heat. Additionally, other water cooling systems are found in furnace side panels, roof panels, exhaust systems, and more. Sensitive equipment is often equipped with instruments to measure and monitor coolant flow and temperature [28]. If there is a shortage of water—such as when the pump room malfunctions or there is insufficient electrical energy—the circuits, particularly in the feeding unit or roof unit, can be supplied with emergency water from a raised gravimetric collapse tank. This emergency supply is designed to maintain adequate pressure and flow rate to prevent damage to people or equipment [26].

2.3.19 Hydraulic System

The hydraulic system is a complex assembly that consists of a central unit along with both rigid and flexible piping. It features various control and adjustment devices that work together to deliver hydraulic fluid under high pressure. This hydraulic fluid is crucial for powering the moving cylinders responsible for functions such as lifting, lowering, and locking. Also, it supports the control servo systems that fine-tune the adjustment of the furnace electrodes. A visual representation of the hydraulic central unit used in the AKS can be found in Figure 2.25.

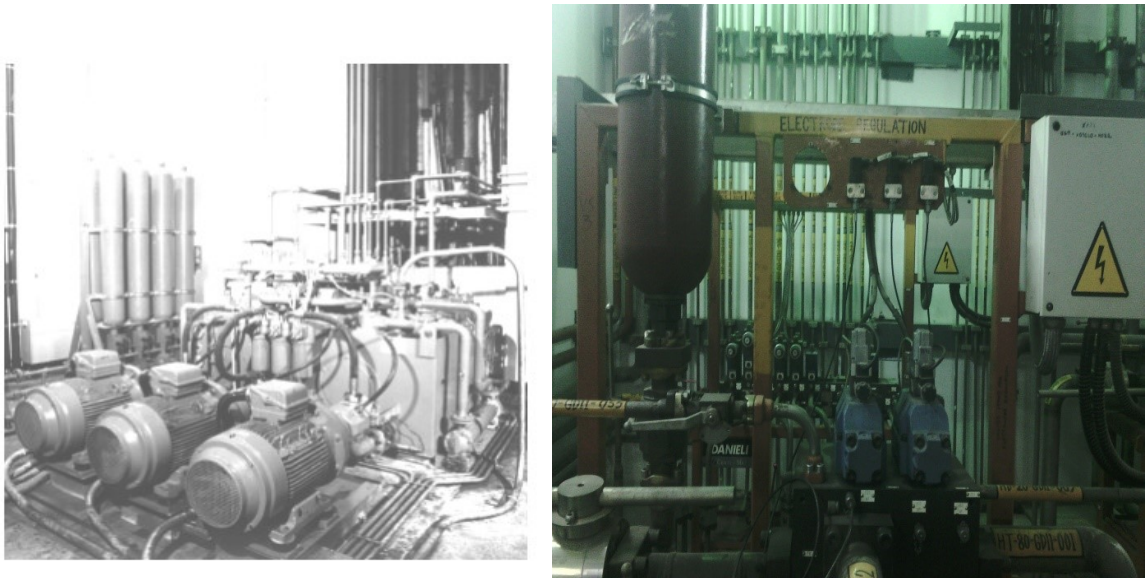


Figure 2. 25 EAF Hydraulic system [setup at AKS melting plant in Chittagong, ref. 27].

2.3.20 Electrodes Conditioning Centre

The electrode conditioning center includes two main components [26]:

Electrode Remaking Station: Located beside the electric arc furnace, this station allows for the transfer of electrode elements from storage. Electrodes are detached from the conveyor, placed in a support structure, and fitted with new elements using a service crane. Once complete, they are moved to parking stations, secured by a pneumatic clamping mechanism.

Electrode Parking Station: Also near the electric arc furnace, this station holds electrode strings after their treatment at the remaking station. There are four designated parking stations where electrodes are secured with pneumatic cylinders until transferred to the furnace.

2.4 RAW MATERIALS IN EAF

In EAF steelmaking, steel scrap serves as the primary raw material. The process can utilize 100% steel scrap, or a combination of Direct Reduced Iron (DRI), Hot Briquetted Iron (HBI), pig iron (PI), and hot metal in conjunction with steel scrap. Statistically, approximately 75% of the raw materials employed in EAF steelmaking are comprised of steel scrap, while DRI and HBI represent around 15%. The remaining 10% is derived from pig iron or hot metal [35].

2.4.1 Scrap

Steel scrap is the predominant raw material utilized for charging in EAF processes. The classification of scrap material is contingent upon the type of steel being produced and the availability of commercial scrap within the marketplace. Several key characteristics are critical for the classification of scrap materials:

Density: The density of scrap varies significantly, ranging from light scrap (typically less than 0.5 t/m^3) to heavy scrap (up to 1 t/m^3). The optimal average density of scrap is approximately 0.7 t/m^3. While light scrap can be melted more readily, it necessitates a greater volume of buckets for processing; conversely, heavy scrap demands increased energy consumption and may lead to higher usage of refractory materials and graphite electrodes during the melting phase [35].

Geometry: A comprehensive understanding of the geometric shapes of scrap allows for the efficient filling of the EAF charge basket. It is important that the maximum dimensions of scrap pieces do not exceed 150 x 50 x 50 cm.

Quality: The quality of scrap is influenced by the presence of detrimental or unwanted elements, as well as various factors affecting yield. Key contaminants include sulfur, phosphorus, copper, and zinc.

Scrap Classifications: Scrap can be categorized into three distinct groups based on its origin:

Obsolete Scrap: This includes components such as old vehicles, appliances, and machinery.

Industrial Scrap: This type is generated during the processing of steel products like strips or bars.

Internal Scrap: This classification encompasses quality rejections, tundish bottoms, and steel recovered from slag.

When charging obsolete scrap, several methods can be employed [2]:

- Fragmentation through shredding
- Pressing into bales
- Oxy-cutting.

Shredded scrap is produced via shredding machines, which recycle materials such as automobiles, machinery, and domestic appliances. Consequently, EAF steelmakers have installed shredding machines to facilitate the acquisition of purified and appropriately sized shredded scrap, thereby significantly enhancing the overall steelmaking process.

The various categories of scrap are delineated as follows [2]:

- No. 1 Heavy melting scrap (HMS 1)
- No. 2 Heavy melting scrap (HMS 2)
- No. 1 Bundles
- No. 2 Bundles
- Busheling
- Turning
- Rail crops
- Rail wheels
- Shredded scrap

The chemical properties of different categories of scrap and other ferrous raw materials are summarized in Table 2.5.

Table 2. 5 Different categories scrap and other ferrous raw materials chemical properties [2]

	HMS #1	HMS #2	Local	Shred.	Bush	Bundle #2	Rails	Internal	Turning	Pig Iron	Liquid Iron	DRI	Average scrap
Density	0.6	0.7	0.7	0.75	0.65	0.85	0.8	2.5	0.6	4	6.9	3.8	0.84
C	0.22	0.22	0.98	0.6	0.3	0.05	0.06	0.58	3.5	4.4	4.4	1.5	0.36
Si	0.16	0.13	0.57	0.3	0.05	0.07	0.22	0.2	0.39	1.5	0.6	0	0.21
Mn	0.66	0.6	0.57	0.43	0.3	0.27	0.38	0.65	0.79	0.3	0.7	0.03	0.55
P	0.02	0.02	0.04	0.05	0.01	0.01	0.02	0.02	0.01	0.08	0.68	0.04	0.03
S	0.04	0.05	0.07	0.04	0.02	0.08	0.1	0.02	0.06	0.02	0.8	0.02	0.04
Fe	93.8	95.6	86.8	95.2	97.1	93.6	91	95.6	88.1	92.7	92.8	88.5	94.7
O	1.48	0.96	3.36	0.4	0.5	3.36	3.52	0.96	1.6	0	0	1.95	1.36
H_2O	0.5	0.8	1	1	0.3	0.6	0.1	0.3	3	0.1	0	0.5	0.68
CaO	0.96	0.8	1.07	0.5	0.3	1.15	0.28	0.45	1.3	0.6	0	2.5	0.82

MgO	0.08	0.2	0.15	0.13	0.06	0.14	0.03	0.01	0.2	0	0	0.79	0.12
Al_2O_3	0.3	0.2	0.1	0.47	0.4	0	0.78	0.02	0.55	0	0	1.12	0.26
SiO_2	1	0.8	0.89	0.87	0.65	0.7	0.7	0.6	0.5	0.3	0	3	0.87
Gangue	2.34	2	2.21	1.97	1.41	1.99	1.79	1.08	2.55	0.9	0	7.41	2.08
Basic	0.96	1	1.2	0.57	0.46	1.64	0.4	0.75	2.6	2	0	0.83	0.99
Cu	0.16	0.11	0.4	0.25	0.1	0.03	0.23	0.08	0.173	0	0	0	0.134
Ni	0.07	0.05	0.15	0.06	0.06	0.03	0.03	0.08	0.111	0	0	0	0.052
Cr	0.11	0.15	0.18	0.19	0.11	0.17	0.09	0.08	0.05	0	0	0	0.109

2.4.2 Direct Reduced Iron (DRI)

Direct Reduced Iron (DRI) is produced through the direct reduction of iron ore using reducing gas mixtures, primarily consisting of carbon monoxide and hydrogen, derived from natural gas or coal. This process occurs at temperatures ranging from 900°C to 1050°C, wherein oxygen is removed from the iron ore, resulting in metallic iron and stable oxides such as SiO_2, Al_2O_3, CaO, and MgO [35]. Most gas-based DRI production facilities are integrated within steel plants and are typically located near Electric Arc Furnace (EAF) operations. DRI serves as a clean iron source that is used in conjunction with steel scrap during the steelmaking process. It's minimal or absent residual elements, such as copper, tin, nickel, and chromium, make it highly suitable for this purpose. DRI can be fed into the EAF in either hot or cold form. Some steel manufacturers operate captive DRI plants where DRI is generated using shaft furnaces or rotary kiln furnaces. The produced hot or cold DRI is then transferred to their EAF, and hot briquett iron (HBI) may also be produced from DRI. The characteristics of DRI can be summarized as follows [35]:

Chemical Composition: The reduction process effectively removes the majority of oxygen and sulfur from the iron ore, although some impurities and gangue remain. Gangue materials include both acidic elements (such as silicon, aluminum, and titanium dioxide) and basic elements (such as magnesium oxide and calcium oxide). DRI is free from tramp elements, containing only trace amounts of sulfur and phosphorus.

Carbon Content: The carbon content in DRI typically ranges from approximately 0.25% to 3%.

Metallization: Metallization refers to the ratio of metallic iron to the total iron present (including FeO), with values varying from about 85% to 95% depending on the reduction process employed. Metallization serves as an important parameter for assessing the efficiency of DRI production.

2.4.3 Hot Briquetted Iron (HBI)

Hot Briquette Iron (HBI) is a refined form of Direct Reduced Iron (DRI) that has been compacted at temperatures exceeding 650^0C. As a result, HBI is dense, and the briquettes can be easily fed into furnaces. In contrast, scrap iron tends to be cumbersome and often requires cutting, which can be a costly process. HBI is manufactured using specially designed roller presses that shape

the material into pillow-shaped briquettes, typically measuring between 50 and 150 mm in length and 25 mm in thickness [35]. This product is produced and compacted from DRI to facilitate shipping, handling, and storage. DRI poses safety risks as it can oxidize violently when exposed to saltwater, potentially leading to extreme temperatures, combustion, or even explosions. Consequently, DRI can only be transported safely under strict precautions, which include regular inspections, temperature monitoring, and the use of inert gas blankets. Due to these risks, DRI is often processed into HBI, which remains stable during shipping [35].

2.4.4 Pig Iron (PI)

Pig iron contains a high percentage of metallic iron and low residual materials, making it suitable for producing high-quality steel. It is produced in a blast furnace and obtained through a casting process. On average, about 5% of pig iron is utilized in Electric Arc Furnace (EAF) steelmaking. In the steelmaking process, a maximum of 15-20% pig iron is used in total charging materials, as it takes more time to melt compared to steel scrap. The characteristics of pig iron are detailed in Table 2.6 below.

Table 2. 6 Typical characteristics of pig iron [31].

Total Fe	94%
Metallic Fe	94%
Metallization	100%
C	3.5 - 4.5 %
P	0.08 - 0.15%
S	≤ 0.05 %
Si	≤ 1.25 %
Mn	≤ 1.0 %
Bulk density	3.3 - 3.7 ton/m3
Apparent density	6.5 - 7.0 ton /m3

2.4.5 Hot Metal (Molten Pig Iron)

Hot metal refers to molten pig iron at a temperature of 1430°C. In integrated steel mills, hot metal is produced in a blast furnace (BF) using iron ore pellets. This hot metal, combined with scrap, is then processed in a basic oxygen furnace (BOF) to create steel. Additionally, some steel plants utilize hot metal in an electric arc furnace to produce steel [35].

2.4.6 Other Charge Materials

In Electric Arc Furnace (EAF) steelmaking, carburizing materials and slag-making materials are utilized alongside scrap, Direct Reduced Iron (DRI), Hot Briquetted Iron (HBI), and pig iron to achieve the desired steel composition.

2.4.6.1 Carbon

Carbon is an essential element in the steelmaking process, contributing to the various grades of steel produced. It plays a critical role in reducing electrical power consumption during the operation. During the melting phase, carbon reacts with oxygen in the furnace, resulting in the production of carbon monoxide through an exothermic reaction. In EAF steelmaking, additional carbon is introduced to further decrease power consumption and to generate foamy slag. Oxygen is injected with coal to create this foamy slag and generate CO gas within it. After carbon injection, it also reacts with iron oxide (FeO), producing additional CO gas. When the slag is foamed, its thickness typically ranges from 10 cm to 30 cm. To effectively create foamy slag in EAF operations, at least 0.3% of carbon must be removed using oxygen. The amount of carbon added is influenced by various factors, including the carbon content of the scrap or DRI, anticipated oxygen consumption, target tapping carbon percentage, the objectives for slag foaming, and the desired iron yield percentage. The typical carbon charging rate for medium carbon steel production is between 2 to 10 kg per ton of liquid steel. In a Direct Current (DC) furnace, the required carbon injection rate for slag foaming falls within the range of 5 to 10 kg per ton [25,36,37].The characteristics recommended or required for the charged carbon are summarized in the following Table 2.7.

Table 2. 7 Charged carbon characteristics [31].

Coal analysis	**%**
Moisture	6 Max
Ash	11 Max
Volatile	1.5 Max
Carbon	85 Max
Sulphur	0.75 Max
Phosphorus	0.025 Max
Coal Size	25 - 50 mm

Using anthracite carbon is preferred because it does not cause wear issues in transport lines. On the other hand, "coke" type carbon can create abrasion problems due to its hardness and sharp edges, which can damage the carbon transport line and the front end of the Carbon-jet carbon pipe. If it is necessary to use "coke" type carbon, the maximum grain size should be limited to 2 mm [31]. The characteristics required for carbon injected with the module system are summarized in Table 2.8.

Table 2. 8 Injected carbon characteristics [31]

Coal analysis	**%**
Moisture	0.7 max
Ash	10 max
Volatile	2 max
Carbon	83 max

Sulphur	0.5 max
Phosphorus	0.5 max
Coal size	%
0.3 - 3.0 mm	100%
1.0 - 3.0 mm	70 % min
0.3 - 1.0 mm	30 % max
Calorific Value	7000 - 7500 Kcal/kg

2.4.6.2 Lime and Dolomite Lime

Lime plays a crucial role as a flux in modern Electric Arc Furnace (EAF) operations. When steelmakers utilize basic refractories, it is essential to maintain a basic slag in the furnace bath to minimize refractory consumption. To achieve effective slag foaming, the slag basicity in the furnace bath should exceed 2.5. Steelmakers need to add lime during the process to reduce the silica and acidic components in the slag. Certain elements such as phosphorus (P), aluminum (Al), silicon (Si), and manganese (Mn) contribute to the acidic content of the slag when they oxidize. Excessive silica levels in the slag can lead to significant refractory erosion. As a result, high levels of iron oxide (FeO) will occur in the slag, as FeO has greater solubility in the presence of silica, which negatively affects the iron yield in the steelmaking process. Therefore, lime is added both during the charging and injection phases.

Also, dolomite lime (a combination of magnesium oxide (MgO) and calcium oxide (CaO)) is incorporated into the steelmaking process to quickly saturate the slag with MgO, thereby reducing the risk of refractory erosion. The characteristics necessary for the lime and dolomite used in slag formation are summarized in the following Table 2.9.

Table 2. 9 Lime and dolomite lime chemical properties [31]

Chemical composition	**Lime**	**Dolomite lime**
CaO (%)	92	58
MgO (%)	1.5	35
SiO_2 (%)	2	2.4
Al_2O_3 (%)	0	0.5
P (%)	0.1	0.1
S (%)	0.1	0.1
Fe_2O_3 (%)	1	1.5
L.O.I (%)	2.5	2

2.5 OXYGEN LANCING IN EAF

Over the past decade, oxygen lancing has become a crucial component in electric arc furnace (EAF) steelmaking. The process involves injecting oxygen to initiate exothermic reactions within the furnace bath, effectively reducing electrical energy consumption. Through oxygen lancing, the oxidation of carbon and iron occurs, contributing to the overall efficiency of the EAF. In contemporary practices, approximately 10-30% of the total energy input is derived from chemical energy sourced from these exothermic reactions. For ultra-high power (UHP) furnaces, oxygen

consumption typically ranges from 18 to 27 Nm^3 per ton of steel produced. Notably, regions with higher electricity consumption, such as Japan and Europe, tend to exhibit elevated oxygen consumption levels [25,38].

However, it is important to recognize the drawbacks associated with high oxygen lancing rates, particularly concerning fume system management and the generation of nitrogen oxides (NOx). Increased lancing leads to higher flue gas volumes and elevated carbon monoxide (CO) production, necessitating careful consideration of these factors when optimizing oxygen lancing strategies [25].

2.6 POST COMBUSTION INEAF

Post-combustion refers to the burning of incompletely combusted components in a mixture. In steelmaking operations, a significant amount of carbon monoxide (CO) is generated due to the process of oxygen lancing and the formation of foamy slag. During the initial stages of scrap melting, large quantities of CO and hydrogen (H_2) are produced as grease, oil, and other combustible materials are released from the surface of the scrap. To ensure the complete combustion of these compounds, an adequate supply of oxygen is necessary. However, in many cases, insufficient oxygen leads to incomplete combustion, resulting in elevated levels of CO. Flue gas emissions from the furnace can contain considerable amounts of unburned CO when inadequate oxygen is available, a phenomenon that has been studied at Vallourec by Air Liquide [39]. The heat generated from the combustion of CO to carbon dioxide (CO2) is three times greater than that produced by the conversion of carbon to CO. This characteristic highlights the role of combustion as a heat source in the Electric Arc Furnace (EAF) operation. Research conducted by Berthet and Grosjean [40] indicates that potential energy savings are significant, with estimates of energy savings reaching up to 72 kWh per ton. Increasing the amount of oxygen lanced can help reduce electrical energy consumption and enhance oxygen utilization. Consequently, more CO can be combusted with the excess oxygen. If CO is burned in the freeboard area, the additional energy gained can be transferred to the furnace bath. Cavaliere [41] has discussed a specific post-combustion system where electricity savings range from 6% to 11%, and reductions in tap-to-tap timing vary between 3% and 11%. Table 2.10 outlines some of the benefits and concerns associated with post-combustion.

Table 2. 10 Benefits and concern for post combustion [25]

Benefits	Concerns
- Reduced heat load to the fume system	- Increased electrode consumption
- Reduced CO emissions to the melting shop andbaghouse	- Increased heat load to the water-cooledpanels and roof

- Higher heat transfer due to more radiation fromcombustion products	- Reduced iron yield
- Reduced water-cooled duct requirement	- Increased costing due toaddition of oxygen
- Improved utilization of energy from oxygenand carbon	
- Decreased electrical power consumption	
- ReducedNOx emissions from the EAF	
- Improved productivity without improved offgas system requirements	

In the operation of an Electric Arc Furnace (EAF), the post-combustion ratio can be measured using a specific equation:

Post Combustion ratio (PCR) = CO_2/ ($CO+CO_2$)

In some processes, oxygen is injected above the slag to facilitate the post-combustion of carbon monoxide (CO). In other processes, oxygen is introduced into the slag to achieve post-combustion before the material moves into the furnace freeboard. It is important that the injection of oxygen is carefully controlled to prevent reactions between the oxygen and the electrode. A thick slag layer is essential to avoid the reaction of carbon dioxide (CO_2) with the molten bath, which could produce additional carbon monoxide and make it difficult to achieve a high post-combustion ratio (PCR).The electrode also needs to be shielded to minimize reactions between carbon and CO_2 that could produce more carbon monoxide. There is a risk that the electrode may react with the available oxygen, which would increase its consumption. Furthermore, injecting oxygen above the slag can raise the oxidation rates of the electrodes due to the reaction of CO_2 with graphite. As a result, increased oxygen injection to ensure adequate post-combustion leads to higher electrode consumption [25].

2.7 SCRAP PREHEATING SYSTEM IN EAF

Steelmaking in EAF is characterized by a high-temperature melting process, with internal furnace temperatures approaching 1650°C. The exhaust gases emitted from the EAF typically range from 900 to 1200°C, representing a significant energy loss. To mitigate this inefficiency, the technique of scrap preheating has been introduced, wherein hot exhaust gases are utilized to elevate the temperature of the scrap in the charging bucket prior to its introduction into the furnace. By preheating the scrap, the required energy for melting is substantially reduced, thereby enhancing energy efficiency during the steelmaking process. Moreover, this preheating approach minimizes the risk of moisture present in the scrap causing furnace explosions during operation. Studies have indicated that scrap preheating can lead to a reduction in electrical energy consumption for the EAF melting process and can enhance productivity by 10 to 20% [25].

It is noteworthy that approximately 20% of the input energy is retained in the exhaust gases, which constitute an underutilized resource that could be efficiently harnessed through the implementation of a scrap preheating system. This system aims to reduce the overall energy consumption associated with EAF operations [42]. Research conducted by Jones and Bowman [25] and Gopal et el. [42] has indicated that preheating steel scrap to temperatures between 300 and 400 °C can result in electrical energy savings ranging from 20 to 40 kWh per ton. The most established scrap preheating technologies employed in EAFs are as follows:

2.7.1 Bucket Preheating System

As one of the earliest scrap preheating technologies, the bucket preheating system is integral to the EAF steelmaking process. This system directs hot exhaust gases exiting the furnace toward the scrap bucket through a ducting and hood arrangement. The hot exhaust gases can reach temperatures around 800 °C as they flow through the bucket, raising the temperature of the scrap to approximately 400 °C, with the cooled off gas exiting the bucket at around 200 °C. Jones and Bowman [25] estimated the energy savings associated with this method to be in the range of 18 to 20 kWh per ton. However, the bucket preheating system has notable disadvantages, which include operational challenges such as scrap adherence to the bucket, limited bucket lifespan, and reduced controllability of the preheating system. The bucket preheating system is shown in Figure 2.26.

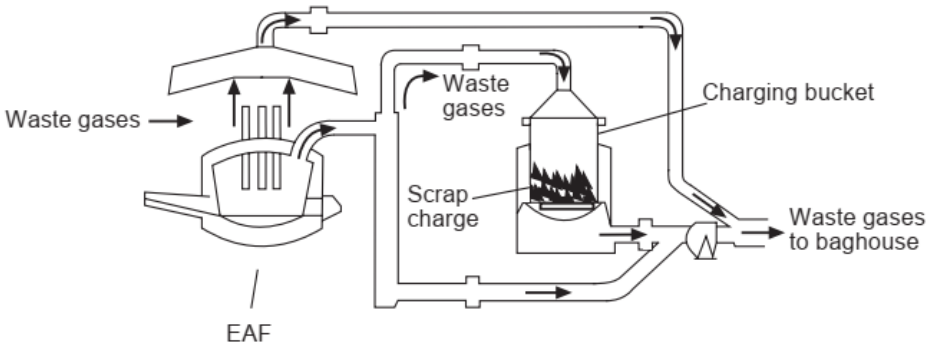


Figure 2. 26 Schematic diagram of bucket preheating system [Adopted from 25].

2.7.2 Continuous Preheating System or Consteel Process

The continuous preheating system, often referred to as the Consteel process, involves the loading of scrap onto a conveyor, which transports it through a dedicated preheating section where it is heated by the flow of off gases from the EAF. Notably, in the Consteel process, the heated scrap is delivered directly into the furnace through an enclosed tunnel, which eliminates the need to open the furnace roof for conventional charging methods. The tunnel facilitates the heating of the scrap via the off gas flow, thereby enhancing the overall efficiency of the melting operation. To

further improve energy savings, natural gas burners may be employed to preheat the scrap as it traverses the conveyor. The energy savings associated with the Consteel process can reach up to 38 to 40 kWh per ton [43]. The consteel process is shown in Figure 2.27. Key advantages of the Consteel process include the reclamation of heat from furnace off-gases for preheating the scrap metal prior to charging, a 10 to 12% reduction in specific electrical energy consumption, decreased utilization of oxygen, carbon, and electrodes, and improved production rates due to reduced tap-to-tap times.

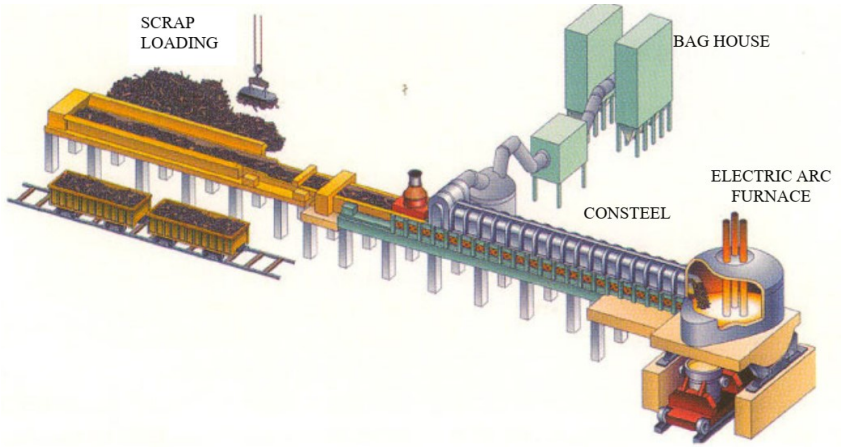


Figure 2. 27 Schematic diagram of consteel process [adopted from 43].

2.8 SHAFT FURNACE

The shaft furnace serves as an alternative to the bucket system, preheating scrap material using off-gas to achieve heat recovery and enhance the efficiency of the Electric Arc Furnace (EAF). In this process, a shaft is positioned above the arc furnace, equipped with a preheating arrangement that heats the scrap material. By utilizing exhaust gas or waste heat, the shaft furnace reduces the electrical power consumption of the EAF [25,41,42]. The concept behind the shaft furnace is to convey scrap into a shaft where it is preheated by off-gas before being fed into the EAF. The scrap is arranged in a column at one end of the furnace, and after preheating, it is charged into the furnace.

There are several types of shaft furnaces used in the EAF process: (i) single shaft furnace, (ii) double shaft furnace, and (iii) finger shaft furnace [42,44]. The single shaft furnace can manage the heating of 50% of the scrap, recovering a total of 72 kWh per ton from off-gas. The double shaft furnace is an advancement over the single shaft furnace, consisting of two identical shafts with a double shell arrangement. A single set of electrode arms provides arcing for both shaft furnaces as needed [42]. Research by Cavaliere [41] has shown that the double shaft furnace can save a total of 110 kWh per ton by preheating the scrap.

The most effective design of a shaft furnace is the "finger shaft furnace", as illustrated in Figure 2.28. In this setup, scrap is fed into the shaft and preheated by off-gas, which flows through the

shaft while the scrap is retained. This design allows for the recovery of heat from the off-gas, effectively preheating the scrap before charging it into the furnace, thereby reducing electrical energy consumption. In the finger shaft furnace, the shaft is positioned overhead, and scrap is held in place by water-cooled fingers; however, the charging of scrap is not continuous. In this process, the preheating temperature of the scrap can reach 500°C or higher, depending on the type and size of the scrap and the degree of post-combustion. The maximum energy savings can reach 100 kWh per ton, with a tap-to-tap time of 35 to 40 minutes achieved in this process. Additionally, the finger shaft furnace can increase productivity by 20% [41].

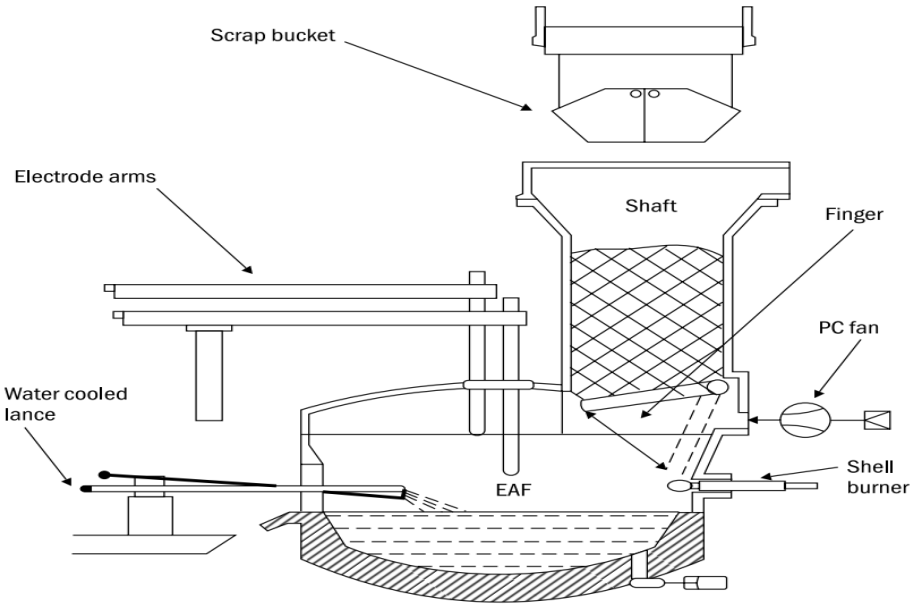


Figure 2. 28 A schematic diagram of finger shaft furnace [adopted from 42].

2.9 CHEMICAL REACTIONS IN THE FURNACE

The oxygen injection strategy emphasized the proficient management of electrical and chemical energy, linking effective dynamic control of the electric arc with a precisely adjusted injection of oxygen and carbon (Figure 2.29). This process was optimized to minimize electrical energy consumption while enhancing the productivity of the Electric Arc Furnace (EAF). To achieve these objectives, the reactions occurring during the melting process were rigorously evaluated and analyzed, leading to the development of various solutions to optimize the process. By examining the fundamental mechanisms and chemical reactions occurring within the furnace, we concluded that it was feasible to augment the contribution of exothermic reactions by precisely regulating the injection of oxygen and carbon.

Importantly, the metallic yield of the charge remained unaffected by the amount of oxygen injected, as the iron oxide generated in the slag was effectively controlled through simultaneous carbon injection at the slag level. The mechanisms discussed are instrumental in understanding

the energy and mass balances within the furnace, as well as in optimizing post-combustion efficiency and controlling the reactions themselves [31].

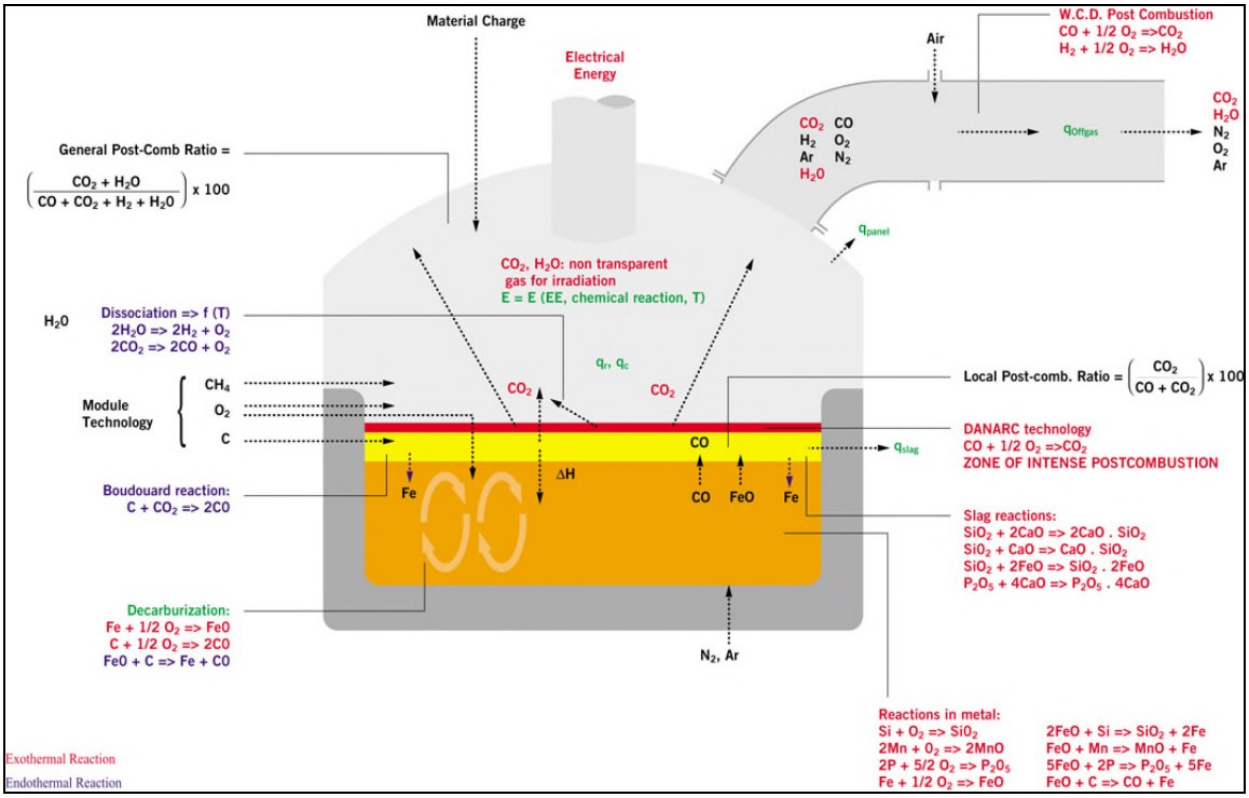


Figure 2. 29 Fundamental mechanism and chemical reaction [adopted from 31].

Chapter -03

Steelmaking Operation and Refining Process

3.1 INTRODUCTION

Steelmaking using EAF represents one of the most efficient and cost-effective methods within the industry, particularly when it comes to operations in casting lines and rolling plants. The primary advantage of steel production in an EAF lies in its significantly lower production costs per ton compared to traditional methods such as blast furnaces and basic oxygen furnaces. Moreover, EAF facilities require a shorter investment period, making them a more economical and feasible choice for modern steelmaking.

The EAF process is characterized by its flexibility in both production methods and the types of raw materials that can be utilized. During the initial charging phase, various materials, primarily steel scrap, are loaded into the furnace. Electrical power is then delivered through the cathode, traveling through the scrap material to the anode, where an electric arc is created. This process generates extremely high temperatures, reaching around 1600^0C, which is well above the melting point of the scrap metal [45]. To ensure the quality of the molten steel, certain elements such as carbon, oxygen, lime, and dolomite lime are introduced into the furnace bath during the melting and refining stages. These additives play a crucial role in reducing impurities within the molten metal. Throughout the operation, the molten steel's carbon content is regularly monitored and measured to meet the specific requirements for various steel grades. When the desired composition is achieved, the molten steel is tapped into a ladle and then moved to a ladle furnace for further refining.

This project focuses on studying the steelmaking and refining processes at AKS melting plant at Chittagong, a reputable Steel Melting Plant in Bangladesh. It encompasses an examination of EAF specifications, the preparation and charging of raw materials, and the overall operational procedures of the furnace. The study emphasizes the significance of raw material selection in steelmaking. Detailed analyses of specific power consumption, carbon usage, lime consumption, and electrode consumption related to different mixtures of raw materials were conducted. Furthermore, the study presents comparative data on these consumption metrics, highlighting the impact of various raw material combinations on the efficiency and effectiveness of the steelmaking process.

3.2 STEEL PRODUCTION

The initial phase of steel production involves processing raw materials, primarily iron ore. Iron ore consists of iron oxides mixed with various metal impurities, including sulfur, phosphorus, and silica. The process begins with crushing the iron ore, followed by separating the metallic impurities using established techniques. Next, the pelletizing process transforms the iron ore, mainly composed of iron oxides, into spherical pellets. After undergoing thermal treatment, these pellets are produced as a final product, also referred to as pellets. In the direct reduction process, these pellets react with carbon to produce pure iron. During this reaction, the pellets lose their oxygen content, resulting in a porous structure similar to directly reduced iron. This final product, known as foamy iron, is stored in specialized tanks for later use as a raw material in subsequent steel production stages [46].

The second phase of steel production is the conversion of direct reduced iron into molten steel. This process uses direct reduced iron as its primary input. At this stage, the specific type and grade of steel, along with its chemical properties, are determined. Direct reduced iron, combined with scrap iron, is melted in EAFs, following predetermined proportions. After the slag is removed from the melt, various additives are introduced based on the desired quality. These additives are mixed into the molten steel through gas blowing to ensure even distribution within the melt [47].

Once this phase is complete, the molten steel is poured into bulk pots for further operations. Quality assurance for the molten steel is conducted through laboratory sampling, leading to melt refining operations to prepare the molten steel for casting. The optimal temperature for casting molten steel is approximately 1650°C, with a critical lower threshold of 1580°C. In the event of potential casting delays, ladle furnaces are used to maintain the melt temperature within acceptable limits. However, it is important to note that such casting delays can incur significant costs. Ultimately, the melt produced during the steelmaking process is solidified into ingots or slabs through continuous casting machines, which are designed in a semi-arched configuration, with the molten ladle positioned atop the casting tower [48].

The casting tower is designed to hold two ladles—one for casting and another for preparation. The molten material flows into the middle pan through a passage located beneath it. The tundish acts as a buffer, ensuring a continuous and uniform flow of melt to the molds during ladle changes. Most casting machines are equipped with dual casting paths, and the tundish has two outlets to direct the melt to the molds. The casting operation is limited by the lifespan of the tundish; once it expires, casting must be paused until it is replaced. A production sequence occurs during replacement intervals, allowing for a limited number of continuous melts that maintain the same quality and casting width. After cooling in the mold, the molten material takes shape, moving in

a semi-arc to form a rectangular strip, which is then cut into specific lengths to produce steel ingots [49].

3.3 ELECTRIC ARC FURNACE SPECIFICATION

This project was conducted at AKS, a leading steel manufacturer in Bangladesh. At AKS, the Electric Arc Furnace (EAF) melting shop is equipped with two independent production lines, each featuring a furnace with a nominal production capacity of 630,000 tons per year. In addition, a single continuous casting machine supports a total nominal billet capacity of 1,275,000 tons per year. The main features of the EAF are as follows [27]:

(a) Each Direct Current (DC) EAF has a nominal molten steel capacity of 85 tons. The design of the shell accommodates a suitable liquid heel of approximately 15 tons, resulting in a total shell capacity of 100 tons.

(b) The EAF's power supply, which is not included in the Danieli scope, consists of four transformers with a capacity of 30.6 MVA, four thyristor rectifiers (27.5 kA - 700 V DC), and four smoothing reactors (4 x 900 μH).

(c) The MORE injection system includes one PALMUR supersonic oxygen and carbon lance, along with three modules (oxyfuel and carbon injectors), manufactured by Danieli& C. Spa in Buttrio (UD), Italy.

The production mix features rebar quality according to widely recognized international standards (ASTM A615 – DIN 488 – EN 10080). Medium and carbon grades are planned according to ASTM A615, encompassing grades 40, 60, 75, 90, and 120. Tables 3.1 and 3.2 provide the technical specifications of the EAF and the chemical energy packages from the steel melting plant.

Table 3. 1 EAF technical specification of AKS melting plant at Chittagong

Liquid steel production capacity		2 × 6,30,000 ton per year
Number of furnace		2 Nos.
Type of furnace		DC Full platform
Type of tapping		EBT (Eccentric bottom tapping)
Tap to tap	(Minutes)	58 – 68 (72-92.5)
Productivity	(Ton/hr)	75 – 87.9(70.8 – 55.1)
Tapped steel	(ton)	85
Furnace capacity	(ton)	100
Hot heel	(ton)	15
Transformer (each furnace)	(MVA)	4 x 30.6
Tapping temperature	(°C)	1630
Scrap density	(t/m^3)	0.50
Shell diameter	(mm)	5800
Inner panel diameter	(mm)	5900
Electrode diameter	(mm)	762
Single piece length	(mm)	2700
Quality of electrodes to be used		High density
Pitch circle	(mm)	n.a.
Bottom refractory thickness	(mm)	900 – 1250
Wall refractory thickness	(mm)	476
Total furnace volume	m^3	127

Table 3. 2 Chemical energy packages (Flow rates) [31]

PALMUR SS oxygen lance PALMUR Carbon lance	(n× Nm^3/hr) (n°×Kg/hr)	1× 1600 Nm3/hr 1 ×15 -45 Kg/min
Oxygen jet	(n× Nm^3/hr) (n ×Power)	3 × 1100 3 × 3.5 MW
Carbon pipe	(n°× Kg/hr)	3 × 15 - 45

3.4 EAF OPERATION

The batch charging process is employed in steelmaking at a prominent melting plant. The production of molten steel through this batch or bucket charging method is referred to as producing "heats." The operating cycle of this production process, or the time required to generate molten steel, is known as "tap to tap timing (TTT)" [42]. A flow diagram illustrating the furnace operation process is presented in Figure 3.1. The operation of the furnace encompasses several critical processes, which are examined in detail in the subsequent section.

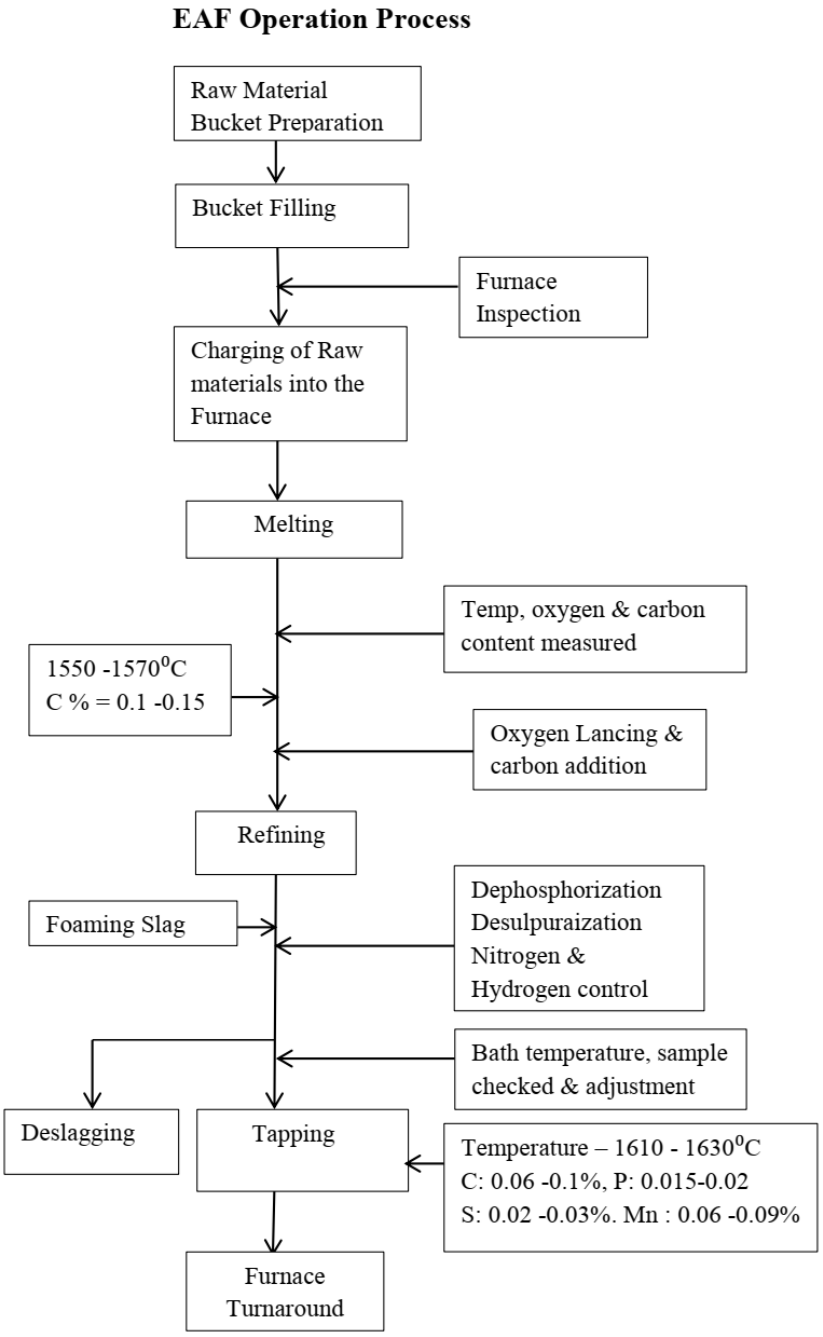


Figure 3. 1 EAF operation process flow diagram [AKSML, Chittagong]

3.4.1 Charging

The furnace charging process encompasses several critical steps essential for ensuring optimal operational efficiency. These steps include the preparation of raw materials, the filling of buckets, and the charging of raw materials into the furnace.

Preparation of Raw Materials Buckets

Prior to the filling of raw materials into the buckets, it is imperative that these materials are appropriately categorized. The preconditions for the scrap to be utilized are summarized as follows:

- The scrap should be of high cleanliness, exhibiting minimal oxidation, and must be devoid of any significant vitreous or other inorganic material enclosures.
- It is crucial to eliminate any lead (Pb) and tin (Sn) content from the scrap.
- The average density of the scrap must not fall below 550 kg/m³.
- The maximum dimensions for any individual scrap piece must adhere to a size not exceeding 1.5 m x 0.5 m x 0.3 m, with a maximum weight limit of 0.5 tons.
- The maximum section thickness of scrap pieces must not surpass 0.1 m.
- The proportion of heavy scrap pieces should not exceed 10% of the total charge.
- The cumulative weight of heavy scrap, which includes heavy melting scrap (HMS), bundles, and large pieces, must not constitute more than 40% of the entire scrap charge.
- Heavy scrap items, such as ingots and large scrap ingot molds, should be charged separately before the bucket is charged, so as to mitigate the risk of damage to the electrodes.

In the final bucket prior to the refining stage, it is advisable to refrain from charging bulky and heavy pieces. When slag-making materials are introduced into the bucket, they should be placed along the walls rather than in the center, thus reducing the likelihood of electrode damage during interactions with non-conductive materials. The introduction of these materials is recommended from the top of the bucket to optimize their distribution. Additionally, lime and coke may be introduced directly into the bucket or injected during the heating process. When loading coke and/or pig iron into the bucket, it should ideally be positioned in the lower layers to ensure optimal yield. Regardless of the configuration, the bucket must be filled adequately but not overfilled.

The design of the scrap bucket volume is calculated to ensure that a complete charge composed entirely of scrap can be contained within two buckets, assuming a standard scrap density of approximately 0.70 tons/m³. Furthermore, when charging the furnace, the volume of scrap within must not exceed 90% of the furnace's total capacity to prevent complications related to roof closing and delays in leveling operations. Proper practices in bucket charging facilitate an even distribution of scrap within the furnace, replicating the layering order established during loading.

The charged materials can be classified into two principal components:
Metallic Charge: This comprises iron scrap, pre-reduced ores, cast iron, and any potential alloying elements.
Slag-Making Materials: These include burnt and dry lime, ensuring that elevated hydrogen contents are not introduced into the molten bath.

Bucket Filling

The guidelines for filling a scrap bucket are:

(a) Start with a 10% layer of light scrap (shredded material or busheling) at the bottom, ensuring it's free of oil or water.

(b) Add a 10% layer of heavy scrap (heavy railway and shipbreaking materials), with internal scrap not exceeding 5% of the total charge.

(c) The next layer should consist of medium to heavy scrap (classes E1 and E3) as the main volume by weight.

(d) Finish with another layer of light scrap at the top.

In general, dense scrap metal takes longer to melt. If aggressive techniques such as high burner activity and oxygen lancing are used, this dense scrap may cause the jet of oxygen to reflect back onto the furnace side walls, potentially leading to damage. When charging the scrap into the bucket, it is essential to consider its size and density to achieve the following goals:

- Promote the formation of a liquid layer of steel.
- Protect the Electric Arc Furnace (EAF) sidewalls and roof from arc radiation.
- Prevent mechanical breakage of the graphite electrodes.
- Reduce the risk of burners and oxygen jet reflection to avoid damage.

It is also crucial to categorize scrap by quality in the yard for optimal bucket stratification in accordance with the steel grade that needs to be produced. By doing this, both charge costs and transformation costs can be optimized. The figure 3.2 below illustrates a typical distribution of scrap inside the bucket:

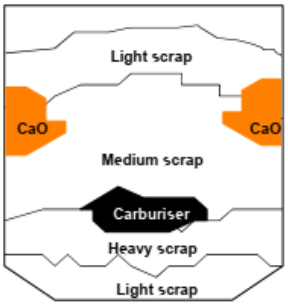


Figure 3. 2 Scrap bucket loading pattern [adopted from 31].

Charging of Scrap into the Furnace

Charging the furnace is a delicate yet crucial step in the melting process. To avoid damage to the furnace and facilitate melting, electric furnaces use buckets with bottom valves for scrap delivery. Before charging, the electrodes are raised, and the furnace roof is lifted and rotated. The scrap bucket is positioned above the furnace using an EOT crane, with the valve operated by a lever through the crane's auxiliary hook. Charging is done progressively, typically using 2 to 4 buckets, though the current trend is to use just two or even one, depending on the electric arc furnace's

volume and scrap density. The charge can also include molten iron or sponge iron. When opening the bucket, it's important to align it with the furnace and maintain a distance of no more than 0.5 meters above the furnace to avoid damage. The sequence for opening the bucket includes:

1. Tensioning the cables while lowering the bucket.
2. Stabilizing the bucket's swing.
3. Quickly opening the valve to discharge scrap into the furnace.
4. After charging, lifting the bucket and closing it for removal.

The correct charging sequence is illustrated in Figures 3.3, 3.4 and 3.5.

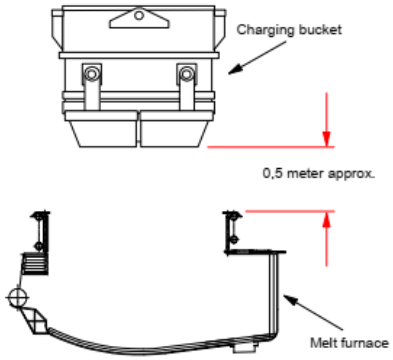


Figure 3. 3 Placing of the Bucket above the Furnace [31].

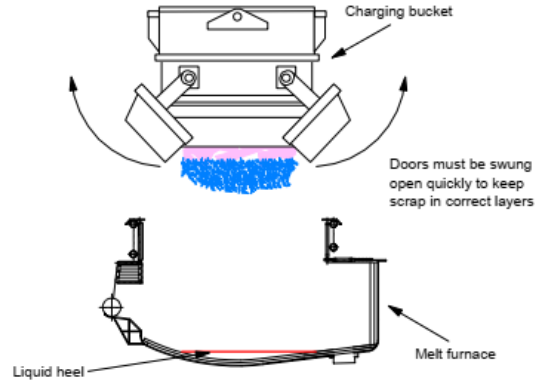


Figure 3. 4 Emptying of the Bucket into the Furnace [31].

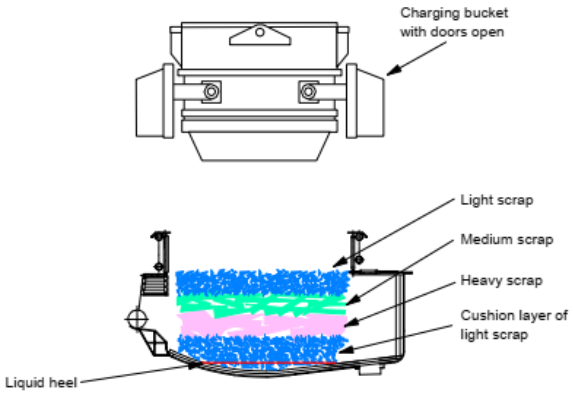


Figure 3. 5 Scrap charged into the furnace [31].

The roof was finally rotated and lowered to close the furnace. Subsequently, the furnace breaker was engaged, and the electrodes were automatically lowered to initiate the arc, preparing the furnace to begin or continue its operations.

Most modern furnaces are designed to minimize the number of bucket charging cycles. During the bucket charging period, the electric arc furnace (EAF) remains inactive, resulting in a complete halt in melting operations. This downtime represents a loss of energy with each roof opening. Research by Jeremy A.T. Jones and Ramesh Singh indicates that the energy loss can amount to 10–20 kWh per ton for each occurrence. Typically, operations aim for 2 to 3 bucket charges per heat production, with some managing to achieve just a single bucket charge. Continuous charging processes, such as the CONSTEEL and ECOARC shaft furnace, help to reduce the energy lost during the charging cycle [41,50].

3.3.2 Melting

The melting process is essential for Electric Arc Furnaces (EAF), which utilize efficient melting systems to optimize their capacity. The primary energy source is electrical energy, supplied mainly through graphite electrodes. Initially, an intermediate voltage tap is used to allow the electrode to penetrate the scrap layer, where lighter scrap is positioned on top. This arc ignition and charging phase lasts about one to two minutes and melts approximately 15% of the scrap while minimizing radiation exposure to the furnace structure.

Once the electrode is submerged, the process transitions to a high voltage tap, creating a long arc that leads to a stable power input and a molten pool. In addition to electrical energy, chemical energy from oxy-fuel burners and oxygen lances accelerates melting in cooler areas of the furnace. The burners ignite after the power is turned on and operate for 15 to 20 minutes, achieving a thermal efficiency of 40-60%. Heat is transferred to the scrap through radiation, convection, and conduction, with smaller scrap pieces melting faster than larger ones.

Oxygen, introduced through pipe lances, helps cut the scrap and enhances the melting process through exothermic reactions, producing iron oxide and generating additional heat. This interaction results in reactions with various components such as Al, Si, Mn, P, C, and Fe, leading to the formation of respective oxides through exothermic reactions. The resulting heat contributes further energy to the bath, facilitating scrap melting. This process also allows for the adjustment of carbon levels as needed, while metallic oxides accumulate in the slag. Carbon monoxide generated during the process can be expelled or combusted when oxygen is present [51].

In the course of the melting process, sufficient scrap material was melted to permit the implementation of the second charge, which necessitated the reiteration of the charging procedure.

Following the completion of the final scrap melt, the Electric Arc Furnace (EAF) sidewalls were subjected to intense radiation emanating from the arc, resulting in a subsequent reduction in voltage [50]. Additionally, HBI and DRI were introduced during the second bucket charging. Simultaneously, the formation of foamy slag played a pivotal role in preserving the arc and providing insulation to the furnace shell. This foamy slag effectively retained a significant quantity of thermal energy, facilitating its transfer to the molten bath and ultimately leading to decreased energy consumption.

Upon the melting of the final charge materials, a molten pool was established within the furnace bath. At this stage, the bath temperature was meticulously measured, and samples were collected for the determination of carbon content and oxygen levels. The carbon concentration was modulated through the strategic addition of charge materials and gas injection, while oxygen levels were managed during the refining phase. These parameters were meticulously adjusted following the completion of the refining process [31,50]. Figure 3.6 illustrates the melting process in a recognized steel melting facility.



Figure 3. 6 Melting process [AKS melting plant in Chittagong].

3.3.2.1 HBI/DRI Continuous Feeding and Melting

The Hot Briquetted Iron (HBI) was continuously charged into the furnace, with the feeding rate carefully regulated to maintain the temperature of the molten steel bath at approximately 1550-1580°C. This regulation system employed instrumental indicators such as energy consumption, actual power input, charge feed rate, as well as a Level 2 forecast of bath temperature, which was corroborated by measurements taken at regular intervals. Melting of the HBI was accomplished by manipulating the active power supplied to the system. The voltage was adjusted to ensure an acceptable arc length, contingent upon the consistency of the foaming slag. Consequently, from

the initial moments of HBI feeding, the injection lances were engaged to introduce oxygen and carbon, fostering the development of a robust foamy slag conducive to the generation of carbon monoxide within the bath. The flow rates of oxygen and carbon injection were critical to the efficacy of the melting process.

To ensure process integrity, bath temperature and oxygen activity were monitored at intervals of every 7 to 10 minutes. The target temperature was maintained within the range of 1550 – 1580 °C, while carbon content was controlled between 0.10 – 0.15 %. These measures were implemented to facilitate the timely conclusion of the charging process in accordance with operational protocols, thereby avoiding prolonged melting times or the necessity for furnace shutdowns to recalibrate carbon levels.

Lower operational temperatures resulted in increased energy consumption due to the propensity for DRI to solidify, which necessitated significant energy input for re-melting the resulting DRI accumulations. Conversely, elevated temperatures led to considerable energy losses via radiation. Crucially, the management of carbon content in the bath was paramount; for safety considerations, it was maintained below 0.15% during the heating process. This precaution was particularly important when temperatures exceeded 1570°C, as higher carbon concentrations could instigate vigorous reactions with oxidized slag, resulting in significant boiling of the bath and hazardous foaming of the slag.

3.3.3 Refining

Refining, or overheating, occurs when nearly all the metal in the furnace has melted completely. At this point, the energy supplied to the furnace increases the temperature of the molten steel and facilitates the complete melting of any remaining scrap or HBI. At this stage, the scrap can no longer protect the cooled panels and refractory, which means that if the electric parameters are modified, the power and arc length may be reduced.

In the EAF refining process, several impurities such as phosphorus, sulfur, aluminum, silicon, manganese, and carbon are typically removed. Additionally, the levels of recently dissolved gases, like nitrogen and hydrogen in the furnace bath, are also monitored. Refining operations are performed once a flat bath is achieved. The refining reactions are carried out based on the available oxygen levels. Oxygen is injected into the furnace at the end of the melting process to reduce the carbon content in the bath to the required level for tapping. During refining, most of the elements that need to be removed have a higher affinity for oxygen than for carbon. As a result, oxygen preferentially reacts with these elements to form oxides, which then become part of the slag.

In modern electric arc furnace operations, oxygen may be blown into the bath throughout the heat cycle, allowing some refining operations to occur simultaneously with melting. The main impurities such as phosphorus, sulfur, silicon, aluminum, and chromium are effectively removed by transferring them into the slag.

The key purposes of the refining process are summarized as follows:

- Regulating the carbon percentage (%C) at tapping
- Increasing the yield of tapped steel, thereby minimizing the FeO percentage in the slag
- Maintaining desirable foamy slag characteristics
- Regulating post-combustion

The refining process flowchart is illustrated in Figure 3.7. The slag per ton of steel is lower in EAF, limiting impurity removal. A bath sample is taken post-refining to measure composition (%C, Mn%, Si%, P%, S%) and temperature. If the temperature is too low, arching continues in the furnace. In modern melt shops, temperature adjustment is also done in the ladle furnace.

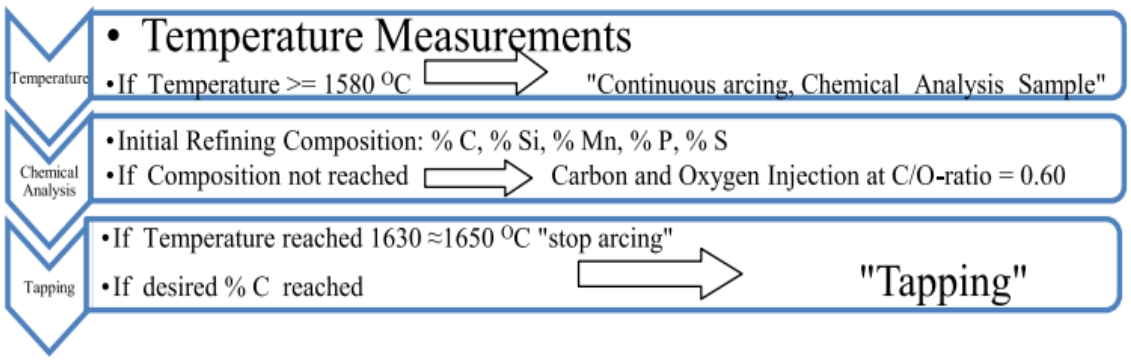


Figure 3. 7 Refining process flowchart [52].

The secondary refining process serves several critical functions, prominently are as follows:

Dephosphorization

The removal of phosphorus from the steel bath is influenced by the basicity of the slag and its iron oxide content. Specifically, phosphoric pentoxide (P_2O_5), which forms as a result of the reaction between phosphorus and iron oxide, becomes fixed in the slag in the presence of free lime, leading to the formation of calcium phosphate. It is preferable to execute phosphorus removal at lower temperatures; thus, operational procedures should be designed to maximize phosphorus extraction during the preliminary stages of the process before the phosphorus can revert to the molten steel at elevated temperatures.

During the melting and oxidation phases within the Electric Arc Furnace (EAF), phosphorus reduction can be effectively conducted. Mincu and Constantin have elucidated methods for minimizing phosphorus content during the melting process in EAF settings. Rapid phosphorus

removal is crucial within the heat cycle. The implementation of a hot heel practice is particularly advantageous for phosphorus extraction, as it allows for oxygen injection into the bath while maintaining relatively low bath temperatures. Initially, the slag's iron oxide (FeO) levels are elevated due to the continuation from preceding heats, which favors phosphorus removal. Additionally, high slag basicity, characterized by elevated lime content, is conducive to phosphorus extraction; however, one must exercise caution to avoid oversaturating the slag with lime. Excess lime can lead to an increase in slag viscosity, thereby diminishing its efficacy in phosphorus removal. To mitigate viscosity issues and enhance slag fluidity, the addition of fluorspar is occasionally employed. Moreover, bottom gas stirring represents another beneficial technique, as it revitalizes the slag/metal interface, thereby facilitating improved reaction kinetics [50,51].

The extraction of phosphorus can be significantly optimized when foamy basic slag is effectively removed from the furnace, resulting in a considerable reduction of phosphorus levels within the slag-metal system. For high carbon heats, ladle phosphorus concentrations below 0.015% can generally be achieved, while even lower concentrations—under 0.010%—are attainable in low carbon heats [31].

Desulphurization

Sulfur is incorporated into the slag as a sulfide and removed during processing. The effectiveness of sulfur removal is influenced by factors such as temperature, slag composition, and basicity; higher basicity and lower FeO content are beneficial. Additionally, low viscosity, high fluidity, presence of manganese, and low oxidation levels in the steel help in sulfur elimination. However, high oxidation levels in modern Electric Arc Furnaces (EAFs) pose challenges. To improve slag basicity, extra lime and fluorspar are added. Typically, meltdown slag is removed before tapping the molten steel, with a secondary slag forming during ladle refining furnace (LRF) operations. Effective sulfur removal mainly occurs during the de-slagging phase and LRF operations, with sulfur content in the ladle from a single-slag EAF heat generally between 0.015% and 0.020%. Lime addition is crucial for optimal sulfur removal, especially under oxidizing conditions.

Furthermore, controlling metallic components in the bath is crucial as it affects the final product's properties, with metallic oxides forming through reactions of oxygen with aluminum, silicon, and manganese before carbon reacts. They would also react with FeO to produce iron into the bath [50,51]. For example:

$$Mn + FeO = MnO + Fe$$

Manganese would usually be lowered to around 0.06% in the bath [51].

To effectively supply heat energy in electric arc furnaces, generating carbon monoxide (CO) from carbon and oxygen is essential, contributing 30% to 40% of the heat. CO bubbles create foaming slag, which submerges the arc and shields it from radiative energy, enhancing thermal efficiency and allowing high arc voltages even in flat bath conditions. This minimizes nitrogen exposure, preventing its diffusion into the steel. Research by Valentin Mincu and Nicolae Constantin [53] shows that desulfurization in the metal bath is improved by bottom stirring with inert gases, as it homogenizes composition and temperature while increasing the contact area between slag and steel.

Nitrogen & Hydrogen Control

The presence of carbon monoxide gas generated within the steel effectively facilitates the removal of nitrogen and hydrogen impurities. Prior to the tapping of molten steel in the EAF, nitrogen levels were successfully reduced to as low as 50 parts per million (ppm). The implementation of eccentric bottom tapping proved advantageous for maintaining low nitrogen levels due to the rapid tapping process and the ability to sustain a constricted tap stream. Elevated oxygen injection into the molten steel was beneficial in achieving low nitrogen concentrations, with the heat being tapped as late as feasible in the oxygen blowing process. It is imperative that the temperature profile be optimized so that the tapping occurs at the requisite temperature correlating with the conclusion of oxygen blowing.

Another approach to nitrogen reduction involves the incorporation of DRI, HBI, and pig iron as raw materials. Nitrogen control can be executed through carbon oxidation, as nitrogen removal diminishes when carbon content falls below 0.3% in the molten bath. With the appropriate proportions of HBI, DRI, and pig iron utilized in steelmaking, nitrogen levels can be maintained below 45 to 50 ppm at the point of tapping. Typically, the nitrogen concentration in steel following tapping ranges from 80 to 100 ppm [31,50,51,54].

Research conducted by Sara Hornby Anderson et al. [55] highlights that elevated nitrogen levels may adversely affect the mechanical properties of hot-rolled (HR) products, leading to embrittlement within the heat-affected zone of welded steel and diminished cold formability. An increased nitrogen content is linked to strain aging phenomena, which results in heightened hardness while concurrently reducing toughness and ductility. Furthermore, studies by Mincu and Constantin [53] indicate that protracted tapping durations within the EAF allow for the ingress of hydrogen (H_2) and nitrogen (N_2) gases from the surrounding atmosphere into the ladle. Consequently, minimizing the tap-to-tap interval in EAF operations is recommended to mitigate this issue.

Decarburization also plays a crucial role in the removal of hydrogen from the steel bath. It is established that a decarburization rate of 1% per hour can effectively reduce hydrogen content from 8 ppm to 2 ppm within a span of 10 minutes [31,50,51].

Foaming Slag

The refining process did not operate at full power, as this had already been used in the flat bath, which could be unsafe for the lining. During this process, foamy slag must be created. A few years ago, an operational practice for producing foaming slag was introduced in EAF operations. Foamy slag was achieved by injecting carbon powder into the oxidized slag. The injected carbon reacted with the FeO present in the slag, resulting in the production of iron and carbon monoxide gas through the reduction of FeO, as indicated below [31]:

$FeO + C = Fe + CO\ (g)$

Foamy slag primarily occurs during HBI/DRI melting operations, where iron oxide (FeO) reacts with carbon from the DRI/HBI in the molten bath to produce carbon monoxide (CO) gas, resulting in the formation of foamy slag [25]. Oxygen is injected into the slag to facilitate this foaming process, as it reacts with coal to produce additional CO gas. Additionally, carbon is introduced to react with iron oxide, producing more CO gas and further contributing to foam formation. During this foaming process, the thickness of the slag cover can increase from 10 cm to 30 cm. In some cases, the slag may overflow from the electrode port due to excessive foaming [25].

According to Jones et al. [25], it is necessary to remove at least 0.3% carbon using oxygen to achieve optimal foamy slag. Once a deep foamy slag is established, it is possible to significantly increase the arc voltage, allowing for a higher power input. Generally, foamy slag develops after a flat bath is achieved; however, slag foaming can commence earlier during hot heel operations. Ito et al. [56] demonstrated that the foaming characteristics are influenced by a reduction in surface tension and an increase in the viscosity of the slag. The best foaming properties are found in a state that is neither entirely liquid nor fully solid, described as “creamy” and “fluffy.” This indicates that the slag is saturated with respect to CaO and MgO.

The formation and stability of the foam are determined by the chemical composition of the slag. Typically, the refractory slag line in the electric arc furnace is basic, requiring saturation of CaO and MgO in the slag composition. For effective foaming behavior and protection of the refractories, a minimum amount of MgO is essential. The required amount of MgO in the slag must be compatible with basic refractories based on a specific basicity ratio. As shown in Figure 3.8, the saturation limit of MgO decreases as the basicity of the slag increases.

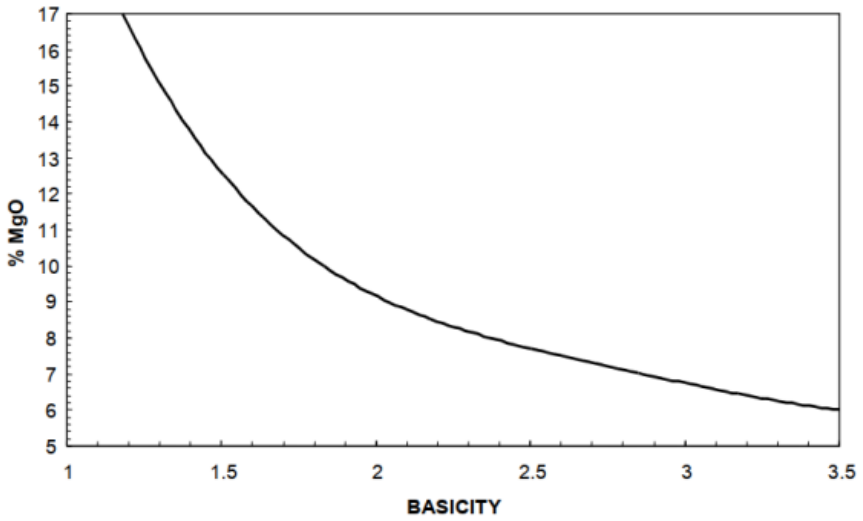


Figure 3. 8 The solubility of MgO for slags that are dual saturated with respect to CaO and MgO at 1600^0C [57].

The stability of foaming slag was enhanced by the addition of silica. Silica reduced surface tension, facilitating the formation of smaller CO bubbles. However, if silica concentrations in the slag became excessively high, it would lead to significant refractory loss. Additionally, increased silica levels would result in elevated FeO concentrations in the slag, as FeO exhibits better solubility in slags with higher silica content. This, in turn, would lead to a greater loss of iron yield in the Electric Arc Furnace (EAF) [25,57].

When oxygen was injected into the bath without the presence of carbon, it resulted in poor slag foaming, despite the adequate generation of gas. This approach was intended to raise the temperature and promote the formation of FeO through the exothermic reactions occurring below, which significantly reduced the viscosity of the slag [57]. The reaction as follow-

$C + ½ O_2 = CO$

$Fe + ½ O_2 = FeO$

The characteristics of slag, particularly its basicity and chemical composition, are crucial for managing slag volume during EAF operation. Increased slag volume often results from carbon monoxide (CO) generation, which enables the use of long arcs while ensuring effective arc coverage through foamy slag.

Key parameters influencing foaming slag formation include the slag basicity index, which should exceed 1.5, and the appropriate concentration of ferrous oxide (FeO). The primary constituents of EAF slag comprise calcium oxide (CaO), silicon dioxide (SiO_2), FeO, and magnesium oxide (MgO), along with minor components like aluminum oxide (Al_2O_3) and manganese oxide (MnO). Maintaining MgO content at around 8 to 10% helps mitigate refractory lining wear and ensures optimal saturation.

EAF operation features three zones based on viscosity and foaming behavior: high viscosity with good foaming, low viscosity with poor foaming, and high viscosity with inadequate foaming. Factors promoting foaming include oxygen and carbon availability, increased viscosity, lower surface tension, and maintaining a slag basicity greater than 2.5 with FeO levels between 15% and 20%. Utilizing foaming slag provides several operational benefits, such as enhanced productivity, reduced electrode consumption, decreased arc noise, and improved thermal efficiency. These advantages highlight the importance of optimizing slag behavior in EAF processes to boost operational efficiency and yield.

3.3.4 Deslagging

The deslagging process was conducted to remove impurities from the furnace. During the melting and refining processes, certain unwanted materials within the furnace bath were oxidized and transitioned into the slag phase. It was advantageous to remove phosphorus as early as possible in the heat cycle, particularly at lower bath temperatures. The slag was discharged into the slag pot through the furnace slag door during the backward tilting of the furnace, which effectively reduced the likelihood of phosphorus re-entering the system during deslagging [51]. Phosphorus reversion occurred during the slag foaming process, which was driven by CO gas generated from the reduction of FeO via carbon injection into the slag. Prior to the foaming slag operation, it was essential to eliminate high-phosphorus slag to prevent any chances of phosphorus relapse in the bath. The slag foaming process could lead to overspill, risking the slag exceeding the steel level in the electric arc furnace and flowing out of the slag door. The slag contains various oxides and other components [50]. A typical slag composition is provided in the Table below – 3.3.

Table 3. 3 Slag composition of EAF [50]

Component	Source	Composition Range
CaO	Charged	40 - 60%
SiO_2	Oxidation product	5 - 15%
FeO	Oxidation product	10 - 30%
MgO	Charged as dolomite	3 - 8%
CaF_2	Charged - slag fluidizer	
MnO	Oxidation product	2 - 5%
S	Absorbed from steel	
P	Oxidation product	

3.3.5 Tapping

After ensuring the ladle was positioned correctly under the EBT and confirming optimal steel temperature, chemical analysis, and additives, tapping could commence. Molten steel flowed into the ladle through the taphole, which then moved to the LRF for secondary refining. Tapping required tilting the furnace while ensuring the switch was off and the electrode holder was locked. To maintain a constant hot heel level, the furnace's tilting angle was restricted to 10.0°-12.5°. This approach enhanced bottom refractory life while limiting iron yield loss when carbon levels fell below 0.1% [54].

During EBT tapping, back-tilting speed needed adjustment to prevent slag transfer into the ladle, which was aided by maintaining an appropriate hot heel. Bulk alloys were added based on bath analysis, and deoxidizers like aluminum or silicon were used to reduce oxygen content. Minimizing slag carryover was a goal, and slag-making materials were added to form a cover before transferring to the LRF. In the LRF, calcium aluminate slag effectively controlled sulfur content, with surplus slag compounds added if cover was insufficient [51]. Fig. 3.9 shown EBT furnace tapping into a ladle at AKS.



Figure 3.9 EBT Furnace Tapping [AKS melting plant in Chittagong].

3.3.6 Furnace Turnaround

Furnace turnaround refers to the duration from the completion of tapping until the release of the first scrap charge into the furnace for the next heat [25]. During this period, the electrodes and roof are raised to inspect the furnace lining for any refractory damage. If necessary, maintenance is carried out on the hearth, slag line, and taphole. In the case of a bottom-tapping furnace, the taphole is filled with sand [50]. Maintenance of the furnace's refractory lining is typically performed using gunned materials. However, in more recent furnace designs, the incorporation of water-cooled panels has significantly reduced the need for patching or fettling between heats. Many operations now regularly turn off the furnace bottom every 2 to 6 weeks to conduct

maintenance tasks while offline. This practice minimizes furnace downtime and boosts production efficiency. Typically, furnace turnaround time represents the most significant dead time within the tap-to-tap cycle. Fortunately, advancements in furnace technology have reduced this duration from 20 minutes to less than 5 minutes in modern furnaces [50].

3.3.7 Furnace Heat Balance

Theoretically, a minimum of 300 kWh per ton of energy is required to melt steel scrap. Therefore, the total theoretical energy needed is between 350 and 370 kWh per ton in modern furnace operations to achieve superheating above the melting point of 1520°C and reach typical tapping temperatures. However, in EAF steelmaking, only 55-60% of this energy is effectively utilized in molten steel. As a result, the total input energy for modern furnaces generally ranges from 560 to 680 kWh per ton. This input energy is sourced from various methods, including electricity (50-60%), oxy-fuel burners (5-10%), and chemical bath reactions (30-40%) [50]. A typical energy balance for both older and more modern EAFs is illustrated in the following Table 3.4.

Table 3. 4 Heat balance of old and new modern EAF [50]

Inputs:	**Low to medium furnace**	**UHP furnace**
Electricity	75 - 85%	50 -60%
Burner	0%	5 - 10%
Bath Reaction	15 - 25%	30 - 40%
Total Inputs	**100%**	**100%**
Outputs:		
Steel	50 – 55%	55 - 60%
Slag	8 -12%	8 -10%
Cooling water loses	5 – 6%	8 -10%
Off gas loses	7 – 10%	17 -28%
Miscellaneous Loses	17 – 30%	1 -3%
Total Output	**100%**	**100%**

The data presented in Table 3.4 is influenced by several factors, including raw material components, power input ratings, and operating practices (such as post-combustion and scrap preheating). These factors can significantly alter the heat balance value. A substantial amount of charge carbon or the use of high-carbon raw materials in furnace operations can result in up to 60% of the energy being contained in the off gases, primarily due to large quantities of unburned carbon monoxide. By recovering this significant energy in the EAF, energy input could potentially be increased by 8-10% [50].

3.5 IMPACT OF RAW MATERIALS ON STEEL MAKING OPERATION

The raw materials utilized in a melting plant include shredded scrap, heavy melting scrap (HMS), HBI, and pig iron, supplemented by lime, dolomite lime, and coke (carbon) to facilitate slag

formation. In the EAF, oxygen is injected to cut and combust the scrap, thus producing slag, with FeO serving as a critical component. Following the completion of the refining process, oxygen lancing is executed to penetrate the slag and react with the molten metal. Notably, this facility lacks both a scrap preheating system and the utilization of hot raw materials in the steel-making process. The optimization of charge mix is crucial, as it has a substantial influence—approximately 75-85% -on the overall cost of liquid steel produced via the electric steelmaking route [56].

On the other hand DRI, HBI, pig iron, iron carbide, and hot metal serve as alternative iron charge materials, which can be combined with steel scrap in various proportions during the EAF steelmaking process. The incorporation of HBI can significantly impact the melting operation, considering the chemical properties of DRI/HBI and their respective percentages in the raw materials, all of which contribute to energy consumption, productivity, and yield [58,59].

The adoption of DRI as a substitute for high-quality scrap in EAFs has garnered increased acceptance due to its freedom from tramp elements, consistent density and shape, improved yield, and higher carbon content, which facilitate ease of charging and offer economic advantages. To achieve the desired special steel grades from scrap materials of high quality, it often becomes necessary to reduce undesirable tramp elements such as Cu, Pb, Cr, Ni, Mo, and Sn through the replacement of scrap with DRI and pig iron [60,61].

The rising global prices of scrap and the scarcity of high-quality steel scrap have rendered the mixture of steel scrap and alternative iron charge materials in electric arc furnace steelmaking more economically viable. For production aimed at achieving specific quality standards—characterized by low nitrogen, very low phosphorus, and low hydrogen levels—DRI/HBI is preferred. The nitrogen content of steel tapped from 100% steel scrap in the EAF typically ranges between 40 and 100 ppm, while nitrogen levels for DRI charges are considerably lower, ranging from 15 to 25 ppm. To maintain low nitrogen levels, large-scale argon purging or vacuum degassing is essential.

Kirschen et al. [61] investigated that the natural gas-based DRI production process yields higher metallization and carbon content compared to coal-based methods. Optimal metallization percentages in DRI, ranging between 94–96%, yield advantageous results in the steelmaking process. A lower metallization level in DRI correlates with an increased presence of FeO that necessitates reduction to enhance iron yield within the EAF process. DRI exhibits a high bulk density, surpassing that of slag in the furnace, thereby facilitating melting at the slag/metal interface. The DRI feeding rate emerges as a critical procedure parameter within the EAF,

typically ranging from 27 to 35 kg/min/MW, influenced by the chemical composition of DRI, bath temperature, carbon-oxygen injection, and bottom stirring.

Further analysis by Kirschen et al. [61] shows that DRI-based EAFs have longer charge melting times than traditional scrap-based EAFs due to the reduction of FeO. DRI introduces SiO_2 and Al_2O_3 gangue materials, generating acidic slag and requiring more lime and dolomite lime for proper slag basicity (approx. $xCaO/xSiO_2 = 2$). This results in larger slag volumes and extended melting times, leading to higher electrical energy consumption, as carbon reduces FeO through an endothermic reaction, resulting in even more slag generation.

The oxygen consumption during the process was similar in both scenarios, influenced primarily by the FeO and carbon content in HBI. When pig iron is combined with HBI in the steel-making process, the oxygen consumption decreases due to the higher carbon content (approximately 4%) in HBI, which leads to reduced oxide formation and lower overall carbon consumption [61].

Research conducted by Heo et al. [60] indicated that utilizing a high quantity of DRI in EAF steelmaking complicates the dephosphorization process. This challenge arises from a reduction in slag basicity and a destabilization of P_2O_5 in the slag. As the percentage of DRI increases, the SiO_2 content in the slag also rises, resulting in a more acidic slag composition. Therefore, it is critical to enhance the slag's basicity to improve dephosphorization efficiency within the EAF process.

Cavaliere [47] highlighted that the incorporation of DRI into the EAF process escalates electrical energy consumption due to the necessity of reducing FeO. The correlation between the percentages of DRI charged and the resultant electrical energy consumption is illustrated in Figure 3.10.

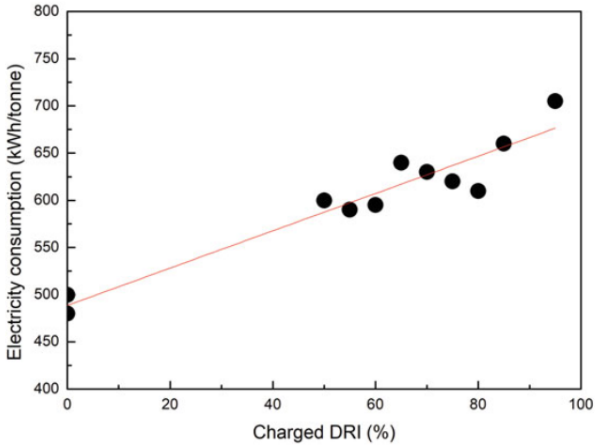


Figure 3. 10 Specific electrical energy consumption versus DRI charging ratio [47].

It is important to note that electrical energy consumption is higher when utilizing DRI compared to scrap. This increase is attributed to the presence of acid gangue in DRI, which necessitates lime

addition to neutralize it and enhance slag basicity in the EAF steelmaking process. Consequently, the volume of slag generated from melting DRI is greater than that from scrap. To manage electrical energy consumption when charging DRI, achieving a high metallization percentage is beneficial. The relationship between electrical energy consumption and DRI metallization across varying percentages of DRI addition to scrap is illustrated in Figure 3.11.

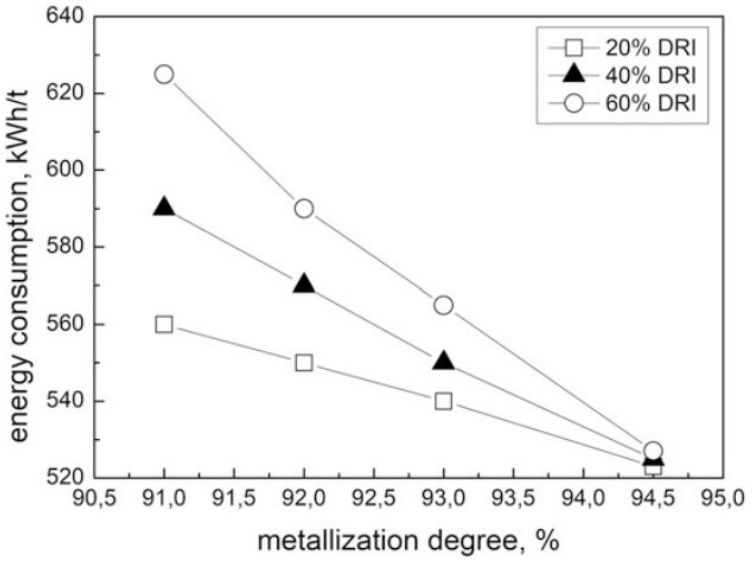


Figure 3. 11 The specific energy consumption versus metallization degree (%) with respect to different percentage addition of DRI to the scrap [47].

Cavaliere [47] reported that a 1% increase in DRI metallization can lead to energy savings of up to 25 kWh/ton. Also, the presence of gangue, primarily SiO_2, contributes to an increase in energy consumption of approximately 10 kWh/ton for every 1% increase in DRI charge, particularly when the DRI content reaches 60%. The type and quality of DRI utilized in EAF significantly influence electrical energy consumption during the process. The carbon content in DRI is crucial, as it serves as an external energy source. When combined with injected oxygen, it generates CO gas through an exothermic reaction, which aids in forming a foamy slag and consequently reduces electrical energy requirements. Furthermore, carbon can react with unreduced FeO to produce additional CO gas, enhancing slag foaming. Generating CO gas within the melt is vital for effective slag foaming, achieved through carbon and oxygen injection via lances or burners.

To optimize foamy slag formation in the EAF process, attention must be paid to slag chemistry. Maintaining a slag basicity above 1.5 is essential, which can be accomplished by controlling the FeO content in the slag. The FeO level should be balanced; too low or too high concentrations can negatively affect operations. Major slag constituents include CaO, SiO_2, FeO, and MgO, with additional components such as Al_2O_3, MnO, and P_2O_5 derived from lime, dolomite lime, scrap oxides, DRI gangue, oxidation byproducts from the metallic charge, carbonaceous ash, and MgO contributions from refractories, as well as residual slag from previous heats.

Increasing the carbon content and temperature of DRI/HBI is associated with a reduction in specific electrical energy consumption. The relationship between temperature, carbon content, and electrical energy use in the EAF process is illustrated in Figure 3.12. Improved performance is linked to the utilization of high-quality DRI/HBI in the charge as shown in Figure 3.13. The gangue content and metallization percentage of DRI significantly impact electrical energy consumption, as depicted in the analysis presented in Figure 3.14.

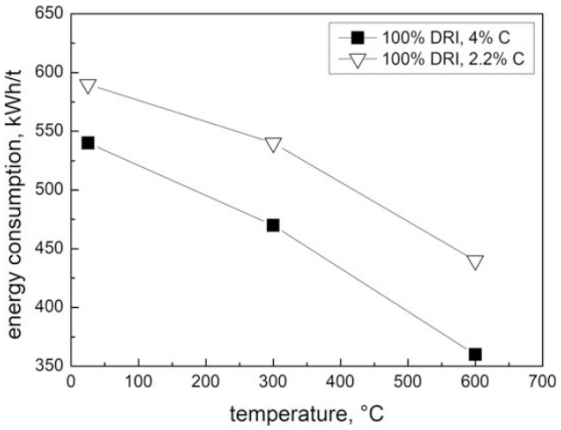


Figure 3. 12 Specific energy consumption versus DRI temperature with carbon % [47].

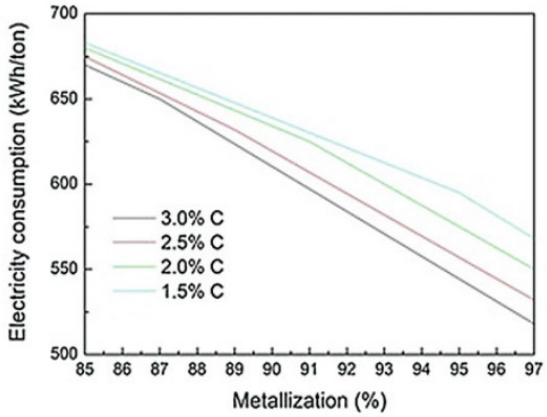


Figure 3. 13 Specific energy consumption versus DRI metallization % with carbon content % [47].

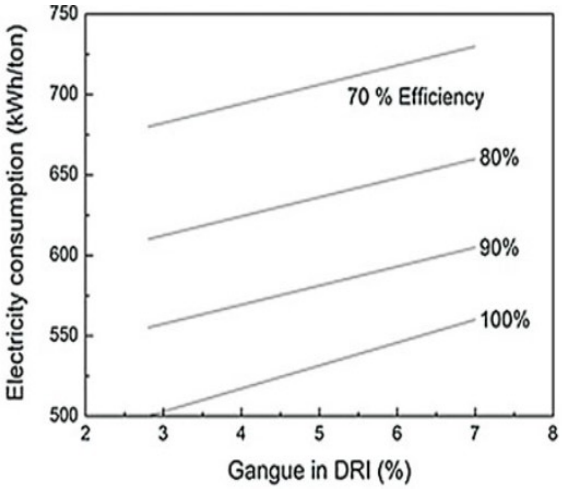


Figure 3. 14 Specific energy consumption versus gangue % (DRI) with efficiency [47].

In HBI, the carbon content ranges from 1.7% to 2%, which is significantly higher than that found in scrap, typically between 0.2% and 0.3%. This higher metallization percentage in HBI allows for reduced carbon consumption when used in conjunction with scrap during steelmaking, compared to a scenario using 100% scrap. However, this scenario leads to increased consumption of electrodes, lime, and energy compared to using solely scrap. Pig iron, with its carbon content of approximately 4% and 100% metallization, presents a distinct advantage when paired with scrap. Its use enhances the chemical energy available during the melting process, thereby accelerating both melting rates and overall productivity relative to a 100% scrap charge [35].

To optimize iron recovery and enhance yield, adequate carbon levels are crucial to balance the FeO content in DRI. Research by Jones and Bowman [25] indicates that around 1% carbon is required in the bath to counteract 6% FeO. Insufficient carbon in the bath can lead to yield losses unless additional carbon is injected into the process. Conversely, introducing carbon into the steel bath allows for reduced electrical energy consumption by enabling the injection of oxygen as an external energy source for the EAF process.

Typically, DRI requires an additional 100 – 200 kWh/ton for melting compared to scrap. In the EAF process, up to 25% DRI can be incorporated into the charge mixture, and it can be introduced continuously through the 5th hole, mitigating thermal losses during DRI charging. Notably, DRI tends to float at the slag bath line while HBI, being denser (2.5–3.3 tons/m^3), sinks and melts similarly to pig iron. The silica content in DRI also plays a critical role in the economic impact on steelmaking; if lime is insufficient to counteract the silica erosion of refractories, additional lime is necessary to achieve the desired slag basicity (2.5 – 3.0) for foamy slag, thereby increasing electrical power consumption for melting.

Incorporating 10-15% pig iron into the charge can result in energy savings during the EAF process due to its high carbon content (4-4.2%) which reacts with injected oxygen, generating substantial heat through chemical reactions that lower energy consumption. Furthermore, the silicon content in pig iron, generally up to 0.65%, can react with oxygen to produce silica (SiO_2), which ultimately contributes to the slag, necessitating additional lime to maintain slag basicity.

The variability of DRI/HBI properties significantly affects the EAF process, with metallization percentage being a key factor as it determines the FeO content retained in DRI/HBI. Excess FeO in HBI reacts with carbon, generating CO through endothermic reactions that subsequently elevate specific energy consumption. Various DRI manufacturers strive to optimize the quality of DRI with sufficient carbon content and high metallization percentages to minimize FeO in the bath [61]. The overall energy consumption in the EAF process is contingent on the specific type of DRI/HBI utilized. The carbon content in DRI serves as an external energy source by generating

CO gas through reactions with injected oxygen, aiding in the formation of foamy slag. Additionally, since DRI/HBI is produced from iron ores with higher gangue content than scrap, more lime is required to achieve the desired slag characteristics. This increased lime demand results in higher energy consumption for melting and slag production, making DRI usage in the EAF process more energy-intensive than a 100% scrap charge [62]. The typical properties of DRI are outlined in the following table – 3.5.

Table 3. 5 Typical properties of DRI [62].

Property	**Value**
Total iron	87 - 94 %
Metallic iron	83 - 88 %
Metallization	91 - 95 %
FeO	6 - 11 %
Carbon	0 - 4.5%
Phosphorus	0.01 - 0.080 %
Sulfur	0.03 - 0.15 %
Silica	1.0 - 4.5 %
Alumina	0.3 - 2.0 %
CaO	0.2 - 1.5 %
MgO	0.1 - 0.6 %
Basicity (B_4) = (CaO + MgO)/(SiO_2 + Al_2O_3)	0.06 - 0.6 %

The operators in EAF have consistently raised concerns regarding the reduced yield associated with the incorporation of DRI, primarily due to insufficient process adjustments. The elevated FeO content in DRI significantly contributes to this yield reduction, as it necessitates either excessive oxygen intake during the process or insufficient carbon injection to counterbalance the oxygen levels [62].

Research by Hornby et al. [63] has indicated that when integrating a 10% DRI charge with raw materials, there is an additional energy requirement of 13.63 kWh/ton, coupled with a tap-to-tap time increase of 2.5 minutes in the EAF. Additionally, the volume of slag tends to rise due to the necessity of incorporating extra lime to neutralize silica, which results in a yield loss of approximately 0.4%. Moreover, every 1% decrease in metallization in DRI charging correlates with an increase in total energy consumption ranging from 7.3 to 14.6 kWh/ton. Interestingly, when 10% of PI (with 4% carbon) is utilized in the charge blend, there is a notable reduction in total energy consumption by 24.6 kWh/ton. While concentrating on the mix of scrap and DRI, it's essential to consider the gangue content, which can exceed 10% when selecting lower quality materials that contain dirt and other non-metallic impurities [63]. A comparative analysis of DRI versus average scrap at AM Mexico is elaborated in Table 3.6.

Table 3. 6 Comparative analysis of DRI & average scarp at AM Mexico [63]

AM Mexico	Total Fe	% FeO	%C	% Gangue
DRI	90.8	6.77	2.08	4.47
Average scrap	93.85	1.88	0.47	4.25

Introducing hot metal or molten pig iron into an EAF as part of the charge mixture at temperatures ranging from 1200 to 1400°C contributes sensible heat to the process. This approach effectively reduces electrical energy consumption required for molten steel production. The hot metal, with its 4.5% carbon content, also facilitates additional chemical energy input through the decarburization process via injected oxygen. As a result, the overall electrical energy demand within the bath is minimized.

Research conducted by Grant et al. [62] demonstrated that increasing the proportion of hot metal in the EAF charge leads to a reduction in electrical energy consumption while simultaneously enhancing furnace productivity. Figure 3.15 illustrates the correlation between electrical energy consumption and the percentage of hot metal charged.

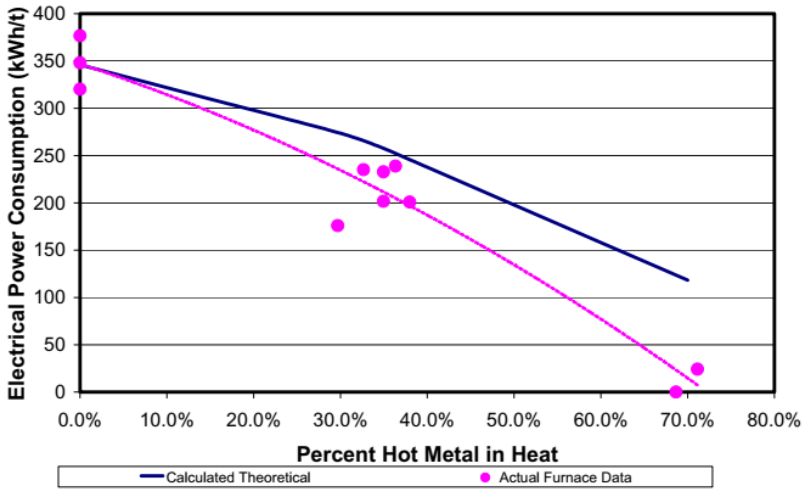


Figure 3. 15 Electrical energy consumption versus percentage of hot metal charged [62].

Grant et al. [62] also demonstrated that for optimal EAF productivity, the proportion of hot metal in the charge mix can be increased up to 40%. An increase in the percentage of hot metal up to this threshold enhances furnace productivity. However, exceeding 40% hot metal leads to a decline in productivity. This drop in efficiency is attributed to the higher volume of oxygen required for decarburizing the elevated carbon content in the hot metal, which ultimately compromises process efficiency and pushes it beyond optimal operational parameters. Figure 3.16 illustrates the relationship between furnace productivity and the percentage of hot metal charged.

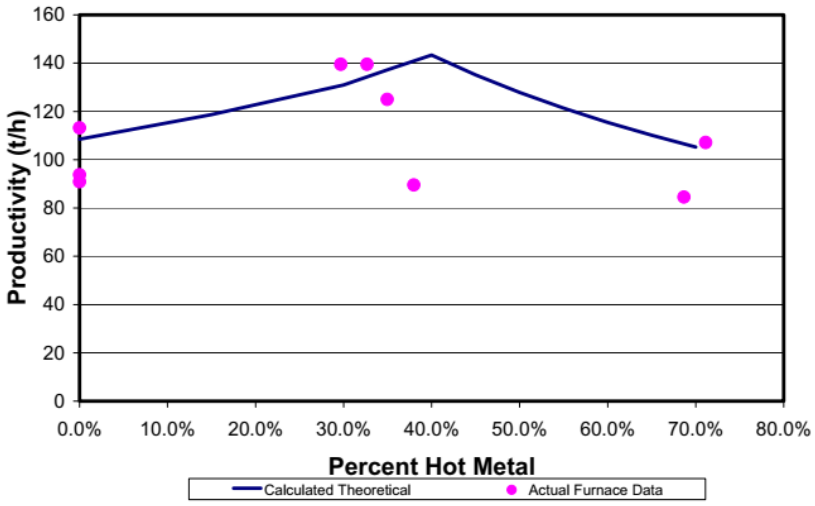


Figure 3. 16 Furnace productivity versus hot metal charged percentage [62].

A study conducted by Ali et al. [10] highlighted the benefits of injecting oxygen into the molten bath, which facilitates an exothermic reaction between oxygen and elements such as carbon, silicon, and iron. This reaction generates additional heat energy, leading to a reduction in both electrical energy consumption and electrode wear, while also minimizing refractory degradation. Consequently, these effects contribute to a decreased melting time and enhanced productivity. Oxygen lancing was implemented at the surface of the steel bath to perform post-combustion reactions with carbon monoxide and hydrocarbons prior to the exhaust gases exiting the furnace. This approach further maximizes heat generation through exothermic reactions within the furnace, allowing for reduced electrical energy requirements.

In the context of DRI and HBI, the primary gangue material present is SiO2, alongside impurities like sulfur and phosphorus. The lime addition in the EAF process is adjusted based on the DRI composition and the percentage of DRI utilized in the charge mix. To enhance slag basicity and decrease sulfur and phosphorus concentrations, lime is introduced, which is essential for attaining the desired steel grade. It is noted that total lime consumption escalates with increased DRI/HBI input into the EAF. A common guideline indicates that for every 10% rise in DRI content within the charge, lime consumption increases by approximately 2.6 kg/ton in the bath [64].

Madias et al. [65] demonstrated that specific electrical energy consumption is contingent upon the materials used and the thermal condition of the charge. When the EAF charge mix contains over 20% hot metal (molten pig iron), the specific energy consumption drops below 300 kWh/ton. Conversely, if pig iron is processed alongside steel scrap, the specific energy consumption ranges between 300 and 400 kWh/ton. The inclusion of hot DRI with scrap material results in a specific energy consumption of 400 to 450 kWh/ton. A significant increase in electrical energy consumption—exceeding 450 kWh/ton—is observed when large quantities of cold DRI/HBI are

charged with scrap in the EAF. Figure 3.17 illustrates the relationship between specific electrical energy consumption and the ratio of raw materials, correlating with input power.

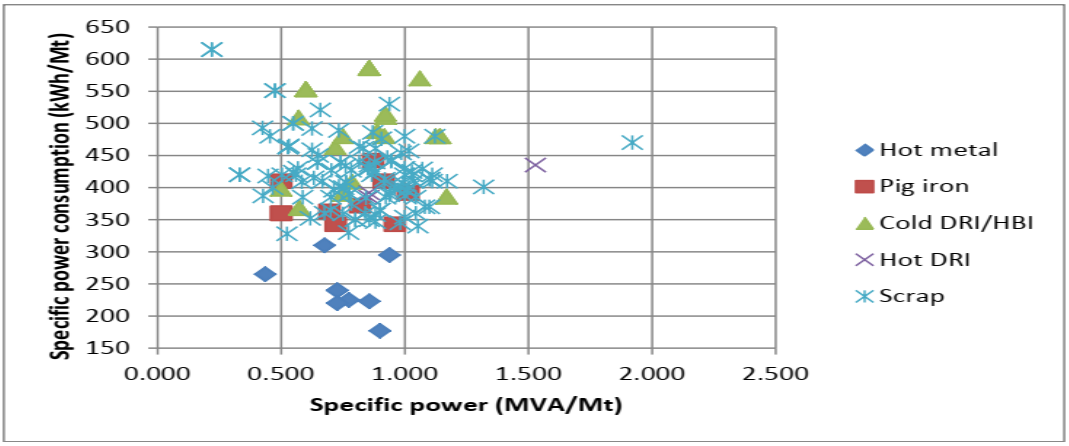


Figure 3. 17 Specific energy consumption versus raw materials ratio with input power [66].

Chapter-04
Data collection and Methodology

4.1 DATA CAPTURING

In this project, a comprehensive analysis of the steel-making operation and refining process was conducted using data collected from a prominent steel melting plant, AKS located in Chittagong. This particular facility operated its EAF with various mixture ratios, each composed of different raw materials. Over a span of five months, four distinct mixture ratios were examined closely, allowing for an in-depth understanding of their impact on the steel production process. The four mixture ratios (MR), along with their respective compositions, are outlined as follows:

1. MR – 1: Scrap -85 % (Shredded – 55% + HMS – 30%), Pig Iron – 5%, HBI – 10%
2. MR – 2: Scrap -87.7 % (Shredded – 67.7% + HMS – 20%), Pig Iron – 12.30%
3. MR – 3: Scrap -72 % (Shredded – 50% + HMS – 22%), Pig Iron – 15%, HBI – 13%
4. MR – 4: Scrap -60 % (Shredded – 40% + HMS – 20%), Pig Iron – 12%, HBI – 28%

In this study, comprehensive data from the steel melting plant has been carefully organized and presented in Tables 4.1 through 4.4 in the Appendices. These tables provide an in-depth analysis of the operational parameters associated with each mixture ratio, highlighting the various refining objectives and outcomes achieved during the steel-making process. Section 4.2.1 exclusively discussed the steelmaking process for mixture ratio 1, as the processing methodology for the other mixture ratios follows a similar approach.

4.2 METHODOLOGY

This project provides a comprehensive examination of the components and operation of the DC EAF in the steelmaking process. It begins with a detailed exploration of the steelmaking process, highlighting the various raw materials used. Key operational stages—including raw material preparation, bucket filling, material charging, melting, refining, tapping, and deslagging were analyzed using data from the AKS melting plant.

The investigation further explored critical parameters associated with the steelmaking process, such as specific power consumption, tap-to-tap timing, carbon and electrode consumption, and lime consumption. These parameters were evaluated in relation to four distinct raw material charge mixtures, with results clearly represented in graphical form. A comparative analysis of these parameters across the different charge ratios was conducted to identify the most cost-effective and productive mixtures for EAF steelmaking.

In addition, the project discusses the incorporation of DRI, HBI, pig iron, and hot metal alongside steel scrap in the melting process. It assesses key properties of the various raw materials, including metallization percentage, carbon content percentage, FeO percentage, and gangue content percentage. The influence of these properties on critical process parameters—such as specific electrical energy consumption, carbon consumption, electrode usage, tap-to-tap time, and lime consumption was also thoroughly analyzed. The whole project work is graphically present in bellow Figure 4.1.

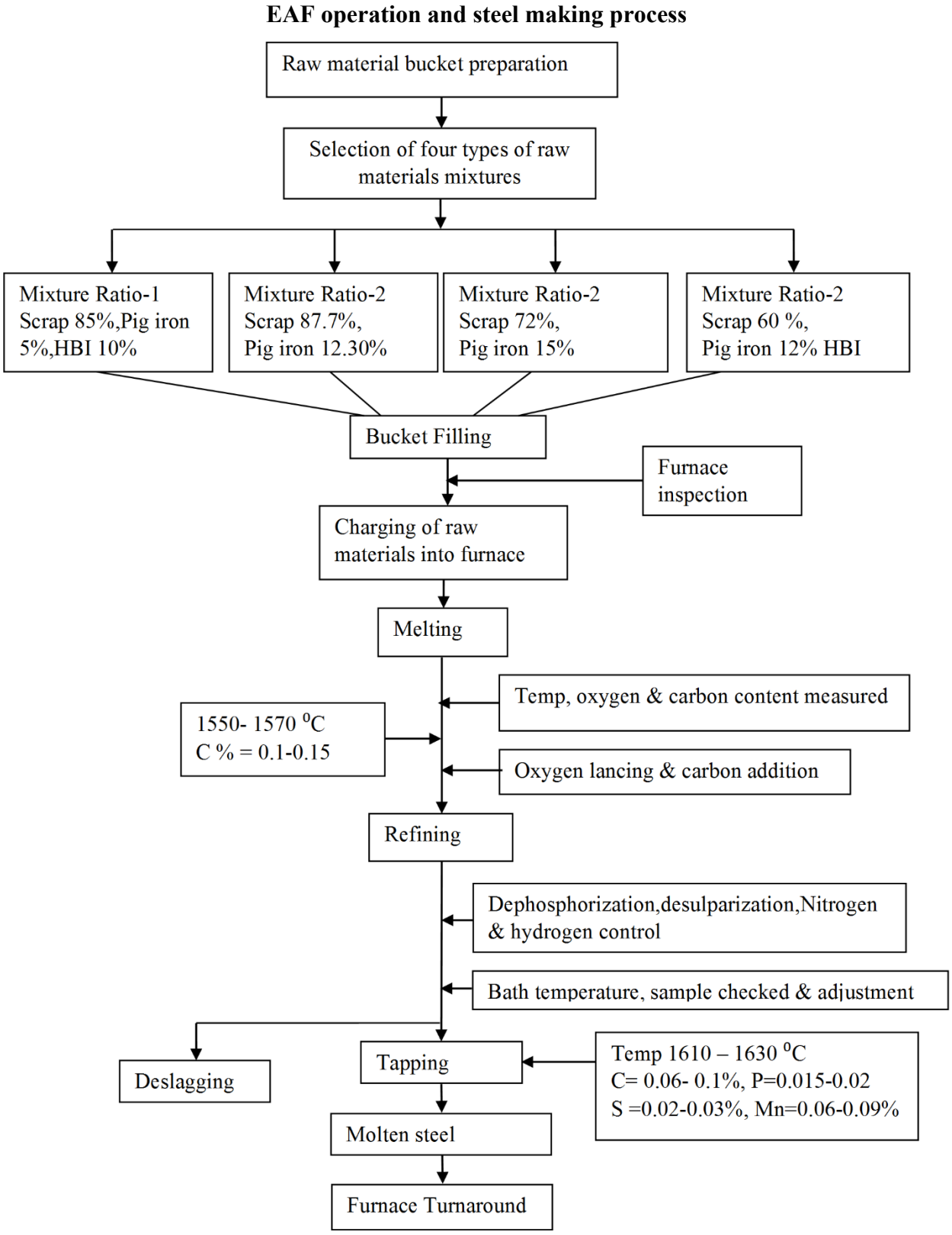


Figure 4. 1 Flowchart of EAF operation and steel making process.

4.2.1 Process Sequence of 85% Scrap, 5% Pi and 10% HBI Mixture

The steelmaking process for the raw materials of MR-1 (at AKS melting plant), which consists of 85% scrap, 5% pig iron (PI), and 10% hot briquetted iron (HBI), is outlined below:

Charge Materials

To produce 85 tons of steel for tapping at the AKS plant, we first determined the necessary proportions of charge materials, considering the different mix ratios. It is essential to maintain a hot heel of approximately 15 tons after tapping. The raw materials will be charged in three buckets: the first bucket will weigh 37 tons, the second will weigh 30 tons, and the third will weigh 27 tons.

Charge Lime and Dolomite Lime

Lime was charged through the fifth hole, totaling approximately 2,680 kg per heat. The distribution of lime is as follows: approximately 900–1,000 kg in the first bucket melting, about 800–900 kg in the second bucket melting, and approximately 800–1,000 kg during the third bucket melting and final overheating phase. This last quantity may be delivered in one or two shots, depending on the availability of the RMH system, with the first shot comprising 400–500 kg and the second shot the same amount.

The total weight of dolomite charged was 1,130 kg per heat, with the entire quantity recommended to be placed in the first bucket. This approach helps achieve MgO saturation in the slag from the early melting phase, thereby reducing refractory wear due to slag attack on MgO-C bricks.

Carbon in Charge

The total carbon charge was calculated at approximately 500 kg per heat, with all carbon added during the first bucket.

Carbon Injection

Consequently, the total carbon injected was around 1,000 kg per heat. This carbon was injected during the operation of the modules and the PARPI slag-door lance at the conclusion of melting for the first, second, and third buckets, as well as during the refining process. The injection timing and flow rate were managed by a Level 2 automation melting profile.

Melting Procedure

In the operational mode, the electric working points and module profiles were controlled via computer systems utilizing level-2 automation. Manual intervention was only employed in emergency situations or in the event of automation malfunctions.

The process of scrap melting commenced with a reduced power setting to minimize radiation exposure, lasting approximately 2 minutes (preliminary working parameters: power 40-45 MW, current 90 kA). Following this initial phase, power inputs were increased once the electrodes were entirely enveloped by scrap material, ultimately reaching the maximum operational parameters of 60-65 MW power at 90 kA current. During the melting of the first half of the scrap bucket, injection of oxygen and carbon commenced. The carbon injection was sustained until the

completion of the initial melting phase. The introduction of both oxygen and carbon facilitated the foaming of the slag, which positively impacted the reduction of refractory material consumption and enhanced the efficiency of heat transfer from the electric arc to the molten steel. At the conclusion of the melting process, the flow rates for oxygen and carbon were set at 1200 Nm^3/hr and 20 kg/min, respectively; the oxy-fuel burner operated at a flow rate of 500-600 Nm^3/hr. It is noteworthy that all flow rates were gradually increased from the commencement of the melting procedure.

Subsequent buckets of scrap were subjected to the same operational protocol, where melting began with the boring phase followed by maximum power application. In cases where the furnace temperature was low, it was deemed necessary to increase specific energy consumption. The burners operated under level-2 set points during the first half of the bucket melting phase, after which the oxygen and carbon lances were activated, continuing the injection until the completion of the melting process to ensure optimal slag foaming conditions. The flow rates for oxygen, carbon injection, and lancing were systematically increased throughout the process.

During the overheating phase, the formation of a well-defined foamy slag was of paramount importance. This required an increased carbon feeding rate along with lime addition to achieve the desired thickness of slag foam. The quantities of dololime, lime, and carbon additions were contingent upon the scrap quality, as dictated by the concentrations of SiO_2, phosphorus (P), and sulfur (S). The slag basicity, essential during the melting process, was maintained within the range of $CaO/SiO_2 = 2.0 – 2.2$.

At the refining stage, temperature readings and samples were taken at 1560 - 1580°C, with the anticipated chemical composition being: carbon (C) at 0.15 – 0.25%, phosphorus (P) < 0.020 – 0.030%, and sulfur (S) < 0.030%. Samples from the molten bath were obtained using a disposable thermocouple probe, linked to a SIDERMAS device for real-time temperature and carbon measurements displayed on the device. Additionally, material composition analysis of the molten metal was conducted using a spectrometer, with the temperature recorded at 1630°C, aligning with expectations. Upon completion of slag reduction and achieving the desired chemical analysis, the process proceeded to tapping, marking the completion of one heat cycle. Table 4.1 presents various technical parameters concerning the specific raw materials utilized in the tapped steel production.

Table 4. 1 Technical parameters of specific raw materials tapped Steel [AKS melting plant in Chittagong]

Description		
Tapped steel	Ton	85
Charge ratio (scrap/PI/HBI)	%	85%/5%/10%
Number of buckets	Pcs	03
Tap to tap timing	mins	47
Power on/Arching time	mins	35.91
Electric power input	MW	65
Specific power consumption	Kwhr/Ton	386.1
Electrode consumption	Kg/Ton	1.18
Lime consumption	Kg/Ton	26.8
Dolomite lime	Kg/Ton	11.3
Carbon consumption	Kg/Ton	14.9
Oxygen consumption	Nm^3/Ton	22

Chapter -05
Data Analysis and Discussion

5.1 INTRODUCTION

The steel industry plays a key role in the national economy and significantly impacts community welfare. Its development catalyzes progress across various economic, industrial, scientific, and social sectors. In particular, the EAF steelmaking process is characterized by its economic efficiency and operational flexibility compared to alternative steelmaking methods [67]. However, it faces notable challenges related to raw material utilization, operational efficiency, and environmental sustainability. A critical issue to consider is that flue gas emissions from the furnace may have significant levels of unburned CO resulting from insufficient oxygen availability during the combustion process [68]. In this context, this report conducted a detailed analysis of several operational parameters, including specific power consumption, tap-to-tap timing, carbon consumption, lime consumption, and electrode consumption, across four distinct raw material mixture ratios. The goal was to determine the most cost-effective and efficient mixture ratio that optimizes these operational metrics. Graphical representations illustrate the comparative analysis of specific power consumption, tap-to-tap timing, carbon and lime consumption, and electrode usage for each mixture ratio. The findings highlight the optimal operational parameters associated with raw material mixtures, offering insights into enhancing both efficiency and productivity within the EAF process. The results and discussions elaborated herein provide a comprehensive understanding of the interplay between raw material composition and operational performance in steelmaking.

5.2 DATAANALYSIS

5.2.1 Graphical Representation of four mixture ratios

In this analysis, the influence of the raw materials mixture ratio (MR) on various operational parameters, including specific power and electric energy consumption, tap-to-tap timing (TTT), as well as the consumption of carbon, lime, and electrodes, was examined through graphical representation. Figure 5.1 presents the analytical results in relation to the number of "heats," a term in EAF operations referring to the melting of 100 metric tons of material which comprised different charge mixture ratios over a duration of 40 to 60 minutes, followed by the transfer of the molten metal into a ladle. In a steel melting plant, the production of molten steel via batch or bucket charging is designated as "heat".

It is noteworthy that the permissible carbon content in HBI ranges from 0.4% to 1.1%, with metallization levels between 92% and 93.5% in the AKS melting plant. For other materials, the carbon content in pig iron is reported at 4%, while scrap metal contains 0.2% to 0.3% carbon. Figure 5.1 illustrates that specific power consumption, TTT, carbon consumption, lime consumption, and electrode consumption exhibit similar trends concerning the number of heats. Notably, the highest specific power consumption, recorded at 401.9 kWh/ton, and the longest TTT of 52 minutes, both occurred during heat number 2.It was noted that due to the similar results recorded over time with several number of 'heat', only the first eight data points were presented graphically for analysis.

Figure 5.2 reveals that the lowest specific power consumption, measured at 338 kWh/ton, was attributed to MR-2, in contrast to other mixing ratios. Conversely, the maximum specific energy consumption, reaching 412 kWh/ton, was documented for MR-4 (Figure 5.4). In MR-2, the composition consisted of 87.7% scrap and 12.3% pig iron, with the carbon content in pig iron being 4% and achieving 100% metallization, contingent upon maintaining low levels of iron oxide (FeO) and gangue content. The elevated carbon content in pig iron facilitates an exothermic reaction with injected oxygen, generating additional thermal energy within the bath. Furthermore, the reduced FeO content in pig iron correlates with diminished energy consumption, as evidenced by literature [33,54]. Furthermore, lower gangue content implies reduced SiO_2 levels, thereby leading to minimized lime consumption and shortened melting durations. The role of pig iron is pivotal in augmenting melting efficiency and overall productivity. For example, a combination of 12% to 15% pig iron with 85% to 87% scrap enhances chemical energy in the steelmaking process, resulting in accelerated melting and increased productivity compared to the exclusive use of scrap.

In MR-3, as displayed in Figure 5.3, the highest recorded specific power consumption and TTT were approximately 385 kWh/ton and 60 minutes, respectively. Lime consumption reached about 28.2 kg/ton, with electrode consumption remaining relatively stable at approximately 1.2 kg/ton.

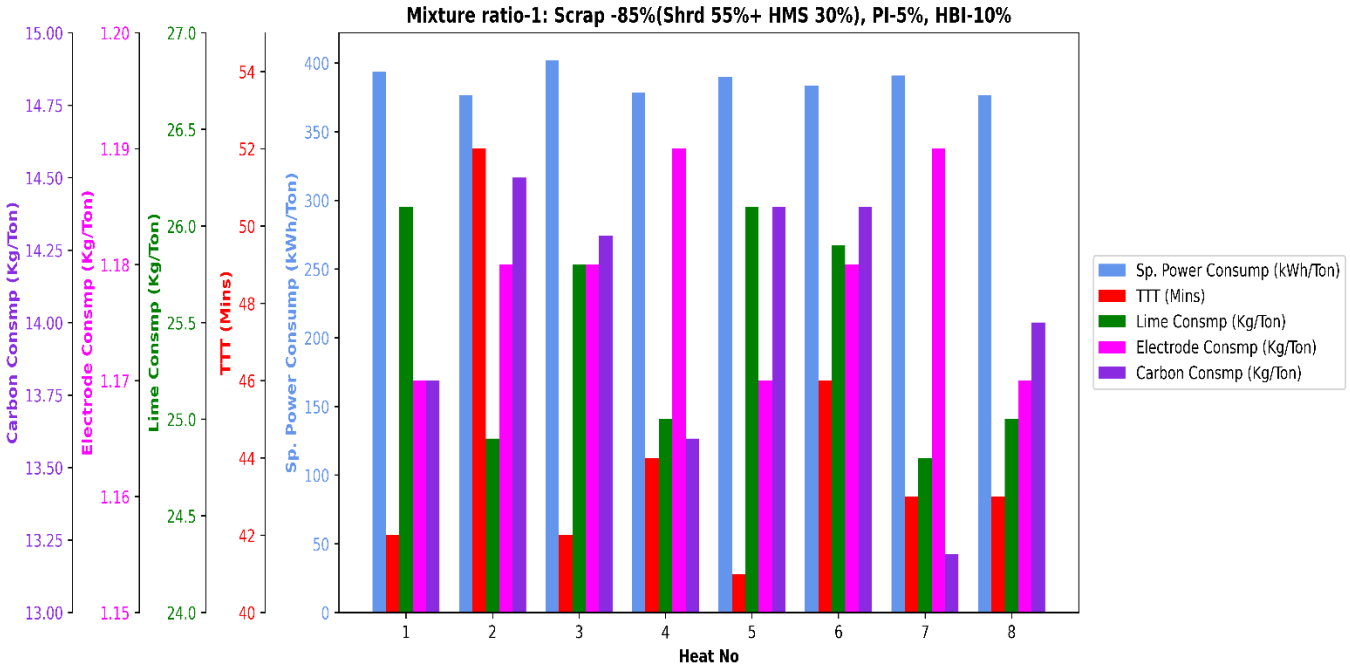


Figure 5.1: MR -1 [Scrap -85 % (Shredded – 55% + HMS – 30%), Pig Iron – 5%, HBI – 10%]

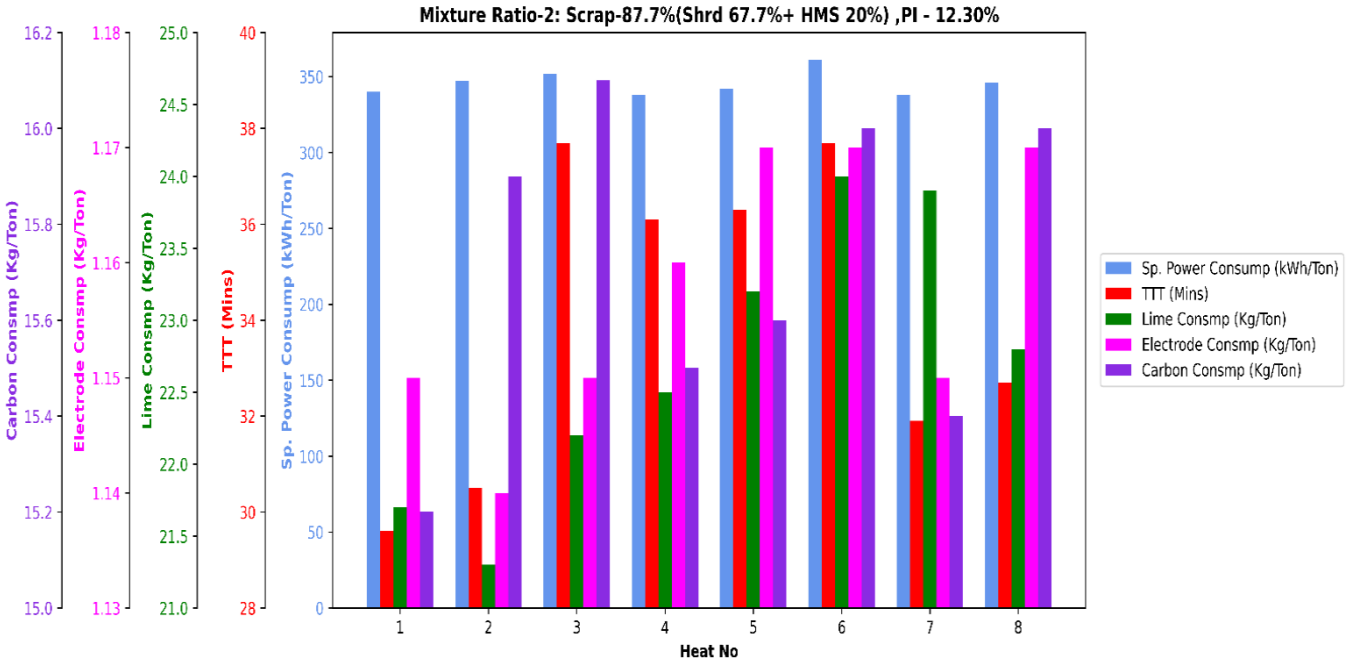


Figure 5. 2: MR-2 [Scrap -87.7 % (Shredded – 67.7% + HMS – 20%), Pig Iron – 12.30%].

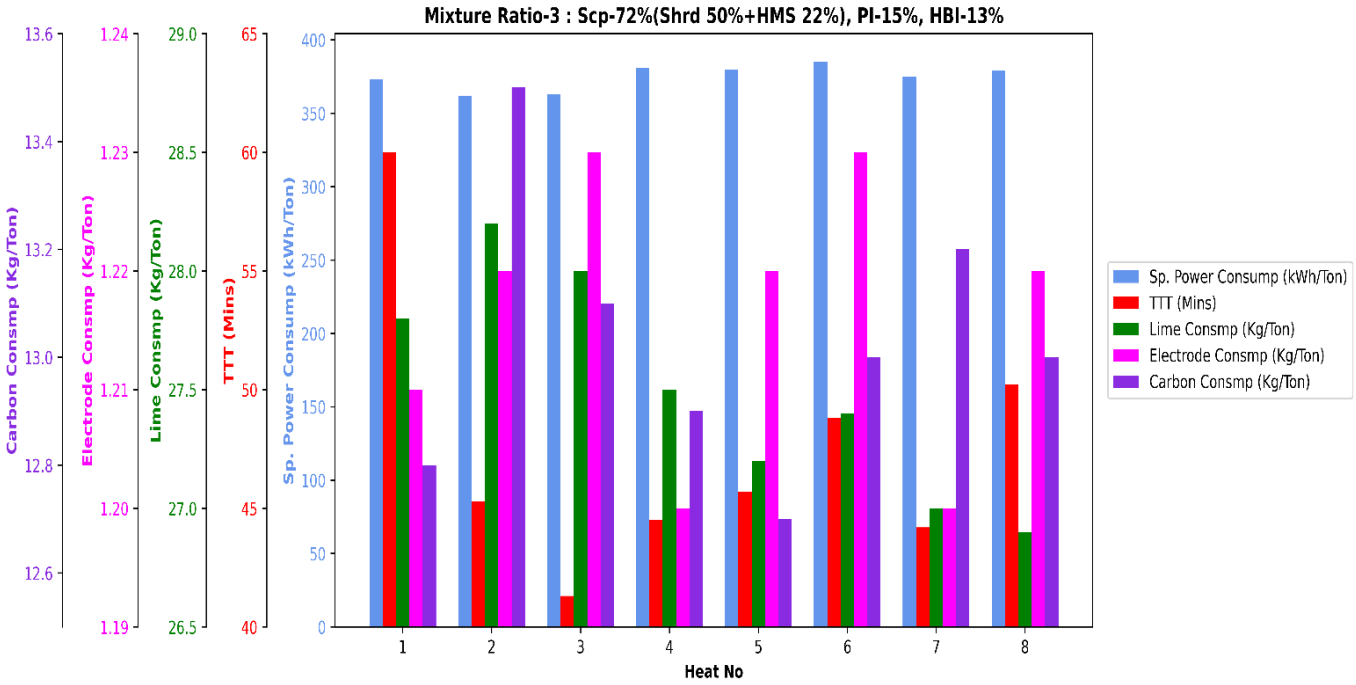


Figure 5.3: MR– 3 [Scrap -72 % (Shredded – 50% + HMS – 22%), Pig Iron – 15%, HBI – 13%].

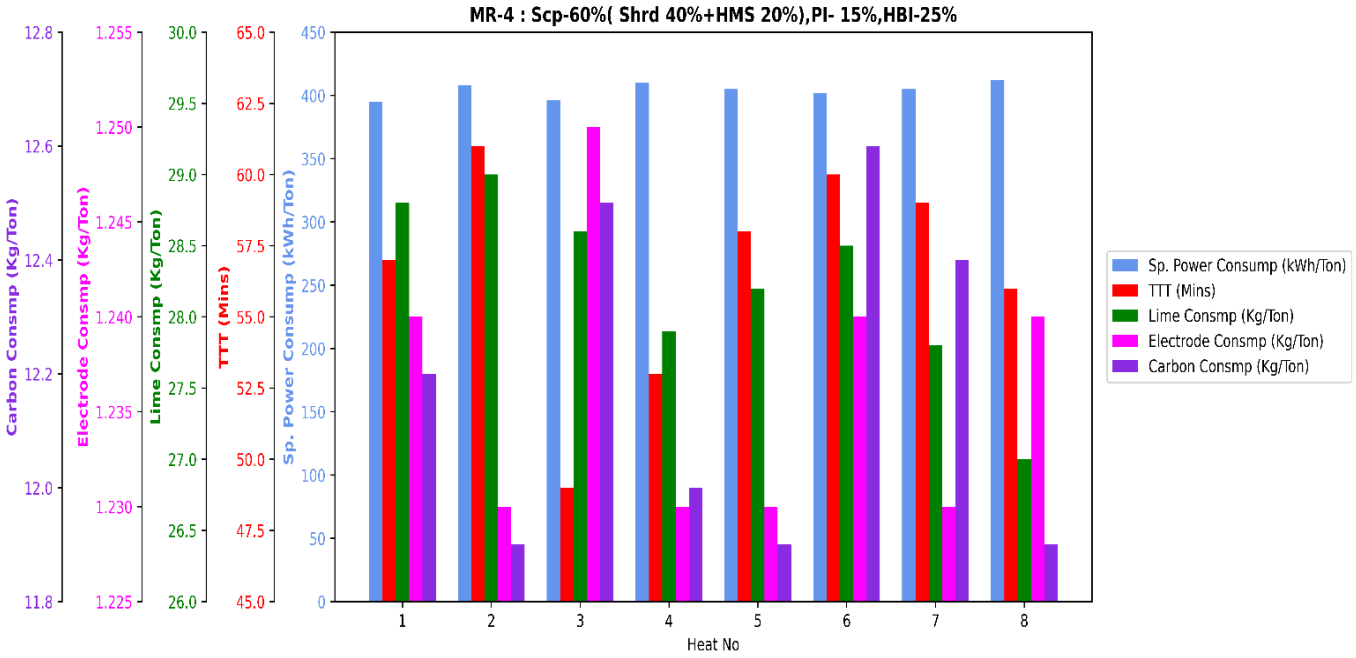


Figure 5. 3 : MR– 4[Scrap -60 % (Shredded – 40% + HMS – 20%), Pig Iron – 12%, HBI – 28%].

5.2.2 Comparative Analysis

Figures 5.5 to 5.9 present a comparative analysis of specific power consumption, TTT, lime consumption, carbon consumption, and electrode consumption across four distinct mixture ratios. According to Figure 5.5, the specific power consumption associated with each mixture ratio is presented. The findings indicate that the lowest specific power consumption was recorded for MR-2, in contrast to the other ratios. Conversely, MR-4 exhibited the highest specific energy

consumption. In MR-2, the composition consisted of 87.7% scrap and 12.30% pig iron, whereas MR-4 incorporated 60% scrap, 12% pig iron, and 28% HBI. It is well established that the electrical energy consumption during DRI/HBI melting exceeds that of scrap due to the presence of acid gangue in DRI/HBI, which increases the silica content in the melt. To offset the elevated silica levels, additional lime is necessary, which results in the formation of foamy slag and enhances the overall slag volume compared to melting scrap. This augmentation in slag basicity necessitates increased power consumption due to the introduction of lime.

Furthermore, a high percentage of metallization is beneficial in managing energy consumption. It is evident that electrical energy consumption is contingent upon the specific type of DRI utilized. The carbon content within DRI/HBI also plays a pivotal role, as it serves as an external energy source when combined with injected oxygen in the EAF, leading to the production of CO gas that promotes foamy slag formation. The reduction of FeO is facilitated by carbon through an endothermic reaction that generates CO gas, contributing to the development of foamy slag. The percentage of FeO in DRI significantly influences energy consumption, as a higher FeO content correlates with elevated electrical energy requirements in the process. This phenomenon is particularly evident when the proportion of DRI in the charge mixture is substantial. As FeO was reduced by carbon, more significant amounts of CO gas were produced, leading to increased electrical energy consumption during EAF operations, particularly when DRI constitutes a larger fraction of the charge mixture [47].

The key property affecting DRI/HBI production was the percent of metallization, as it indicated the amount of FeO present. More FeO reacted with carbon, increasing energy consumption due to endothermic reactions. DRI is produced from iron ores with higher gangue content than steel scrap, requiring more lime to create appropriate slag and balance silica. This additional lime increased power consumption due to the extra energy needed for melting [62].When 25% or more HBI is used with scrap in steelmaking, it results in higher energy consumption for melting compared to other raw material mixtures. Consequently, the specific power consumption for the MR-4 is higher in relation to the others, as illustrated in Figure 5.5. In contrast, the specific power consumption for MR-1 and MR-3 is lower than that of MR-4. Therefore, we can summarize the specific power consumption as follows:

- Specific power consumption for MR-4 > MR-1> MR-3 > MR-2.

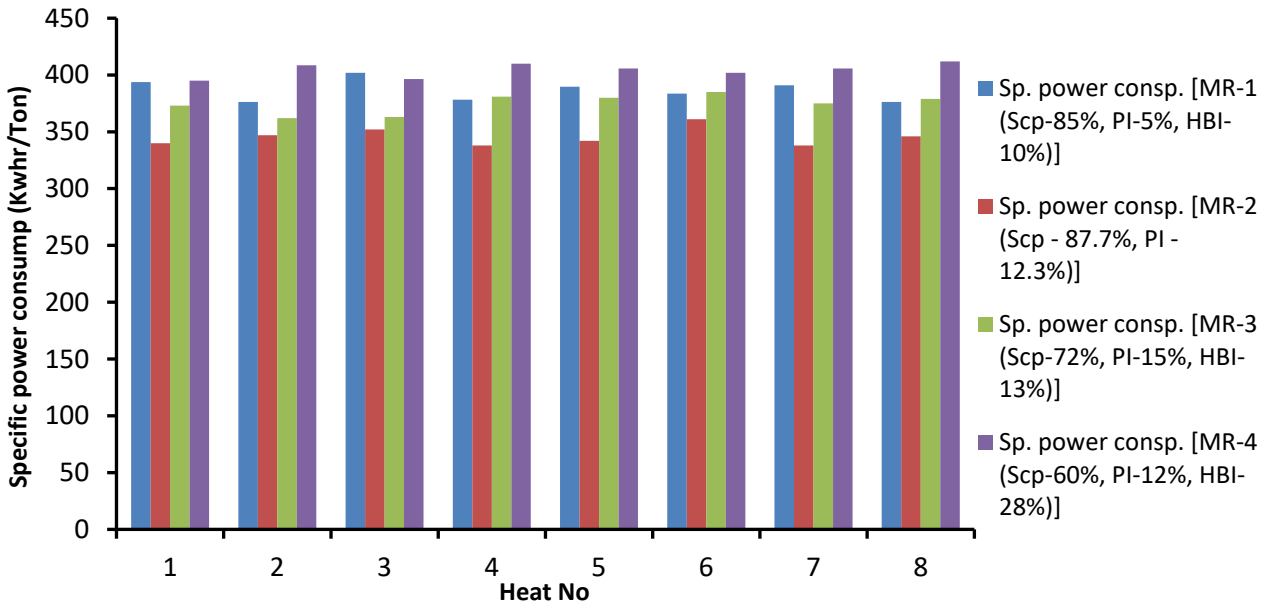


Figure 5. 4: Comparison of specific power consumption for the four mixture ratios.

The TTT values for the four different mixture ratios are illustrated in Figure 5.6. It is evident that the MR-4, which consists of 60% scrap material (composed of 40% shredded materials and 20% HMS), 12% PI, and 28% HBI, recorded the highest TTT at approximately 61 minutes. This indicates that this particular mixture ratio requires the most time to complete the processing cycle when compared to the other ratios evaluated. Conversely, MR-2 exhibited the lowest TTT among all the studied ratios. The minimum TTT recorded for this ratio was 29.6 minutes, highlighting a significant reduction in processing time relative to the other ratios. The data suggests a distinct correlation between the composition of the mixture and its efficiency in processing time. Due to the significant amount of scrap metal and the inclusion of pig iron present in MR-2 led to a reduced melting time. Once again, it is important to note that the 4% carbon content in pig iron, when fully metallized, results in low FeO levels. The excess carbon reacts with the injected oxygen, producing additional heat energy through an exothermic reaction. The lower FeO and gangue content in pig iron contributes to a decreased melting time, which in turn lessens lime consumption and accelerates the TTT. Conversely, in MR-4, the use of 28% HBI led to an increase in both TTT and lime consumption compared to other mixture ratios. Therefore, the relationship between TTT and mixture ratios can be expressed as follows:

- TTT for MR - 4 > MR - 3 > MR - 1 > MR - 2.

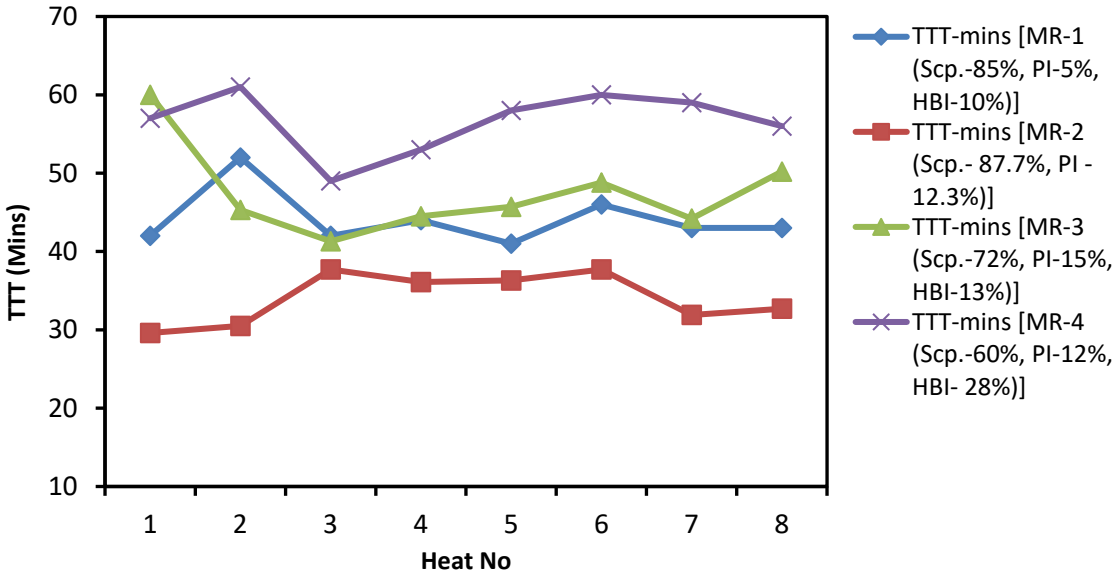


Figure 5. 5: Comparison of tap-to-tap timing (TTT) for the four mixture ratios.

In Figure 5.7, the comparison results indicate that lime consumption was maximized for MR-4 in comparison to the other mixture ratios. DRI/HBI typically contains silica as the primary gangue material, along with low levels of other impurities such as sulfur and phosphorus. The quantity of lime needed in the EAF process varies based on the ratio of DRI in the charge mixture and the impurities present in the DRI. Additional lime is required to neutralize the silica in the bath and to reduce sulfur and phosphorus levels to acceptable standards for producing the desired grade of steel. Consequently, the increased lime contributes to a higher slag basicity, facilitating the formation of foamy slag [64]. The total lime consumption rises in parallel with the percentage of DRI/HBI in the EAF charge mix. According to the rule of thumb, an increase of 2.6 kg of lime per ton of liquid steel is expected for every 10% rise in DRI in the charge mix [64]. Figure 5.7 further illustrates that the minimum lime consumption occurs at MR-2 compared to the others. In fact, when a higher proportion of scrap metal is used in steelmaking, lime consumption significantly decreases. This reduction is attributed to the lower gangue content in scrap and pig iron, resulting in much lower lime consumption than in the HBI-based mixture ratio. Therefore, a relationship can be established among the four mixing ratios as follows:

- Lime consumption for MR 4 > MR 3 > MR 1 > MR 2.

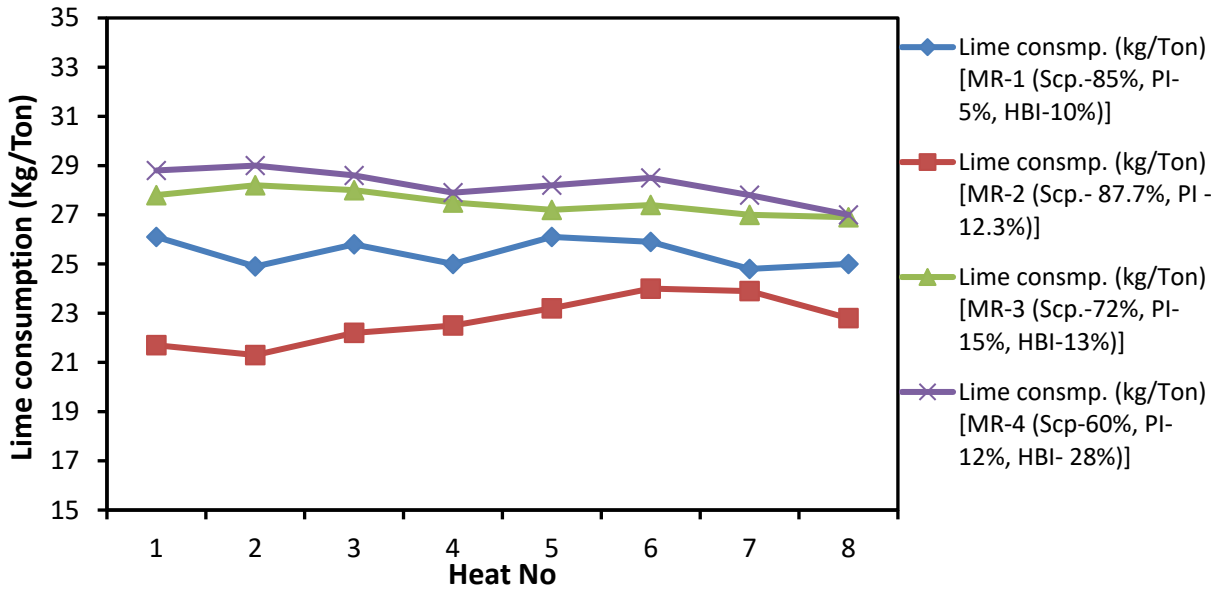


Figure 5. 6: Comparison of lime consumption for the four mixture ratios.

Figure 5.8 illustrates the results of comparing carbon consumption data across four different mixture ratios. The findings reveal that carbon consumption was highest for MR-1 compared to the other ratios. This mixture contained a significant amount of scrap, with 10% HBI and 5% pig iron (PI). It is well established that the presence of FeO in HBI necessitates greater carbon consumption to produce CO gas. Additionally, the low carbon content (0.2–0.3%) in 85% scrap further contributed to increased carbon consumption in the bath. Consequently, the carbon requirement for MR-1 was high. In contrast, MR-4 exhibited the lowest carbon consumption among all the mixture ratios. This particular ratio utilized a higher proportion of pig iron and HBI while incorporating less scrap. Due to the high amount of carbon content present in this mixture, minimal additional carbon consumption was needed in the bath reaction to produce molten steel. Thus, the relationship for carbon consumption can be summarized as follows:

- Carbon consumption for MR-4 < MR-3 < MR-2 < MR-1.

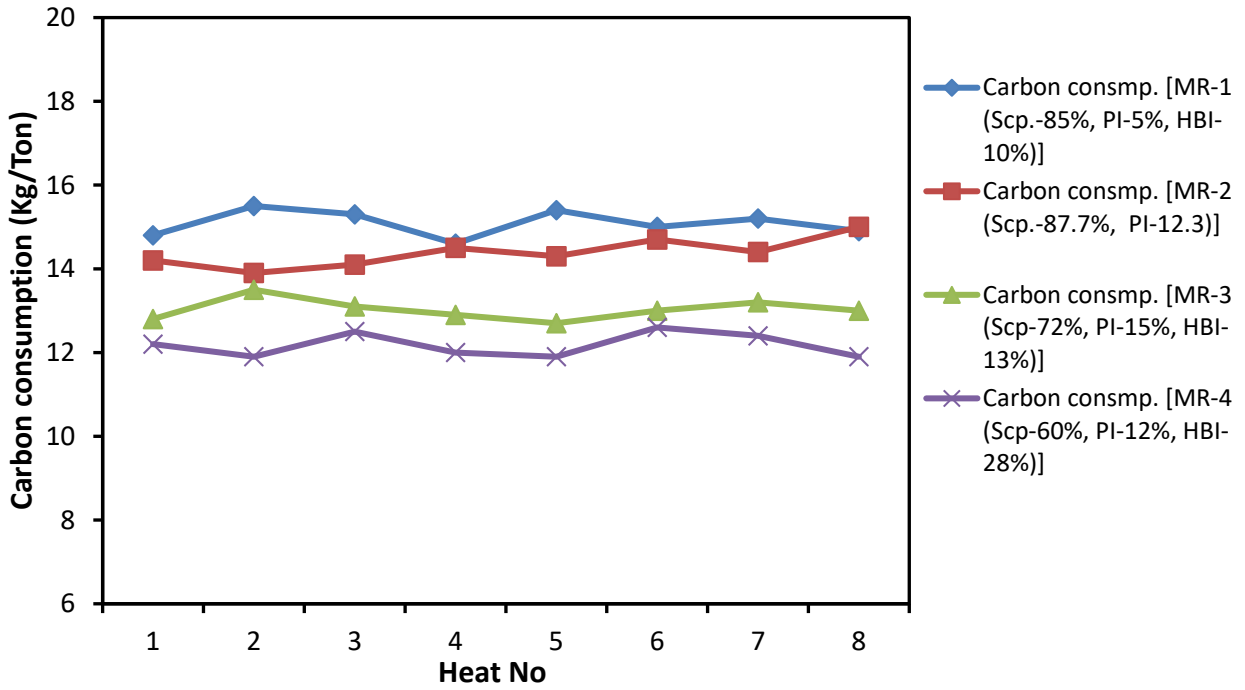


Figure 5. 7: Comparison of carbon consumption for the four mixture ratios.

In Figure 5.9, it was observed that electrode consumption was the highest for the MR-4 compared to all other ratios. Notably, as the proportion of HBI/DRI in the raw materials increased, or when mixed with scrap, the consumption of electrodes also rose. The addition of HBI to the EAF charge mixture led to an increase in the levels of FeO% and gangue (silica) in the bath. The formation of foamy slag is facilitated by the CO gas generated from the endothermic reaction between FeO and carbon. In addition, a greater amount of lime is required to enhance the slag basicity by neutralizing silica, resulting in increased power demand and longer melting times, which in turn higher electrode consumption. Conversely, the consumption of electrodes was observed to be minimal for the MR-2 ratio, where a higher quantity of scrap was present and no HBI was included. This composition reduced both melting time and energy consumption, leading to lower electrode usage compared to the other mixtures. The relationship regarding electrode consumption can be summarized as follows:

- Electrode consumption for MR-4 > MR-3 > MR-1 > MR-2.

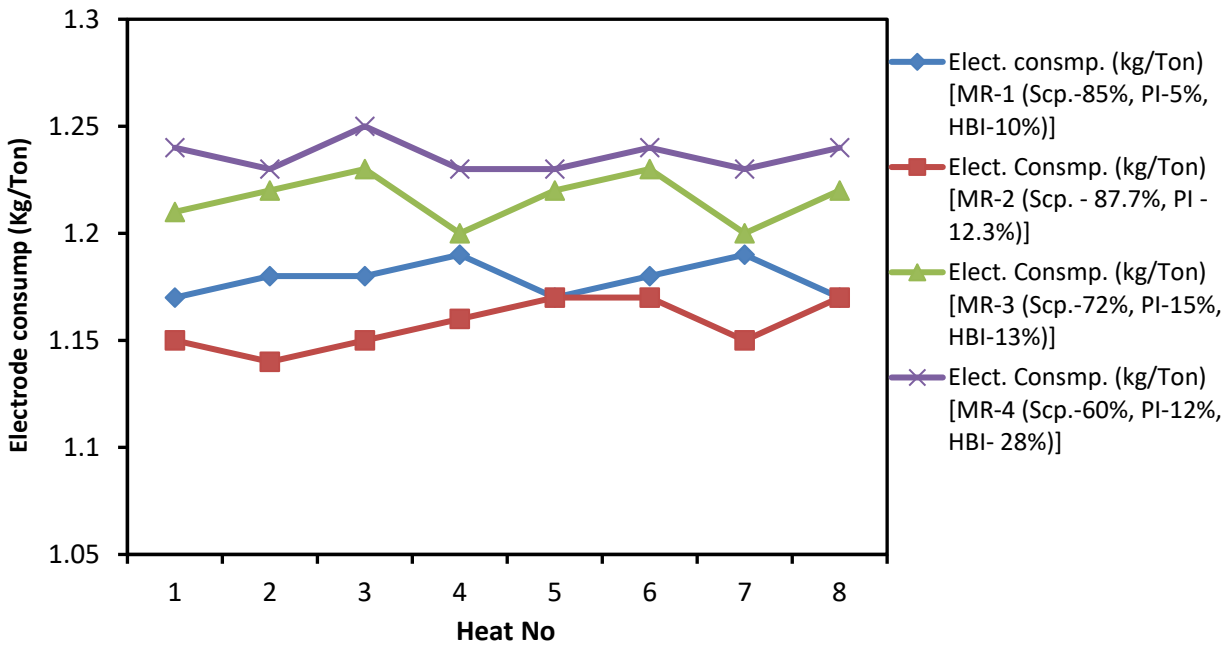


Figure 5. 8: Comparison of electrode consumption for the four mixture ratios.

5.3 DISCUSSION

Based on the analysis above, the most efficient outcome was achieved with MR-2, indicating that the raw mixture proved to be more effective than the alternatives discussed. When incorporating more than 25% HBI/DRI into the charge mixture, it has the potential to reduce energy consumption, provided that the quality of HBI is maintained (specifically, 95% or higher metallization, carbon content between 2.5-3.1%, and minimal gangue content). A lower degree of metallization necessitates the reduction of additional FeO in the EAF, which in turn results in increased specific power consumption. To enhance yield and productivity, DRI/HBI should be utilized in EAF operations with FeO levels kept below 6%. An excess of FeO reacts with carbon and leads to energy consumption through endothermic reactions, thereby further escalating power usage in the EAF.

Utilizing hot DRI in the EAF leads to reduced electricity consumption and enhanced productivity. When hot DRI (ranging between 600-700°C) is combined with scrap, there is a notable savings of 131.9 kWh per ton in specific power consumption, along with a reduction of 0.054 minutes in tap-to-tap time and 0.3 kg per ton in electrode consumption. The productivity gains from charging with hot DRI can be substantial, as it decreases the tap-to-tap time, enabling a productivity increase of up to 20% compared to charging at ambient temperatures. Furthermore, when using 100% DRI for EAF charges, each 100°C increase in DRI temperature corresponds to a reduction in electricity consumption of approximately 20 kWh per ton. Consequently, charging at temperatures exceeding 600°C can yield savings of around 120 kWh per ton [63,69].

Utilizing more than 20% hot metal (molten pig iron) in conjunction with scrap can lead to improved specific electrical energy consumption, achieving levels below 300 kWh/ton for MR-2. Thus, increasing the proportion of hot metal (at temperatures between 1200-1400°C) in the steelmaking process can significantly reduce specific energy consumption, as well as electrode usage, TTT times, and input material consumption. This shift greatly decreases the electrical energy required to produce a batch of steel. Moreover, hot metal typically contains approximately 4.5% carbon, and the additional chemical energy generated during the decarburization of a high-carbon bath with oxygen contributes to further electrical energy savings. However, research indicates that exceeding a 40% hot metal content in the charge mixture can adversely affect furnace productivity due to increased oxygen demand [62,66,70].

Currently, most steel melting plants do not employ a scrap preheating system (such as bucket preheating). Introducing scrap preheating using off-gases can elevate the scrap temperature to 300-400°C, resulting in a reduction of 18-20 kWh/ton in specific power consumption. Continuous scrap preheating has proven to be more efficient than bucket preheating. Therefore, incorporating preheated scrap or hot Direct Reduced Iron (DRI)/Hot Briquetted Iron (HBI) into the steelmaking process could yield lower specific electrical energy consumption and reduced TTT. This enhancement would not only boost furnace productivity but also be more cost-effective.

Maintaining slag basicity within the range of 2.0 to 2.5 is essential for achieving foamy slag during the steelmaking process. Several factors contribute to the formation of foamy slag, including increased slag viscosity, reduced surface tension, and optimal levels of FeO and silica, with FeO ideally between 15-20% and silica between 5-15%. The stability of foaming slag was enhanced by specific silica content, as silica reduced surface tension and encouraged the formation of small CO bubbles. However, if the silica (SiO_2) content in the slag is permitted to rise excessively, it can lead to significant refractory erosion. To achieve foamy slag while minimizing refractory loss, it is necessary to increase the consumption of lime and dolomitic lime. Furthermore, elevated FeO levels in the slag can occur since FeO is more soluble in high-silica slags, potentially resulting in higher yield losses in the EAF and increased dephosphorization.

The FeO percentage in the slag will rise if decarburization is reduced or if there is less carbon injection in the EAF bath, indicating that less FeO is being reduced in the bath. An increase in FeO concentration within the slag will consequently decrease Iron yield percentage and accelerate phosphorus removal. Additionally, the FeO percentage will escalate in the slag as the carbon content (%C) at tapping decreases.

Chapter –06
Conclusion and Recommendations

6.1 CONCLUSION

The EAF play a crucial role in modern steel production, with significant advancements enhancing their efficiency over the past 30 years. Current operations achieve a tap-to-tap time of 30 minutes, consume less than 300 kWh/ton of electrical energy, and have an electrode consumption of 1.0-1.2 kg/ton. Due to limited scrap availability, high-quality DRI/HBI, pig iron, and hot metal can be used alongside scrap to boost chemical energy through exothermic reactions. Proper selection of charge materials reduces energy consumption and enhances productivity. Recent trends include the use of oxy-fuel burners, which increase chemical energy input and decrease melting times, further saving electrical energy. Efficient heat utilization, such as post-combustion processes, helps reduce exhaust losses and improve overall energy efficiency. The DC electric arc furnaces are more efficient than their AC counterparts, consuming less energy and electrodes. Advanced controls featuring multiple sensors facilitate power savings and precise monitoring of key parameters, further optimizing the modern EAF process.

In this study, the steelmaking operations and refining processes associated with Electric Arc Furnaces (EAF) are described in detail. An analytical examination of various raw materials utilized in steel production and their respective impacts is presented. Based on the analytical and experimental findings, the outcomes are summarized below.

- The lowest specific power consumption was recorded for MR-2, in contrast to the other ratios. Conversely, MR-4 exhibited the highest specific energy consumption.
- The MR-4, which consists of 60% scrap material, 12% PI, and 28% HBI, recorded the highest TTT at approximately 61 minutes. Conversely, MR-2 exhibited the lowest TTT among all the studied ratios. The minimum TTT recorded for this ratio was about 29.6 minutes.
- The lime consumption was maximized for MR-4 in comparison to the other mixture ratios. The results also show the minimum lime consumption occurs at MR-2 compared to the others. In fact, when a higher proportion of scrap metal is used in steelmaking, lime consumption significantly decreases.
- The carbon consumption was highest for MR-1 and the lowest for MR-4 compared to the other ratios.
- The electrode consumption was the highest for the MR-4 compared to all other ratios as the proportion of HBI/DRI in the raw materials increased, or when mixed with scrap, the consumption of electrodes also rose. Conversely, the consumption of electrodes was observed

to be minimal for the MR-2 ratio, where a higher quantity of scrap was present and no HBI was included. This composition reduced both melting time and energy consumption, leading to lower electrode usage compared to the other mixtures.

- We got only best mixture ratio with respect to four mixture ratio based on sp. Power consumption, tap to tap timing, carbon consumption, lime consumption and electrode consumption. We could not make any decision about steel quality from these four mixing ratio and which mixture ratio was good for steel quality was also not measured.

6.2 RECOMMENDATIONS

- Due to the unavailability and high cost of steel scrap, it is essential to use high-quality and well-educated DRI/HBI for the EAF (Electric Arc Furnace) charge mixture to achieve better performance. When using more than 25% HBI/DRI in the charge, the following properties of DRI must be maintained during the steelmaking process: metallization percentage (greater than 95%), carbon content (between 2.5% and 3%), FeO percentage (less than 6%), and gangue content (less than 4%).
- To lower electrical energy consumption, reduce electrode wear, and improve productivity, hot DRI (at temperatures between 600°C and 700°C) can be used in the EAF process. Additionally, it is advisable to incorporate 10% to 15% pig iron as an alternative iron source in the EAF charge mixture to save on power consumption. However, care must be taken regarding the silicon content in the pig iron, as it can lead to the production of silica (SiO_2) in the bath.
- To further decrease electrical energy consumption and the use of carbonaceous materials, a portion of hot metal or molten pig iron (at temperatures between 1200°C and 1400°C) can be mixed with the scrap charged materials in the EAF process. It is recommended that no more than 40% of hot metal be included in the EAF charge mixtures to maintain optimal furnace productivity.
- A scrap preheating system is recommended for the EAF steelmaking process to reduce electrical energy consumption. This system can increase the scrap temperature by 300°C to 500°C using exhaust off gases, thereby enhancing furnace productivity by 10% to 20%.
- To achieve foamy slag in the electric arc furnace steelmaking process, the slag basicity index should be maintained between 2.0 and 2.5. It is also advisable to conduct slag composition analysis in the EAF process to properly maintain FeO%, SiO_2%, and MgO levels, ensuring a productive and cost-effective steelmaking operation.

References

[1] A. S. Christopher, E. W. Saturday, B. G. Oladeji and O. O. Biodun, "Process Modeling of Steel refining in Electric Arc Furnace (EAF) for Optimum Performance and Waste Reduction", Chemical and process engineering research, Volume-28, ISSN 2224-7467 (Paper) ISSN 2225-0913 (Online), 2014.

[2] J. Madias, "Electric Furnace steelmaking", Chapter – 1.5, Treatise on Process Metallurgy, Volume -3, Page 271-301, 2014 (http://dx.doi.org/ 10.1016/B978-0-08-096988-6.00013-4).

[3] Yuri N. Toulouevski, Ilyaz Y. Zinurov, "Innovation in Electric arc Furnaces", Second Edition, Springer-2013 (DOI 10.1007/978-3-642-36273-6).

[4] Rodney T. Jones, "DC Arc Furnaces – Past, Present, and Future", Mintek, National Research Foundation (NRF) of South Africa.

[5] M. A. Haque, A. Abdullah, "Bangladesh Steel Industry Review", EBL Securities Ltd, December-2019.

[6] I. Z. Yildirim and M. Prezzi, "Chemical, Mineralogical, and Morphological Properties of Steel Slag", Advances in Civil Engineering, Volume 2011, Article ID 463638,July – 2011(doi:10.1155/2011/463638).

[7] J. Madias, Electric Arc Furnace, Chapter – 16, Springer International Publishing Switzerland-2016 ,P. Cavaliere (ed.), Ironmaking and Steelmaking Processes, (DOI 10.1007/978-3-319-39529-6_16).

[8] Swaren S. Bedarkar and Narendra B. Dalal, "Energy Balance in Induction Furnace and Arc Furnace Steelmaking," International Journal of Engineering Research and Applications, ISSN: 2248-9622, Vol. 10, Issue 6, (Series-V) June 2020, pp. 57-61(DOI: 10.9790/9622-1006055761).

[9] "Understanding Electric Arc Furnace operation", The EPRI Centre for Materials Production, CMP TechCommentary1997, Electric power research institute, Tech Commentary/ TC-107714.

[10] A. M. Ali, and S. Amani, "Using oxygen reaction as electricity saving in Electric arc Furnace steel making," International Journal of Chem Tech research, ISSN: 0974-4290, Vol-1, No-1,PP – 62-70,March-2009.

[11] S. Ahamed, "Coronavirus effect on Bangladesh's steel industry", New Vision Solutions Ltd, May – 2020.

[12] M. Hasan, "The Steel Industry of Bangladesh: Constructing A Compact Foundation of Growth A midst Economic Instability", IDLC Monthly Business Review, November-2023.

[13] "Introduction to Electric Arc Furnace" The EPRI Centre for Materials Production, CMP Tech commentary, 1985 Electric power research institute, USA, Tech Commentary/ TC-107713.

[14] E. Hajidavalloo, H. Dashti, and Nejad M. Behbahani, "Exergy and Energy Analysis of An AC Steel Electric Arc Furnace Under Actual Conditions", International Journal of Exergy 12(3): 380-404, 2013.

[15] N. Arzpeyma, "Modeling of Electric arc furnace (EAF) with Electromagnetic Stirring", Department of materials science and Engineering, Royal Institute of Technology, Sweden – 2011.

[16] A. Ghodrati, R. Zahedi, A. Ahmadi, "Analysis of Cold Thermal Energy Storage Using Phase Change Materials in Freezers. Journal of Energy Storage 51: 104433, 2022.

[17] O. Martin, Tenova, ORI Martin embrace Industry, 2019.

[18] D. Mazumder and S.C. Korea, "Lecture –15, Electric Furnace Steelmaking," National Program on Technology Enhanced Learning (NPTEL), Department of Material Science & Engineering, IIT, Kanpur.

[19] G. Boyd, H. K. Stephen, N. Mark, R. Marc, "Energy Intensity Improvements in Steel Minimills", Contemporary Economic Policy 11(3): 88-100.

[20] Y. N. Toulouevski and I. Y. Zinurov, "Innovation in Electric Arc Furnaces", Springer, p. 1-23, 2010.

[21] S. K. Dutta andY. B. Chokshi, "Electric Furnace Processes. In: Basic Concepts of Iron and Steel Making. Springer, Singapore, 2020. https://doi.org/10.1007/978-981-15-2437-0_16.

[22] B .Bowman "A technical comparison between AC & DC furnaces" Lecture at the Steel Industries conference, Bangkok, December – 1992.

[23] "Direct Current Electric Arc Furnace", The EPRI Centre for Materials Production, CMP Tech commentary, 1991 Electric power research institute, USA, Tech Commentary/ CMP 063.

[24] S. K. Sarna, "DC Electric Arc Furnace", Article at Ispat Guru, 15 May -2013.

[25] J.A.T Jones, B. Bowman, and P.A. Lefrank, "Electric Furnace Steelmaking, Chapter-10", 1998, The AISE Steel foundation, Pittsburgh.

[26] Danieli Technical Department, DANIELI & C. Spa – Buttrio (UD) – ITALY, "Operating and Maintenance Instructions for the Electric Arc Furnace", Document Number - TP02BB-GD11-M1001-KB012, 08/06/2012.

[27] Operational Manual, AbulKhair Steel melting plant, Chattogram, Bangladesh.

[28] MatteoSprchio, "Electric Arc Furnace AC (Part-1) –Layouts & Components", Products for Steelmaking, May- 08-2019.

[29] H. Gripenberg, M. Brunner, and M. Petersson, “Optimal Distribution of Oxygen in High Efficiency Arc Furnaces,” Iron and Steel Engineer 67:7, 33–7, 1990.

[30] K. Bergman and R. Gottardi, “Design Criteria for the Modern UHP Electric Arc Furnace with Auxiliaries,” Ironmaking and Steelmaking, 17:4 282–7, 1990.

[31] Danieli Technical Department, DANIELI and C. Spa – Buttrio (UD) – ITALY, “EAF DC Operating Manual AbulKhair”, Danieli Reference Number: DP02BBT3.80.15, JDN Document Number: TP02BB – GD11 – M1100 – BB001, 04/12/2013.

[32] D. Mazumder and S.C. Korea, “Lecture –16, Developments in EAF steelmaking,” National Program on Technology Enhanced Learning (NPTEL), Department of Material Science & Engineering, IIT, Kanpur.

[33] D.H. Hubble, R. O. Russel, H. L. Vernon, and R. J. Marr,“ Steelmaking Refractories, Chapter -4” The Making, Shaping and Treating of Steel, 11th edition, Steelmaking & Refining volume – 1998, The AISE Steel foundation, Pittsburgh.

[34] S. Bisaws and D. Sarkar, “Refractory practice in Electric Arc Furnace - Chapter -5” Introduction to Refractories for Iron & Steelmaking © Springer Nature Switzerland AG 2020, ISBN 978-3-030-43807-4. (https://doi.org/10.1007/978-3-030-43807-4).

[35] Matteo Sprchio “Electric Arc Furnace AC (Part-2) –Raw materials” Products for Steelmaking, August, 26-2019.

[36] L. L. Teoh, “Electric Arc Furnace Technology: Recent Developments and Future Trends,” Iron making and Steelmaking 16, 303–13, 1989.

[37] R. J. Fruehan, “Scrap in Iron and Steel making: Technologies to Improve the Use of Scrap,” Iron & Steelmaker 12:7, 31–36, 1985.

[38] H. Gripenberg, M. Brunner and M. Petersson, “Optimal Distribution of Oxygen in High Efficiency Arc Furnaces,” Iron and Steel Engineer 67:7, 33–7, 1990.

[39] N. Perrin et al., “Continuous Fume Analysis at Vallourec Saint-Saulve,” Electric Furnace Conference Proceedings 49 (Warrendale, PA: Iron and Steel Society, 233–41, 1991.

[40] A. J. Berthet and J-C. Grosjean, “The 90s Electric Arc Furnace Steelmaking Route: The Leap Forward,” Proceedings of the Sixth International Iron and Steel Congress, Nagoya, Japan: 1990, 180–9.

[41] P. Cavaliere, “Electric Arc Furnace: Most Efficient Technologies for Greenhouse Emissions Abatement, Chapter–6” Clean Ironmaking and Steelmaking Processes, Springer – 2019. https://doi.org/10.1007/978-3-030-21209-4_6.

[42] E. N. Gopal, A. Ganguly and N. Vasudevan, “Energy Efficient technology packages for Electric Arc Furnace” The Energy & Resources Institute, New Delhi -2017 (Published for UNDP).

[43] A. Dicion, “Innovative Energy Conservation through Scrap Pre-heating in an Electric Arc Furnace” Willis Energy Services (ONT) Ltd, ACEEE Summer Study on Energy Efficiency in Industry- 2013.

[44] J. Clayton et al., “The Sheerness Shaft Electric Furnace,” Steel Technology International, (1993): 97–101.

[45] I.Ekmekci, Y. Yetisken, and U. Camdali, “Mass Balance Modeling for Electric Arc Furnace and Ladle Furnace System in Turkey” Journal of Iron and Steel Research, International, Volume-14, -2007.

[46] D. C. Yang, “Reagents in iron ore processing, in Reagents in mineral technology”, Routledge, London, United Kingdom, pp: 579-644, 2018.

[47] P. Cavaliere, “Direct Reduced Iron: Most Efficient Technologies for Greenhouse Emissions Abatement”, in Clean Ironmaking and Steelmaking Processes, pp. 419-484, 2019.

[48] R. Zahedi and A. B. Rad, “Numerical and Experimental Simulation of Gas-Liquid Two-Phase Flow in 90-degree elbow. Alexandria Engineering Journal 61(3): 2536-2550, 2021.

[49] Z. Mengjing, W. Yong, Y. Shufeng, L. Jingshe, S. Zhaoqi et al. (2021) Flow behavior and heat transfer of molten steel in a two-strand tundish heated by plasma. Journal of Materials Research and Technology 13: 561-572.

[50] Jeremy A.T. Jones, “Electric arc furnace steelmaking” Nupro Corporation, American Iron & Steel Institute-2008.

[51] R. Singh, “Production of Steel, Chapter-5” Applied Welding Engineering (2nd Edition), 2016, Page: 37- 55. https://doi.org/10.1016/B978-0-12-804176-5.00005-0.

[52] M. M. Elkoumy, M. El-Anwar , A. M. Fathy, G. M. Megahed, I. El-Mahallawi, H. Ahmed “Simulation of EAF refining stage” Ain Shams Engineering Journal 9, 2781–2793, 2018. https://doi.org/10.1016/j.asej.2017.10.002.

[53] V. Mincu and N. Constantin, “Refining steels produced in electric arc Furnace” U.P.B. Sci. Bull., Series B, Vol. 75, Iss. 2, 2013. ISSN:1454 – 2331.

[54] Eugene Pretorius, Helmut Oltmann “The EAF Operating Cycle –Charging, melting and refining” EAF Fundamentals- Process Technology Group (LWB Refractories).

[55] S. H. Anderson, D. Trotter, D. Varcoe, and R. Reeves, “Use of HBI and DRI for Nitrogen control in Steel Products” -2002, ResearchGate Publications, https://www.researchgate.net/publication/265107012.

[56] K. Ito and R.J. Fruehan, “Slag Foaming in Electric Furnace steelmaking”, Transactions of ISS & I&SM, pp.55-60, August 1989.

[57] E. B. Pretorius and R. C. Carlisle, “Foamy slag Fundamentals and their practical application to Electric Furnace Steelmaking” Baker Refractories- 1998 EAF conference.

[58] Gregory L. Dressel, “Direct reduced iron process effects & applications: part-4” Use of DRI in EAF-1998, PawleysIsland, SC, USA.

[59] M. Kovacic, K. Stopar, R. Vertnik, and B. Sarler, “Comprehensive Electric arc furnace electric energy consumption modeling” Energies -2019,12,2142 (doi: 10.3390/en12112142)

[60] J. H. Heo and J. H. Park, “ Effect on Direct reduced iron on Dephosphoraization of molten steel by Electric arc furnace slag” The minerals, metals & materials society and ASM International, 2018 (https://doi.org/10.1007/s11663-018-1406-5).

[61] M. Kirschen, K. Badr, and H. Pfeifer, “Influence of Direct Reduced Iron on the Energy Balance of Electric Arc Furnace in Steel Industry”, Energy 36 (2011) PP 6146-6155 (https://doi.org/10.1016/j.energy.2011.07.050)

[62] Michael G. K Grant, Kenneth C Kaiser, and Serban M Cantacuzene, “Optimization of Oxygen steelmaking in non- conventional EAF operations”, AISTech 2005 Proceedings-Volume-1, 2005.

[63] S. Hornby, J. Madias,and F. Torre, “Myths & Realities of Charging of DRI/HBI in Electric Arc Furnace” AISTech 2015 Proceedings.

[64] M. Satyendra “Use of Direct Reduced Iron in Electric Arc Furnace” Ispatguru, May 2013

[65] J. Madias, A. Bilancieri, and S. Hornby, “Influence of Metallics and EAF type on Specific Consumptions & Productivity” AISTech 2017 Proceedings.

[66] H. Pfeifer, M. Kirischen, “Thermodynamic Analysis of EAF Energy Efficiency and Comparison with Statistical Model of Electric Energy Demand”, Institute of Industrial furnace & heat engineering in Metallurgy, RWTH Aachen, Germany, May-2002.

[67] D. Klein and K. Wimmer, “DC Electrodes—A Key Factor for Progress in EAF Production,” Metallurgical Plant and Technology International 18:4 (1995): 54–63.

[68] A. D Bennett, “Methods of Controlling Fume Emissions From Electric Arc Furnaces,” Steel Technology International (1993): 32–8.

[69] S. Hornby Anderson, “Educated use of DRI/HBI improves EAF energy efficiency and yield and downstream operating results” Midrex Technologies Inc., Charlotte, NC, USA-2002.

[70] T. Battle, U. Srivastava, J. Kopfle, R. Hunter, and J. McClelland, “The Direct Reduction of Iron, Chapter – 1.2” Treatise on Process Metallurgy, Volume -3; Industrial process -2014, page -89-176. https://doi.org/10.1016/B978-0-08-096988-6.00016-X.

Appendices

A. 1 Mixture Ratio – 1 [Scrap -85 % (Shredded – 55% + HMS – 30%), Pig Iron – 5%, HBI – 10%]
Date: 29-08-2020; EAF – 01; Average heatwise charge weight – 97 Ton

Heat no	Lime Consmp. (Kg/T)	Dol. lime Consmp. (Kg/T)	Oxygen Consmp (Nm^3/T)	Carbon Consmp (Kg/T)	Sp. Power Consmp. (Kwhr/T)	TTT (mins)	Tap Temp. (^0C)	Avg. Power input (MW)	Arch. time (min)	Electrode Consmp. (Kg/T)	%Carbon at Tapping
1	25.3	10.7	24.5	15.2	386	47	1593	60	38.93	1.18	0.07
2	26	14.4	23	15.7	401.9	44	1641	68	34.58	1.19	0.06
3	25.6	11	24.8	15.5	386.5	47	1593	62	37.13	1.18	0.08
4	24.9	13.2	23.5	14.5	395.9	47	1617	68	34.95	1.17	0.1
5	26.8	11.3	22	14.9	386.1	47	1617	65	35.97	1.18	0.06
6	26	13.6	23.7	15.6	399.7	48	1588	68	35.23	1.19	0.07
7	25.5	14.4	22.9	15	405.8	45	1620	68	36.2	1.18	0.08
Date : 20-08-2020											
1	26.1	15.3	24.5	14.8	393.8	42	1621	68	34.45	1.17	0.1
2	24.9	10.1	23	15.5	376.3	52	1639	60	37.98	1.18	0.06
3	25.8	14.8	24.4	15.3	401.9	42	1613	71	33.7	1.18	0.08
4	25	10.7	25	14.6	378.2	44	1600	65	35.5	1.19	0.1
5	26.1	14.4	23.8	15.4	389.7	41	1612	68	33.47	1.17	0.09
6	25.9	11.2	25	15	383.6	46	1607	63	37.92	1.18	0.08
7	24.8	14	24.3	15.2	390.9	43	1600	67	34.87	1.19	0.07
8	25	11	25.2	14.9	376.3	43	1625	66	34.58	1.17	0.06

A. 2 Mixture Ratio – 2 [Scrap -87.7 % (Shredded – 67.7% + HMS – 20%), Pig Iron – 12.30%]
Date: 11-07-2020; EAF – 01; Average heatwise charge weight: 96.5 Ton

Heat no	Lime Consmp. (Kg/T)	Dol. lime Consmp. (Kg/T)	Oxygen Consmp (Nm^3/T)	Carbon Consmp (Kg/T)	Sp. Power Consmp. (Kwhr/T)	TTT (mins)	Tap Temp. (^0C)	Avg. Power input (MW)	Arch. time (min)	Electrode Consmp. (Kg/T)	%Carbon at Tapping
1	21.7	9.8	22.2	14.2	340	29.6	1592	63.5	31	1.15	0.08
2	21.3	10.5	23.8	13.9	347	30.5	1636	66.4	31	1.14	0.1
3	22.2	11	25.5	14.1	352	37.7	1613	69.7	30	1.15	0.06
4	22.5	10.4	24.7	14.5	338	36.1	1622	68.3	29	1.16	0.06
5	23.2	9.8	24.2	14.3	342	36.3	1601	63.6	32	1.17	0.07
6	24	10.2	26.5	14.7	361	37.7	1619	66.6	32	1.17	0.1
7	23.9	11.3	23.3	14.4	338	31.9	1615	68.4	29	1.15	0.06
8	22.8	9.9	23.3	15	346	32.7	1618	67	31	1.17	0.08
9	24.2	10.5	24.9	14.8	352	29.7	1570	61.1	34	1.15	0.07
10	23	10	25.1	15	354	37.2	1631	70.9	30	1.16	0.08
11	23.8	9.8	25.4	14.9	349	38.7	1618	70.5	30	1.18	0.07
12	22	11.2	24.8	15.2	346	39.2	1630	72.3	28	1.17	0.09
13	22.7	10.6	25.7	14.9	362	40.2	1618	68.4	31	1.17	0.08

14	23.1	10.8	23.3	14.7	339	34.4	1591	68.8	29	1.16	0.08
15	23.6	11	23.4	14.3	338	35.3	1576	69.1	28	1.14	0.1
16	24.2	11.5	23.7	14.9	332	37	1605	66.8	29	1.15	0.09
17	25	10.4	24	15	345	38	1615	68.6	29	1.17	0.08
18	23.9	10.7	21.5	14.5	376	37.5	1601	66.4	33	1.16	0.05
19	22.6	11.2	26.4	14	363	39.6	1606	65.9	33	1.17	0.07
20	21.8	9.7	23.9	14.7	358	35.5	1600	67.9	31	1.15	0.09
21	21	10	24.5	15	346	35.4	1587	66.7	30	1.17	0.1
22	22.5	10.6	23.3	14.4	345	31.6	1595	68.4	29	1.16	0.08
23	22.9	11.1	24.2	15	352	34.8	1601	66.9	30	1.16	0.09
24	23.2	9.5	23.9	15.1	351	34.2	1593	68.5	29	1.17	0.07
25	22.4	9.8	22.8	14.6	348	31.8	1592	69	29	1.16	0.09
26	24.4	10.4	23.5	14.9	354	34.3	1586	67.2	31	1.17	0.08
27	23.8	10.7	24.8	15	348	36.2	1592	66.5	30	1.15	0.1
28	22.2	11.1	22.7	14.4	345	31.2	1591	68.6	29	1.17	0.09
29	23.5	10.8	24.2	14.7	358	37.1	1611	67.6	31	1.14	0.08

A. 3 Mixture Ratio – 3[Scrap -72 % (Shredded – 50% + HMS – 22%), Pig Iron – 15%, HBI – 13%]
Date: 18-06-2020; EAF – 01; Average heatwise charge weight – 96 Ton

Heat no	**Lime Consmp (Kg/T)**	**Dolomite Consmp (Kg/T)**	**Oxygen Consm (Nm^3/T)**	**Carbon Consmp (Kg/T)**	**Sp. Power Consmp (Kwhr/T)**	**TTT (mins)**	**Taping temp (^{0}C)**	**Avg. Power input (MW)**	**Arch. time (min)**	**Electrode Consmp. (Kg/Ton)**	**%Carbon at Tapping**
1	27.8	15.6	29	12.8	373	60	1615	64.9	35	1.21	0.07
2	28.2	16.3	26.5	13.5	362	45.3	1590	65.2	32	1.22	0.1
3	28	16.3	26.3	13.1	363	41.3	1622	65.4	33	1.23	0.07
4	27.5	16.3	26.9	12.9	381	44.5	1593	66.2	34	1.2	0.06
5	27.2	16.4	27.8	12.7	380	45.7	1585	68.3	33	1.22	0.09
6	27.4	16.5	29.4	13	385	48.8	1655	65.2	34	1.23	0.06
7	27	16.5	27.2	13.2	375	44.2	1618	68.3	32	1.2	0.06
8	26.9	16.5	29.2	13	379	50.2	1601	67.1	33	1.22	0.07
9	27.1	16.3	29.2	12.9	365	52.5	1591	66.4	32	1.22	0.05
10	27.4	15.8	27.5	13.3	368	48.4	1601	68.7	31	1.19	0.05
11	27.8	16.3	24.7	12.9	361	40	1600	66.6	32	1.21	0.07
12	26.9	16.5	22.8	13.1	391	34.3	1581	67.4	34	1.22	0.1
13	27.2	15.9	25.9	13	401	43.7	1603	67	37	1.2	0.06
14	27.6	16.4	24.2	13.5	399	34.8	1603	66.8	34	1.23	0.07
15	27	16.5	26.3	12.9	380	43.1	1626	70.2	29	1.21	0.06
16	27.3	15.7	25.5	13	374	41.6	1600	71.3	30	1.22	0.04
17	26.8	16.2	25.2	13.1	380	38.9	1604	68.8	31	1.23	0.07
18	27.2	16.4	24.2	13.6	386	49.9	1633	68.3	33	1.21	0.07
19	27	16.4	25.1	12.9	375	46	1612	71	31	1.2	0.1
20	27.7	16.4	25.3	13.3	371	46.2	1639	70.3	31	1.21	0.06
21	28.1	16.3	24.8	13.2	365	44.2	1622	71.1	30	1.21	0.08

22	28	16.4	25.2	13.7	369	44.9	1606	70.9	30	1.2	0.07
23	27.9	16.4	24.2	12.7	363	41.1	1625	71.4	30	1.21	0.07
24	27.6	16.4	25	12.6	359	43.3	1613	68.9	30	1.19	0.05
25	28.1	16	24.8	12.6	363	42.4	1637	70.2	31	1.2	0.07
26	26.9	16	26	13.7	365	46.9	1610	67.7	32	1.23	0.08
27	27.4	16.7	25.4	13.2	371	43.8	1601	69	33	1.22	0.07
28	27	15.9	25.9	13	372	47.5	1600	69.4	32	1.19	0.04

A. 4 Mixture Ratio – 4 [Scrap -60 % (Shredded – 40% + HMS – 20%), Pig Iron – 12%, HBI – 28%]
Date: 06/05/2020; EAF – 01; Average heatwise charge weight: 95 Ton

Heat no	**Lime Consmp (Kg/T)**	**Dolomite Consmp (Kg/T)**	**Oxygen Consmp (Nm^3/T)**	**Carbon consmp (Kg/T)**	**Specific Power Consump (Kwhr/T)**	**TTT (mins)**	**Tap temp (^{0} C)**	**Avg. Power input (MW)**	**Arch. time (min)**	**Electrode Consump (Kg/Ton)**	**%Carbon at Tapping**
1	28.8	13.7	23.8	12.2	395	57	1598	68	39.5	1.24	0.05
2	29	15.4	24	11.9	408.5	61	1631	67	38.6	1.23	0.07
3	28.6	14	24.8	12.5	396.5	49	1615	69	40.13	1.25	0.06
4	27.9	14.2	25	12	410	53	1610	70	39.65	1.23	0.1
5	28.2	13.9	25.2	11.9	405.7	58	1596	71	38.77	1.23	0.08
6	28.5	14.2	24.7	12.6	402	60	1612	68	37.83	1.24	0.06
7	27.8	14.4	24.1	12.4	405.8	59	1625	71.5	38.2	1.23	0.09
8	27	13.7	23.9	11.9	412	56	1597	70	39	1.24	0.08
9	28.2	13.8	24.2	12	398	62	1604	69	40.2	1.25	0.08
10	28	14	25	12.4	406	55	1613	68	38	1.24	0.05

report

ORIGINALITY REPORT

13%	8%	8%	2%
SIMILARITY INDEX	INTERNET SOURCES	PUBLICATIONS	STUDENT PAPERS

PRIMARY SOURCES

1	ar.scribd.com Internet Source	2%
2	Subir Biswas, Debasish Sarkar. "Introduction to Refractories for Iron- and Steelmaking", Springer Science and Business Media LLC, 2020 Publication	1%
3	www.slideshare.net Internet Source	1%
4	Pasquale Cavaliere. "Clean Ironmaking and Steelmaking Processes", Springer Science and Business Media LLC, 2019 Publication	1%
5	etech.lwbref.com Internet Source	1%
6	Submitted to TU Delft Student Paper	<1%
7	www.americancombustion.com Internet Source	<1%
8	Sujay Kumar Dutta, Yakshil B. Chokshi. "Basic Concepts of Iron and Steel Making", Springer Science and Business Media LLC, 2020 Publication	<1%
9	Jorge Madias. "Electric Furnace Steelmaking", Elsevier BV, 2024 Publication	<1%
10	www.ispatguru.com Internet Source	